



DEPARTMENT OF TELECOMMUNICATION AND MEDIA INFORMATICS
BUDAPEST UNIVERSITY OF TECHNOLOGY AND ECONOMICS

ROUTING IN OPTICAL NETWORKS BASED ON PHYSICAL
EFFECTS

By
Szilárd Zsigmond

SUBMITTED IN PARTIAL FULFILLMENT OF THE
REQUIREMENTS FOR THE DEGREE OF
DOCTOR OF PHILOSOPHY (Ph.D.)

Supervised by

Dr. Tibor Cinkler
Department of Telecommunications and Media Informatics

High Speed Networks Laboratory
Budapest University of Technology and Economics

Budapest, Hungary

2010

Table of Contents

| | |
|---|-----------|
| TABLE OF CONTENTS | II |
| KIVONAT | IV |
| ABSTRACT..... | V |
| ACKNOWLEDGEMENT..... | VI |
| INTRODUCTION..... | 1 |
| 1.1 PREFACE..... | 2 |
| 1.2 OVERVIEW OF OPTICAL NETWORKS | 2 |
| 1.2.1 <i>Optical network components</i> | 4 |
| 1.2.2 <i>Optical modulation formats</i> | 6 |
| 1.2.3 <i>Performance evolution criteria</i> | 8 |
| 1.3 WAVELENGTH ROUTING IN OPTICAL NETWORKS | 9 |
| 1.3.1 <i>Impairment aware routing</i> | 11 |
| 1.4 OVERVIEW OF DISSERTATION AND CLAIMS..... | 12 |
| MODELING THE PHYSICAL IMPAIRMENTS IN WDM OPTICAL NETWORKS..... | 13 |
| 2.1 CLAIM 1.1: ANALYTICAL METHOD OF Q-FACTOR ESTIMATION..... | 14 |
| 2.1.1 <i>Introduction</i> | 14 |
| 2.1.2 <i>Q-factor estimation</i> | 18 |
| 2.1.3 <i>Validation of the calculation</i> | 35 |
| 2.2 CLAIM 1.2: CALCULATION OF OPTIMAL SIGNAL POWER FOR WDM OPTICAL NETWORKS | 38 |
| 2.2.1 <i>Introduction</i> | 38 |
| 2.2.2 <i>Model description</i> | 39 |
| 2.2.3 <i>Results</i> | 40 |
| 2.2.4 <i>Conclusion</i> | 51 |
| PHYSICAL IMPAIRMENT BASED ROUTING..... | 52 |
| 3.1 CLAIM 2.1: DYNAMIC IA-RWA ALGORITHM..... | 53 |

| | | |
|-------|--|-----------|
| 3.1.1 | <i>Introduction</i> | 53 |
| 3.1.2 | <i>Graph model</i> | 54 |
| 3.1.3 | <i>Routing model</i> | 55 |
| 3.1.4 | <i>Results</i> | 57 |
| 3.1.5 | <i>Conclusion</i> | 66 |
| 3.2 | CLAIM 2.2: ADAPTIVE CONFIGURATION METHOD | 67 |
| 3.2.1 | <i>Introduction</i> | 67 |
| 3.2.2 | <i>Physical feasibility</i> | 68 |
| 3.2.3 | <i>Conclusion</i> | 73 |
| 3.3 | CLAIM 2.3: HEURISTIC RWA FOR THE ADAPTIVE CONFIGURATION SCHEME | 74 |
| 3.3.1 | <i>Introduction</i> | 74 |
| 3.3.2 | <i>Graph model</i> | 75 |
| 3.3.3 | <i>Routing model</i> | 76 |
| 3.3.4 | <i>Results</i> | 79 |
| 3.3.5 | <i>Conclusion</i> | 83 |
| | CONCLUSION: | 85 |
| | BIBLIOGRAPHY | 86 |
| | INDEX | 93 |
| | APPENDIX: | 96 |
| 5.1 | CONSTANTS | 96 |
| 5.2 | VARIABLES | 97 |
| 5.3 | OBJECTIVE FUNCTION | 98 |
| 5.4 | CONSTRAINTS | 98 |
| 5.5 | EXPLANATION | 99 |

Kivonat

A disszertáció célja, hogy adjon egy jó kompromisszumot az útvonalválasztás és hullámhossz hozzárendelés (RWA - Routing-and-Wavelength-Assignment) probléma megoldására úgy, hogy a lehető legjobban vegye figyelembe az optikai hálózat specifikusságait. Az optikai hálózat teljesítőképességének modellezésére analitikus számolásokat alkalmaztam. A helyességüket szimulációkkal, illetve ahol lehetett mérésekkel ellenőriztem. Ezeket a módszereket beépítettem az általam javasolt RWA módszerekbe. Az eredményeket az alábbi két téziscsoportban foglaltam össze.

Az első téziscsoportban a fizikai hatások modellezésével foglalkozom. Az irodalomban publikált módszerekből kiindulva, ezeket a számolásokat kiterjesztve, vagy éppenséggel korlátozva, új számolási módszereket mutatok be, amelyek kielégítik az útvonalválasztó algoritmusok által felállított követelményeket. Minden fizikai hatásra kidolgozok egy-egy számolási módszert, amellyel az adott fizikai hatás, a megfelelő pontosság mellett, kvantitatívan lehet jellemezni, azaz vissza lehet vezetni a vevő oldalon mérhető bithiba arányra.

A második téziscsoportban az RWA probléma megoldását tűztem ki célul, a fizikai korlátok figyelembe vétele mellett. Mint ismeretes, két fő esetet különböztetünk meg az optikai hálózatok konfigurációjánál, a statikus és a dinamikus konfigurációt. Mindkét módszerre algoritmusokat fejlesztettem ki, amelyek képesek a fizikai hatások figyelembevételére. Ezen új módszerek előnyeit szimulációkkal igazolom.

A disszertációm alapját az ipari partnerekkel való eszmecsere során felmerült problémák adták. Ezek segítségével a jövő optikai hálózataiban az útvonalválasztók a fizikai hatások által támasztott korlátokat is figyelembe tudják venni.

A disszertációmban ismertetett eredményeimet 10 folyóirat és 10 konferencia cikk, egy könyvfejezet és egy nemzetközi szabadalom támasztja alá.

Abstract

The aim of my dissertation is to give a good compromise to the routing and wavelength assignment (RWA) problem, to be able to take into account the most accurate way the specifics of optical networks. For investigating the performance of optical networks I have used analytical calculations. The accuracy of the models were validated by simulations and where it was possible also measurements were done. These calculations were built in the proposed RWA methods. The results are classified in two areas which are strongly correlated.

In the first thesis group the modeling of physical effects is presented. Based on the already published models, these methods are extended or even in some cases restricted. I also present new calculation methods which fulfill the requirements of the RWA algorithms. For every physical effect I have developed a method which is able to characterize it in a quantitative way i.e., to calculate its effects onto the bit error ratio, measured at the receiver.

In the second thesis group the aim is to give a solution to the RWA problem which takes into account the physical effects. As it is well known two main cases are distinguished in configuration of optical networks, the static and the dynamic configuration. For both cases I have developed new methods which fulfill the physical constraints. The advantages of these effects are presented by simulations.

All the algorithms and solutions of this dissertation are strongly motivated by the telecommunications industry. They can equip the switches of the future optical networks to be able to handle the requirements of physical impairments.

The obtained results are supported by 10 journal and 10 conference papers, a book chapter and an international patent.

Acknowledgement

I would like to thank to my supervisor: Tibor Cinkler, whose help was essential in becoming a researcher in the field of telecommunication.

I would also like to thank to Géza Paksy for every day discussions, and his deliberate advices which made my research more adequate and useful. It was my honor to work with him.

My work was done in the research cooperation framework between Ericsson and the High-Speed Networks Laboratory (*HSNLab*) at the Budapest University of Technology and Economics. I am grateful to Tamás Henk and Robert Szabó for their continuous support.

I had the pleasure of spending one year at National Institute of Information and Communications Technology (NICT) Tokyo, Japan as guest researcher where I was able to work together with excellent researchers such as Dr. Tetsuya Miyazaki, Dr. Naoya Wada and Dr Hideaki Furukawa. I also made good friends there, Dr. Ben Puttnam and Dr. Kazi Sarwar Abedin. I will never forget the time spent together.

Of course, I am grateful to my parents, Ildikó and Sándor Zsigmond, for their patience and love. I would like to thank to my brother Péter for all his support, sometimes financially sometimes just a phone call. I am also thankful to all my relatives especially to my uncle József and to my grandparents for their trust on me.

I am also grateful to two excellent teachers from the elementary school: to my math teacher Ferenc Pál and to my first physics teacher László Erdélyi. Thanks to them I become interested in science.

Last but not least I wish to thank to all my friends for all the fun we had together.

Budapest Hungary
January 28. 2010

Szilárd Zsigmond

Chapter 1

Introduction

1.1 Preface

Reliability in dynamic, wavelength division multiplexed (WDM), photonic communication networks is becoming an increasingly important research topic. The combination of the ever-increasing demand for capacity, the generalization towards meshed network topologies, and widespread availability of dynamic optical switching, leads to severe constraints on quality of service (QoS) provisioning. These result from the difficulty in maintaining a uniform and acceptable quality for any optical path across a transparent optical network comprising multiple fiber types, signal formats and data rates [1]. Furthermore, the quality of each optical path is often correlated with other optical paths due to optical impairments such as crosstalk, limited amplifier output power, or transients in optical amplifiers, among others. In this scenario, newly emerging unforeseen demands often cannot be satisfied without modifying the network design, which is costly and time consuming. A solution for the interoperability issues among network layers based on the introduction of dynamic management and control (M&C) capabilities must cope with the escalating complexity inherent to the deployment of more reliable transparent networks. The need to achieve higher performance levels and to enhance the network reconfiguration capability and autonomy is also spreading from core to metro and access networks [2]. In communication networks, routing generally performs the identification of a path (route), per connection request, between a source and a destination node, across the network. In optical networks, the particular wavelengths along the path should also be determined. The resulting problem is often designated as routing and wavelength assignment (RWA) problem in literature [3]. The existing RWA proposals can be classified into two main categories: (a) considering the effects of impairments on network performance and (b) network design without impairment consideration. Although this is a widespread research topic, for transparent networks the incorporation of physical impairments in the RWA problem is still to be explored in full width.

1.2 Overview of optical networks

Since their first development and deployment, optical transmission networks offer improved possibilities for dealing with ever growing demands on transmission bandwidth and system capacity. In the last 20 years, the optical transmission networks have become one of the most important parts in the telecommunication hierarchy, whose seamless integration with conventional network applications and services forces a further development and a broader deployment of optical networks in all telecommunication areas. Making a classification of different optical transmission networks, it can be distinguished between Access, Metro and

Core (or back-bone) networks (Figure 1-1:) [4]. This is the most convenient network classification made regarding the transmission distance or network diameter. Access networks as the base of the telecommunication hierarchy, are characterized by the interaction between numerous different network technologies based on different transmission media e.g. wire, wireless or fiber. The implementation and deployment of optical networks in this region e.g. fiber-to-the-home (FTTH) and fiber-to-the-business (FTTB) would address the bottleneck problems, hence enabling an even broader bandwidth access than with conventional wire based technologies (e.g. DSL). But this is rather a question of deployment strategy and cost than of the achievable transmission performance. Metro area networks (MANs) accumulate the traffic from the access networks with different protocols and services, enabling its further transmission over longer distances. The MANs are based on optical transmission technologies and they are characterized by a limited transmission distance (< 200 km) and an increased network complexity. Furthermore, MANs have to deal with different communication protocols, thus requiring close interaction between the network management and transmission infrastructure, which results in the fact that the channel data rates used here are rather small (≤ 10 Gb/s/ch, at the moment). It has to be mentioned that in the last years a merge has been seen between the metro and core technologies, thus the metro networks becomes short range (< 1000 km) core networks as well.

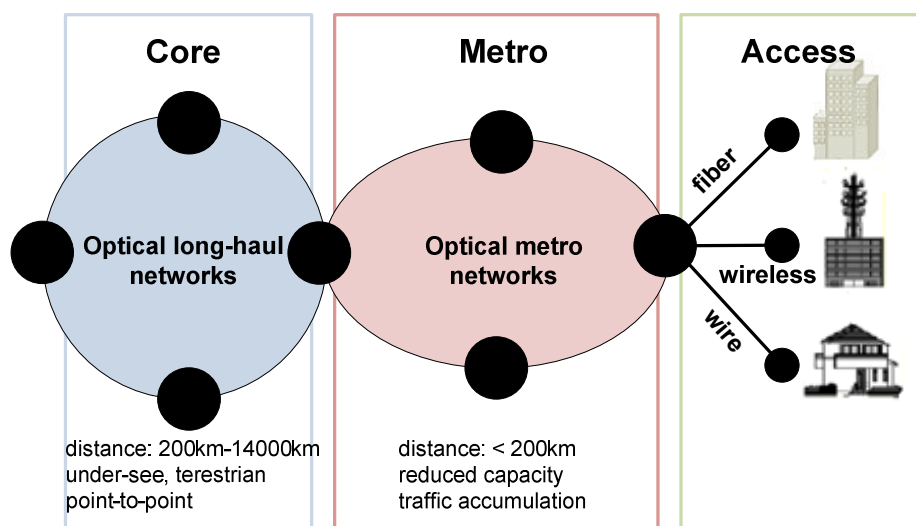


Figure 1-1: Network classification

The core networks connect numerous MANs over distances larger than 200 km. Basically, it can be distinguished between terrestrial and under-sea core networks. The under-sea networks are characterized by point-to-point transmission, ultra long-haul transmission distances (>1000 km), and specialized component characteristics (e.g. component life times

and customized fiber types). The core networks possess an increased transmission capacity based on larger channel data rates.

1.2.1 Optical network components

Figure 1-2 shows a generic block diagram of a typical WDM optical communication system. It consists of a transmitter, a communication channel, and a receiver, the three elements common to all communication systems.



Figure 1-2 Block diagram of an optical communication system

In optical networks the only difference being that the communication channel is an optical fiber cable. The other two components, the optical transmitter and the optical receiver, are designed to meet the needs of such a specific communication channel. In this section the basic elements of such systems are presented. The objective is to provide an introductory overview of them.

1.2.1.1 Optical transmitters

The role of an optical transmitter is to convert the electrical signal into optical form and to launch the resulting optical signal into the optical fiber. It consists of an optical source, a modulator, and a channel coupler. Semiconductor lasers or light-emitting diodes are used as optical sources. The optical signal is generated by modulating the optical carrier wave. Two types of modulation methods exist: the direct modulation and the external modulation. Semiconductor optical source can be modulated directly by varying the injection current. Such a scheme simplifies the transmitter design and is generally cost-effective but has much worse transmitter parameters than the external modulated transmitters. The coupler is typically a microlens that focuses the optical signal onto the entrance plane of an optical fiber with the maximum possible efficiency.

1.2.1.2 Optical fibers

The evolution of optical communication was strongly correlated by the evolution of optical fibers since its loss was the main bottleneck of such systems. The availability of low-loss fibers led to a revolution in the field of lightwave technology and started the era of fiber-optic communications. Several books devoted entirely to optical fibers cover numerous advances made in their design and understanding [5][6]. The International Telecommunication Union

has standardized the main optical fiber types and its parameters [7]. In nowadays networks the most widespread fiber type is defined by ITUT-G. 652, and it is a single mode optical fiber with zero dispersion at 1310 nm wavelength.

1.2.1.3 Optical amplifiers

Optical amplifiers represent one of the crucial components in an optical transmission system. Despite of the minimum attenuation at 1550 nm, fiber losses significantly limit the transmission performance with increased transmission distance. Optical amplification can be realized using different amplifier concepts and mechanisms e.g. semiconductor optical amplifiers (SOA), rare-earth doped fiber amplifiers or more recently Raman amplifiers. All these amplifier types are based upon different physical mechanisms resulting in different device characteristics and implementation areas. The most important representative of these amplifiers are the erbium doped fiber amplifiers (EDFAs), which are today's widely used amplifier types in optical transmission systems due to the fact that they provide an efficient optical amplification in the 1550 nm region.

1.2.1.4 Optical Nodes

The traffic entering/leaving a node can be described by the switching granularity: optical fiber, wavelength, time-slot. Thus, a "perfect" switching node would perform a complete permutation, i.e. the traffic from any fiber, any wavelength, and any time slot would be possible to switch to any other fiber, wavelength, time slot. However, due to considerations of cost and scalability, different node architectures are deployed in reality that have less than perfect switching capability. Considering WDM architecture where multiple wavelengths are multiplexed into one carrier optical fiber. If a node is able to add and drop some of the channels in all-optical way it is so called optical Add-Drop-Multiplexer (OADM). In contrast to OADMs, which usually have predetermined add/drop wavelengths, Reconfigurable OADMs (ROADMs) allow a network administrator or operator to dynamically select what wavelengths to drop or by-pass. In the last years for ring interconnection purposes new types of ROADMs were developed called multi-degree ROADM (MROADM). These optical nodes have the feasibility to switch the channels in several directions i.e., in as many directions as the degree, typically eight in nowadays MROADM nodes [8]. For the interconnection of multiple optical fiber carrying multiple channels optical cross connects (OXC) are used. These nodes are usually able to switch from any input fiber any channel to any output fiber, maintaining the wavelength continuity constraint.

1.2.1.5 Optical receivers

An optical receiver converts the optical signal received at the output end of the optical fiber back into the original electrical signal. It consists of a coupler, a photodetector, and a demodulator. The coupler focuses the received optical signal onto the photodetector. Semiconductor photodiodes are used as photodetectors because of their compatibility with the whole system. The design of the demodulator depends on the modulation format used by the lightwave system. The use of frequency-shift keying (FSK) and phase-shift keying (PSK) formats generally requires heterodyne or homodyne demodulation techniques. Most lightwave systems employ a scheme referred to as “intensity modulation with direct detection” (IM/DD). Demodulation in this case is done by a decision circuit that identifies bits as 1 or 0, depending on the amplitude of the electric signal. The accuracy of the decision circuit depends on the signal to noise ratio (SNR) of the electrical signal generated at the photodetector.

1.2.2 Optical modulation formats

In this section different optical modulation techniques are presented. Since the modulation is crucial on the performance of a lightwave system it is important to distinguish these techniques.

1.2.2.1 Amplitude modulation

Amplitude-Shift-Keying (ASK) known as “On-Off”-keying (OOK) is the technique of modulating the intensity of the carrier signal. In the simplest form, a source is switched between on and off states. A basic classification of the various ASK-based modulation formats can be made according to the shape of the optical pulses. All modulation formats can be divided into two groups: non-return-to-zero (NRZ), and return-to-zero (RZ). The NRZ is the major applied modulation format in today’s optical transmission systems. The pulse duration of the NRZ pulses is equal to the length of the time slot. During one time slot NRZ pulse retains the same amplitude and between successive 1’s no change of the signal amplitude occurs. In contrast to NRZ the RZ pulses occupy just a part of the bit slot, resulting in a duty cycle value smaller than 1. The main characteristic of RZ modulated signals is a relatively broad optical spectrum. The large spectral width results in a reduced dispersion tolerance and a reduced spectral efficiency of RZ-based WDM systems. The RZ pulse shape enables an increased robustness to fiber nonlinear effects [9], [10] and to the effects of polarization mode dispersion (PMD) [11].

1.2.2.2 Phase modulation

Phase Shift Keying (PSK) uses the phase of the signal to encode information. Optical PSK signals possess a narrow spectrum and a constant signal envelope, which enables improved nonlinear tolerance, but on the other hand the PSK signals are sensitive to a phase modulation induced by multi-channel effects, which can result in decoding errors at the receiver side. At the same time, PSK-based modulation enables an improved receiver sensitivity (up to 6 dB) [12] compared to ASK-formats. Especially interesting method of PSK modulation is differential PSK (DPSK). In DPSK signals, the information is encoded in the phase change between two successive bits. In spite of increased realization complexity of PSK modulation, the DPSK and differential quadrature PSK (DQPSK) investigations in 40Gb/s based WDM systems [13], [14], identified these formats as good alternatives to ASK-based modulation formats in future high speed WDM systems.

1.2.2.3 Frequency modulation

Frequency Shift Keying (FSK) is realized by switching the laser light frequency between two frequency values for marks and spaces. The FSK-based formats are not used in already deployed transmission systems because of complex signal detection. More recently, FSK-based modulation known as dispersion supported transmission format was intensively investigated for the implementation in MAN networks [15].

1.2.2.4 Polarization modulation

Polarization shift keying (PolSK) is the most exotic modulation format among all already presented. The optical PolSK signals are generated by switching the signal polarization between two orthogonal states of polarization. The PolSK is characterized by a constant signal envelope enabling an improved nonlinear tolerance [16], an improved sensitivity (3 dB) [17] compared to ASK-based modulation, and enables a better utilization of the system bandwidth by the use of orthogonal polarization as an additional degree of freedom. PolSK is a good alternative for the realization of multilevel modulation formats [18]. The drawbacks of PolSK are an increased complexity of signal generation and detection, as well as, the sensitivity to polarization disturbances (e.g. PMD, polarization dependent loss (PDL)) in the transmission line, whose impact increases with an increased channel data rate. Despite the fact that, PolSK may not be interesting for the implementation in commercial transmission systems, because of its complexity and sensitivity, it can be used as additional modulation stage for the improvement of nonlinear tolerance of ASK-based modulation formats.

1.2.2.5 Duobinary modulation

Duobinary modulation can be described as a combination of a conventional ASK-based modulation and phase shift keying (PSK). Depending on the realization, optical duobinary transmission can be understood as a multilevel transmission with phase encoded bits and a reduced spectral width. The reduction of the spectral width of the optical duobinary signal is the reason for its better dispersion tolerance compared to NRZ signals and enables an improved spectral efficiency in WDM systems. The main disadvantage of duobinary signals, similar to NRZ signals, is a relatively strong impact of fiber nonlinearities, which represents the main limiting factor for the maximum transmission length and the achievable transmission quality.

1.2.3 Performance evolution criteria

Performance monitoring traditionally refers to monitoring at the SONET/SDH (electrical) layer for bit error rates (BER) and other quality-of-service (QoS) measures. Due to the diversity of the optical layer several other performance evolution criteria has been introduced, which are not necessarily correlated with digital performance.

1.2.3.1 Bit error ratio (BER)

Performance requirements are usually characterized in terms of an acceptable bit error rate (BER), whose value generally depends on a specific source-to-user application. It might be as high as 10^{-3} for applications such as digitized voice or as low as 10^{-12} for scientific data. The tendency is towards lower and lower BER requirements. Also the received BER highly depends from the input signal power. The other problems with the BER that for low BER values the measuring time can increase drastically. The other disadvantage is that it describes the system overall performance and gives no details about the error occurring phenomena.

1.2.3.2 Q-factor

The Q-factor provides a qualitative description of the receiver performance because it is a function of the optical signal to noise ratio (OSNR). The Q-factor suggests the minimum OSNR required to obtain a specific BER for a given signal. Equation 1-1 shows the definition of the Q-factor.

$$Q = \frac{\mu_1 - \mu_0}{\sigma_0 + \sigma_1}$$

Where σ_0 , σ_1 are the noise variances, μ_0 , μ_1 are the mean values of the marks/spaces voltages or currents. In case of Gaussian noise distribution there is a relationship between the BER and the Q-factor as presented in [19].

1.2.3.3 Optical signal to noise ratio (OSNR)

The OSNR is determined whenever a dense WDM system is installed. It characterizes the difference between the peak power and the noise floor at the receiver for each channel. Optical noise, which has taken on new importance since the introduction of optical amplifiers in transmission systems, is due mainly to amplified spontaneous emission (ASE) in the EDFAs. Although the manufacturer has almost certainly tested the EDFAs individually, it is important to check their performance on-site, with all optical channels in operation and all cascaded amplifiers present, to confirm that overall performance expectations are being met. Gain variation merits special attention in multi-amplifier systems, as it will directly affect system power flatness. ASE noise figures can be particularly significant in some configurations, since this phenomenon degrades the signal-to-noise ratio in all optical channels. System gain will vary over time because of temperature changes, local stress, component degradation, and network modifications.

1.3 Wavelength routing in optical networks

The accelerating growth of data traffic is motivating the research for more efficient, flexible and intelligent optical network architectures. In this direction, IP over WDM is becoming accepted as one of the most promising candidates to fulfill these ever-increasing bandwidth demands. On the other hand, there is a global industry consensus to consider the generalized multi-protocol label switching (GMPLS) protocol suite [20] to be an integral part of next-generation transport networks, especially as enabler for the automatically switched optical network (ASON) [21] control plane, because it renders optical networks intelligent. However, the huge transport capacity of WDM technology is accepted to not be fully used by current optical networks [22]. Such inefficiency on the bandwidth utilization is due to the use of expensive optical-electrical-optical (OEO) transponders, which causes the well-known electronic bottleneck. These opaque networks have important advantages such as electronic signal regeneration as well as the capability of wavelength conversion, or grooming, on the hops of the connection. However, opaque networks also present important drawbacks: a complex layered structure, sensitive to signal format and data rate, elevated capital and operational costs (capex and opex), and suboptimal use of WDM's capacity. As a consequence, future optical networks are expected to overcome these limitations and take full

advantage of the WDM technology. This will be achieved using all-optical switches (e.g., reconfigurable optical add drop multiplexers, ROADMs, and/or optical cross-connects, OXCs) which allow to switch/route entirely an optical connection (lightpath) over the optical domain (i.e., transparent networks). Thus, the introduction of transparency in optical networks eliminates the need for expensive OEO transponders (reducing capex) during the switching of a lightpath. However, this also results in losing the electrical regeneration of signals, which in turn makes the optical signal not oblivious to the accumulation of the impairments due to fiber transmission (attenuation, dispersion, nonlinearities, etc.), optical amplification (ASE), insertion losses and crosstalk introduced by optical elements such as switches, filters or mux/demux in ROADMs and OXCs. Considering a transparent network scenario, the signal quality degradation will increase the importance of performance monitoring. The BER computation is not as fast as desired (minutes) in the context of a dynamic, transparent optical network, in which changes may take place in msec-sec order. Other parameters such as optical signal noise ratio (OSNR), Q-factor or polarization mode dispersion (PMD) penalty are thus being investigated to be used for guaranteeing on-line QoS with lower opex and delays.

Considering a nowadays (2009) more realistic scenario the translucent networks are located in the path toward the transparent optical networks (full optical) networks. Since all optical regeneration (re-amplification, re-shaping and re-timing) are not mature enough, translucent networks are inevitable. Optical-Electrical-Optical regeneration not only affects the routing and wavelength assignment strategies, due to their impact of physical layer performance, but also paves the way for other functions like traffic grooming.

A central issue in wavelength routing (WR) networks is the resource allocation of wavelength channels to lightpaths. Lightpaths provide end-to-end, circuit-switched connections between a pair of physical nodes using a single, previously specified wavelength. First, in order to establish such a connection, one needs to find a reasonably short sequence of physical network links between the endpoints – this process is called routing; the resulting sequence will be the assigned route or path of the lightpath. In a WR network, a set of wavelengths is available on each physical link; lightpaths, on every link belonging to the assigned route, need exactly one of these for exclusive use from setup until termination. Also, a lightpath requires all optical nodes traversed along the assigned route to be set to states in which the wavelengths belonging to the lightpath on subsequent links are connected.

Another important question is the distinction between two kinds of problems: static and dynamic routing. There is a wide range of literature available on the subject [23][24][25][26][27][28]. Consider the operation of a network where all connections are

provisioned for long periods of time, e.g., months or years; it can always be sure that the set of held calls does not change frequently. Also, when admitting a new call to the network, there may be no stringent requirement that the route be established in a very short period of time: there may even be enough time available for the operator to find the best solution of the nondeterministic polynomial-time hard (NP-hard) optimization problem and route all calls accordingly.

In general it can be said that the RWA problem is an NP-complete problem with computational effort increasing exponentially with the problem size. Thus, a wide range of optimum approximation methods and heuristics have been proposed to solve various network optimization problems. Integer linear programming (ILP) could be employed [29], but it requires heavy computational efforts. Other heuristic algorithms such as Tabu-search [30], simulated annealing [31], and genetic algorithms [32] with to some extent scalable computation effort have also been proposed. It has also been used to solve single objective RWA problem [33], to optimize amplifier placement [34], as well as to optimize multicasting sessions [30].

1.3.1 Impairment aware routing

In case of optical networks the signal gets slightly degraded after traversing a link or a node; it is obvious, that lightpaths can not be arbitrarily long as signal regeneration is not yet possible purely in the optical layer. Thus in WR networks signal degradation due to transmission impairments cannot be neglected; however, their adverse effects on the performance of routing and wavelength assignment have not been studied extensively. Most impairment aware RWA (IA-RWA) approaches recently proposed, still consider the quality of the transmission separately from the RWA problem [35][36]. A common strategy employed is to incorporate impairments into the cost function. However, a cost function for both linear and nonlinear impairments is still an open question. Different analytical models have been developed to describe reference links with or without compensation of fiber impairments [36][37]. Only few studies, consider the simultaneous impact of chromatic dispersion (CD), polarization mode dispersion (PMD), amplified spontaneous emission (ASE), and nonlinear phase shift [38]. Therefore, other more universal metrics have been used, including the average measured Q [39] or noise variance [37]. In any case, accurate Q-path estimation is not a trivial task and in some cases can have heavy computation, even in the static RWA problem demanding offline calculation. For an IA-RWA strategy to be actually implemented, one needs to consider also fundamental aspects like enabling Optical Impairment Monitoring (OIM) for indirect evaluation of signal quality, or enabling direct Optical Performance

Monitoring (OPM) [40]. In 2004, ITU-T defined a list of OPM parameters that might be used for impairment-aware RWA [41]. The most important performance parameters: (a) residual chromatic dispersion (CD), (b) total EDFA input and output powers, (c) a channel's optical power budget, (d) optical signal-to-noise ratio (OSNR), and (e) Q-factor as an estimator of the overall optical performance. In this dissertation the focus is on the utilization of intelligent routing algorithms which take into account physical layer attributes as input parameters (i.e., constraints) for the path computation, with the aim to achieve quality-enabled services. Such routing algorithms are known in the literature as impairment aware RWA (IA-RWA).

1.4 Overview of dissertation and claims

The Dissertation consists of five chapters.

In Chapter 1 a short introduction is given where the basics of optical networks and routing in such networks, are presented. The concept was to give a very short and brief state of art of these topics.

In Chapter 2 an analytical calculation method is presented for estimating the Q-factor of an optical connection. The novelty of the method is that it allows calculating a link Q-factor in relatively short time, e.g. several seconds, which makes it possible for use in IA-RWA methods. The other advantage of the method is that it takes into account all important physical effects which have influence onto the signal quality in case of, up to 10 Gbit/s NRZ amplitude modulated direct detected systems.

In Chapter 3 an IA-RWA method is given for both static and dynamic routing cases. In case of dynamic routing; a new scheme is proposed where it is able to consider multilayer networks besides the constraints of the optical layer. In case of static routing a new method is proposed, called adaptive configuration method, where the control plane is able to adjust the signal power of each channel. In this way it is possible to configure the optical network in a more accurate way.

In Chapter 4 a short overview and conclusion is given of the dissertation. The Chapter 5 is an appendix, the ILP formulation is given for the adaptive configuration method.

Chapter 2

Modeling the physical impairments in WDM optical networks

2.1 Claim 1.1: Analytical method of Q-factor estimation

Claim 1.1: "I have proposed an analytical signal quality calculation method, which has low computation requirements while it still takes into account the main degrading effects of intensity modulated direct detection 10 Gbit/s bit-rate wavelength division multiplexed all-optical networks."

Claim 1.1 describes an analytical method to calculate the Q-factor. Several methods have been proposed in the literature so far and it is quite hard to distinguish between them, since the basic method is to calculate the variance of the noise at the receiver side. The method presented in this dissertation also calculates the variance of the noise, but it has two main advantages comparing to the already published ones.

The first difference is, that it is able to calculate nearly all physical effects which occur in WDM optical networks concerning the assumptions mentioned in previous section. To the best of the author knowledge this is the first method which can handle EDFA noise, node crosstalk, fiber nonlinearities like four-wave mixing (FWM), stimulated Raman scattering (SRS), cross-phase modulation (XPM) and also the effects of PMD simultaneously.

The other very important issue of the proposed calculation method is that the original problem is divided into sub problems. Considering a point-to-point connection where a chain of optical elements fibers, EDFA, optical nodes, etc. are used the proposed method is reduced to several sub calculations, where each of the calculations can be done separately. The advantage of it is the cooperation possibility with the impairment routing schemes, as presented in Chapter 3.

2.1.1 Introduction

In the last fifteen-twenty years the optical technology had been widespread in the telecommunication networks. Various technologies were developed for each segment of the network. In the access part of the network short range passive optical networks were proposed. In the metro networks the WDM and Dense WDM (DWDM) technology were deployed together with OADM-ROADM-MROADM optical nodes. In the core and long haul networks low noise figure amplifiers, Raman amplifiers, and accurate dispersion mapping is used. And all these technologies can be used with various modulation formats and bit rates. Thus, to make a calculation method of the impairments which is valid in each segment of the network is impossible. The only solution is to distinguish between the certain technologies and to define the main impairments which have the most influence onto the signal quality.

Since the dissertation is based on routing in WDM optical networks the calculation of the physical constraints have the following assumption:

- WDM metro-core network
- high performance, externally modulated distributed feedback lasers (DFB) for transmitters
- amplitude modulated NRZ or RZ signals
- direct detection receiver, PIN or Avalanche APD photodiode
- channel bit rate up to 10 Gbit/s
- channel spacing 50 or 100 GHz

As it can be seen, these assumptions are not sever assumptions, nearly all types of nowadays (2009) deployed WDM systems fulfill these requirements. However, it has to be mentioned, that several companies have 40 Gbit/s channel bit rate phase modulated systems. In this case the proposed calculation method must be improved.

The signal quality of a connection is characterized by Bit Error Ratio (BER). Experimental characterization of such systems is not easy since the direct measurement of BER takes considerable time. Another way of estimating the BER is to degrade the system performance by moving the receiver decision threshold value, as proposed in [42]. This technique has the additional advantage of giving an easy way of estimating the signal quality (Q) of the system, which can be more easily modeled than the BER. In section 1.2.3.2 the definition of Q-factor was already given. [43].

It is an obvious question that if the BER is the most well-known parameter of an optical system why the Q-factor has been introduced. The answer is that both the modeling and measuring the BER is very difficult. For a given design at a BER such as 10^{-12} and a line rate of 155 Mbps, the network would have one error in approximately 10 days. It would take 1000 days to record a steady state BER value. Of course if the line rate is increased for example to 10 Gbit/s typically used in nowadays WDM systems this time will scale down but still if we would like to know a system BER floor which could be lower than 10^{-30} these measurements are nearly impossible. That is the reason why BER calculations are quite difficult. On the other hand, Q-factor analysis is comparatively easy and from the estimated Q-factor the BER can be calculated as well.

Let as consider the definition of BER:

$$BER = \frac{\text{Number of errors}}{\text{Number of transmitted bits}}$$

2-1

As mentioned previously the error counting method has several drawbacks thus another definition has been proposed for BER estimation. Considering a two level amplitude modulated system (i.e. '0' and '1' bits). A typical eye diagram of such systems can be seen in Figure 2-1, source [44].

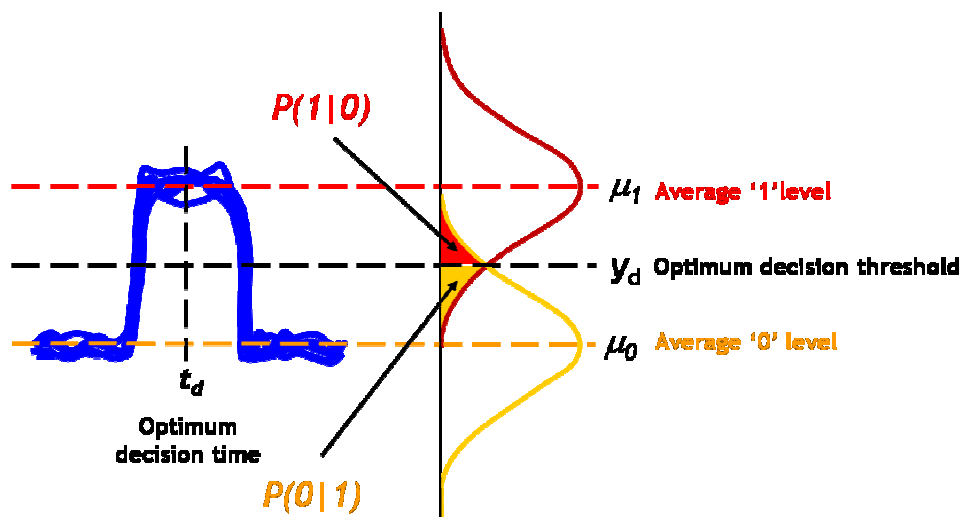


Figure 2-1 Bit Error Rate (BER) estimation

Due to noise, the '1' level and the '0' level are not fixed. It not only varies from bit to bit, but also fluctuates within a bit. Over a large number of bits, the '1' and '0' levels are statistically represented by distributions, each with its own mean and variance.

- the mean level of '1' is given by μ_1
- the variance of the distribution of '1' is given by σ_1
- the mean level of '0' is given by μ_0
- the variance of the distribution of '0' is given by σ_0

In this case the BER can be defined as follows:

$$BER = p(1)P(0|1) + p(0)P(1|0)$$

2-2

Where:

- $p(1)$ is the probability of '1' transmitted ~ proportion of '1's in the transmitted sequence
- $p(0)$ is the probability of '0' transmitted ~ proportion of '0's in the transmitted sequence

- $P(0|1)$ is the probability of detecting a '0' given that a '1' is actually received
- $P(1|0)$ is the probability of detecting a '1' given that a '0' is actually received

If the same number of '0's as '1's are sent, then $p(0) = 0,5 = p(1)$ so the BER simplifies to

$$BER = \frac{1}{2} [P(0|1) + P(1|0)] \quad 2-3$$

The two BER values give the same results in case of infinite number of bits. Assuming a Gaussian noise distribution, which is typical in WDM systems, expressions for the various probabilities may be written explicitly in terms of the means, variances of the '0's and '1's, and the decision level y_d :

$$p_1(y) = \frac{1}{\sigma_1 \sqrt{2\pi}} \exp \left[-\frac{(y_d - \mu_1)^2}{2\sigma_1^2} \right] \quad 2-4$$

$$p_0(y) = \frac{1}{\sigma_0 \sqrt{2\pi}} \exp \left[-\frac{(y_d - \mu_0)^2}{2\sigma_0^2} \right] \quad 2-5$$

$$P(1|0) = p(y > y_d | y \sim p_0) = \frac{1}{\sigma_0 \sqrt{2\pi}} \int_{y_d}^{\infty} \exp \left[-\frac{(y_d - \mu_0)^2}{2\sigma_0^2} \right] = \frac{1}{2} \operatorname{erfc} \left[\frac{y_d - \mu_0}{\sqrt{2}\sigma_0} \right] \quad 2-6$$

$$P(0|1) = p(y < y_d | y \sim p_1) = \frac{1}{\sigma_1 \sqrt{2\pi}} \exp \int_{-\infty}^{y_d} \left[-\frac{(y_d - \mu_1)^2}{2\sigma_1^2} \right] = \frac{1}{2} \operatorname{erfc} \left[\frac{\mu_1 - y_d}{\sqrt{2}\sigma_1} \right] \quad 2-7$$

Substituting 2-6 and 2-7 in 2-3 we obtain:

$$BER = \frac{1}{4} \left[\operatorname{erfc} \left(\frac{\mu_1 - y_d}{\sqrt{2}\sigma_1} \right) + \operatorname{erfc} \left(\frac{y_d - \mu_0}{\sqrt{2}\sigma_0} \right) \right] \quad 2-8$$

As it is to be seen the BER values highly depends from the decision threshold. The optimum y_d gives minimum BER. erfc stands for the well known error function. Several techniques have been proposed in experimental setups to determine the optimum [45]. In case of optimum y_d the following equation holds:

$$p_1(y_d) = p_0(y_d) \quad 2-9$$

In general this equation must be solved numerically. In case of Gaussian noise distribution a common but accurate approximation is that for an optimum threshold:

$$P(0|1) = P(1|0) \quad \Rightarrow \quad y_d = \frac{\sigma_0 \mu_1 + \sigma_1 \mu_0}{\sigma_0 + \sigma_1} \quad 2-10$$

in this case the

$$BER = \frac{1}{2} \operatorname{erfc}\left(\frac{Q}{\sqrt{2}}\right) \quad \text{where} \quad Q = \frac{\mu_1 - \mu_0}{\sigma_0 + \sigma_1} \quad 2-11$$

where Q is the Q-factor of the signal. As it is to be seen in case of Gaussian noise distribution the BER is determined fully by Q-factor. Thus if it is possible to measure or calculate the Q then the BER can be determined. The method presented enables a good BER estimation, but according to the inaccuracy of Gaussian distribution the predicted BER values are typically larger than the minimum expected BER [45] and determined y_d may deviate from the real optimum.

2.1.2 Q-factor estimation

An optical link consists of several optical elements in chain as presented in Figure 2-2. An accurate calculation method to determine the signal quality must handle all of these elements simultaneously.

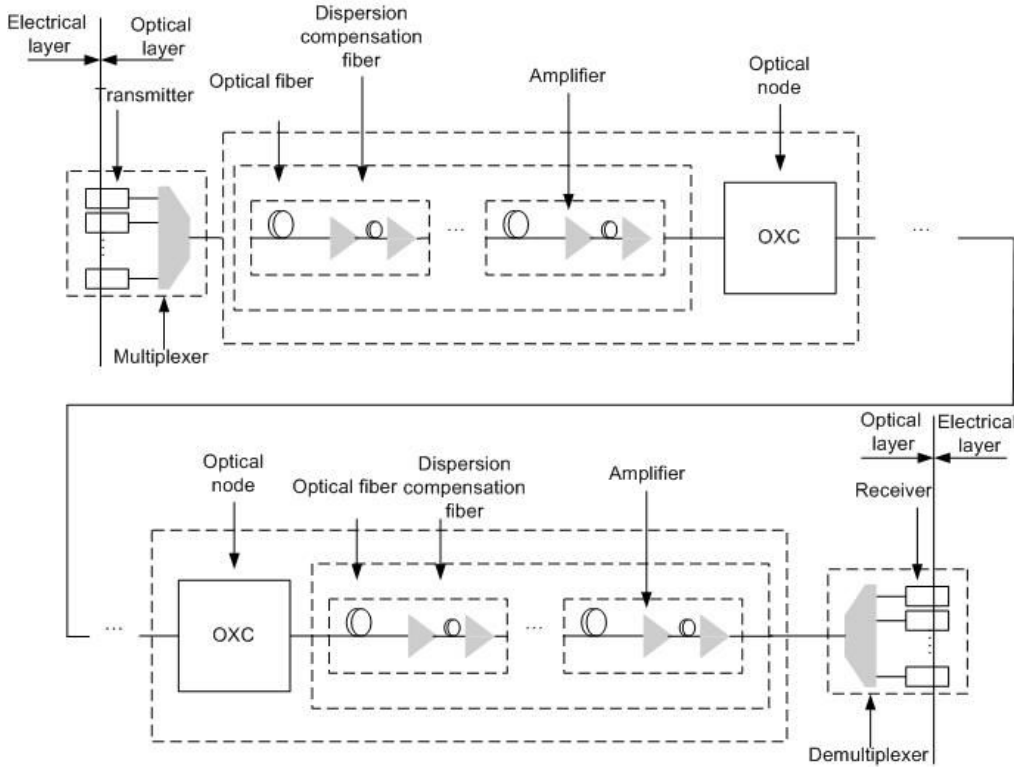


Figure 2-2 Optical link elements

Using the definition of Q-factor and with a simple mathematical rearranging as shown in equation 2-12 it is possible to calculate the Q-factor after one optical element (Q_{end}) while knowing the input Q-factor (Q_{start}) and the degradation effects of the element. Using the previously presented method it is possible to calculate Q-factor while the signal passes through the network as follows.

$$\begin{aligned}
 Q_{end} &= \frac{\mu_{1end} - \mu_{0end}}{\sigma_{1end} + \sigma_{0end}} = \left(\frac{\mu_{1end} - \mu_{0end}}{\mu_{1start} - \mu_{0start}} \right) \times \left(\frac{\sigma_{1,start} + \sigma_{0,start}}{\sigma_{1,end} + \sigma_{0,end}} \right) \times \left(\frac{\mu_{1start} - \mu_{0start}}{\sigma_{1,start} + \sigma_{0,start}} \right) = & 2-12 \\
 &= \left(\frac{\mu_{1end} - \mu_{0end}}{\mu_{1start} - \mu_{0start}} \right) \times \left(\frac{\sigma_{1,start} + \sigma_{0,start}}{\sigma_{1,end} + \sigma_{0,end}} \right) \times Q_{start} = (\text{Eye Penalty}) \times (\text{Noise Penalty}) \times Q_{start}
 \end{aligned}$$

As presented in equation 2-12 a system overall Q-factor can be determined by the calculation of each element physical degradation i.e. the eye and noise penalty. The Eye related penalties are the dispersion related penalties such as chromatic dispersion (CD) and polarization mode dispersion (PMD). The Noise related penalties are the amplifier spontaneous emission (ASE) and crosstalk.

The CD in nowadays metro-core optical networks is compensated. Since the CD has wavelength dependency the residual dispersion can deteriorate the signal quality. Hopefully it does not have high influence on the signal quality in case of typically used C or L bands and just several hops, less than 20 compensation points for current networks.

The situation is different in case of PMD. Since in networks in used nowadays the PMD is not compensated, thus even for 10 Gbit/s system it can have high influence onto the signal quality [46].

The noise related penalties include ASE noise from EDFA the crosstalk from the nodes and also the nonlinearities in the optical fiber. Here we assumed that the influence of each phenomena to the others is very small, i.e., it results in a larger or smaller perturbation around the mean value of a channel. The phenomena under consideration (ASE, crosstalk (XT), FWM, XPM, and SRS) are treated as statistically independent, and their overall contribution to the Q-factor is approximated by a Gaussian variable.

Using the equations for a p-i-n photodiode in the receiver and the previously stated assumptions, the Q-factor is approximately given by [47]:

$$Q_i = \mu_{SRSi} \frac{\mu_{1i} - \mu_{0i}}{\sigma_{0ASEi} + \sqrt{\sigma_{1ASEi}^2 + \sigma_{XTi}^2 + (\sigma_{XPMi}^2 + \sigma_{FWMi}^2 + \sigma_{SRSi}^2)}} \quad 2-13$$

Where σ_{0ASEi} , σ_{1ASEi} are the noise variances excluding the nonlinear effects, μ_{0i} , μ_{1i} are the mean values of the marks/spaces voltages or currents, and σ_{XPMi} , σ_{FWMi} , σ_{SRSi} , are the induced optical power deviations due to the respective effect at i^{th} channel. μ_{SRSi} is the SRS-caused signal level deviation normalized by the output power.

Combining the equation 2-12 and 2-13 it is possible to calculate the performance of an optical link containing a chain of optical fibers and different elements such as optical switches, EDFAs, etc.

The Q-factor unlike the OSNR is an electrical performance monitoring parameter thus it also includes the receiver parameters. In this dissertation for Q-factor estimation the following calculation method is used. The method is an extension of [48] to be able to calculate other impairments as well.

Let as assume an optical signal before the receiver in the presence of disturbing contributions like ASE, XT, nonlinearities:

$$E_R(t) = E_{sig}(t) + E_1(t) + E_2(t) + E_3(t) + \dots + E_n(t) \quad 2-14$$

where $E_R(t)$ is the lightwave received, the first term $E_{sig}(t)$ represents the lightwave for the desired signal component and $E_1(t)-E_n(t)$ represents the disturbing effects such as ASE, XT etc. The received lightwave, after photo detection, produces a photocurrent given by:

$$i_p(t) = R \langle E_R^2(t) \rangle + i_{sh}(t) + i_{th}(t) \tag{2-15}$$

where the first term represents the square-and-average response of the photodetector to the incident lightwave $E_R(t)$ with R representing the responsivity of the photodetector, the second term is the shot noise produced by the incident lightwave, and the third term accounts for the receiver thermal noise. Assuming that the signal power is much higher than the receiver sensitivity the shot noise and the thermal noise can be neglected. The first term of $i_p(t)$ in (2-15) can be expressed as:

$$R \langle E_R^2(t) \rangle = i_{sig}(t) + i_{sig-1}(t) + i_{sig-2}(t) + \dots + i_{sig-n}(t) + other \tag{2-16}$$

where $i_{sig}(t)$ represents the desired signal component while the remaining terms account for the beat noise components between signal and the deteriorating effects. In the other component all the other cross components are involved such as $i_{1-1}(t)$ or $i_{1-2}(t)$.

Considering that the dominant beat noise terms are contributed by the signal-disturbing effect, and representing all the noise components as a combined noise process the equation 2-15 can be approximated as:

$$i_p(t) \approx i_{sig}(t) + [i_{sig-1}(t) + i_{sig-2}(t) + \dots + i_{sig-n}(t)] \tag{2-17}$$

$$= I_{sk} + n_k(t) \tag{2-18}$$

$$= RP_{opt} b_k + n_k(t) \tag{2-19}$$

where k in the subscripts of all the terms in (2-18) and (2-19) represents the data bit (1 or 0) being received, I_{sk} with $k=1$ or 0 represents the corresponding signal components of the photocurrent, P_{opt} represents the average value of the received optical signal power, and $b_k=2$ or 0 for $k=1$ or 0 , respectively. The combined electrical noise $n_k(t)$ is modeled as a zero-mean Gaussian random process with a variance given by

$$\sigma_k^2 = \sigma_{k sig-1}^2 + \sigma_{k sig-2}^2 + \dots + \sigma_{k sig-n}^2 \tag{2-20}$$

The receiver Q-factor is evaluated with a given decision threshold choice. One can maximize the Q-factor by an optimum selection of it. However, an optimum choice of the threshold can only be made with a prior knowledge of the received power levels of signal, crosstalk, and ASE components and the other deteriorating effects.

Assuming a perfect laser extinction (i.e., $b_0 = 0$, and hence $I_{s0} = 0$), in the following fix receiver threshold is used in the calculation, the value is $I_{s1}/2$. Using the above threshold and noise variances, the Q-factor of the system can be express by :

$$Q = \frac{I_{s1}}{\sigma_1 + \sigma_2} \tag{2-21}$$

The novelties of the proposed method are as follows: It is able to calculate step-by step each physical effect as the equation 2-12 indicates. The receiver model presented in [48] was extended to be able to take more physical effects into account. Also to fulfill the step-by-step model the receiver noise at this point was neglected. Finally the cross effects between physical effects was neglected.

In the following sections form 2.1.2.1 to 2.1.2.4 the detailed calculation of each physical effect is presented.

2.1.2.1 Calculation of ASE noise

Optical amplifiers represent one of the crucial components in an optical transmission system. Despite of the minimum attenuation at $1.55\mu\text{m}$ (theoretically, 0.16 dB/km), fiber losses significantly limit the transmission performance with increased transmission distance ($>20 \text{ km}$). Optical amplification can be realized using different amplifier concepts and mechanisms e.g. semiconductor optical amplifiers (SOA), rare-earth doped fiber amplifiers (e.g. erbium, holmium, thallium, samarium) or more recently Raman amplifiers. All these amplifier types are based upon different physical mechanisms resulting in different device characteristics and implementation areas. The rare-earth doped fiber amplifiers provide optical amplification in the wavelength region from $0.5\text{-}3.5\mu\text{m}$. The most important representative of this amplifier type is erbium doped fiber amplifier (EDFA), which is today's widely used amplifier type in optical transmission systems due to the fact that it provides an efficient optical amplification in the $1.55\mu\text{m}$ region.

Considering a chain of EDFAs besides the signal amplification the noise is also generated as shown in Figure 2-3.

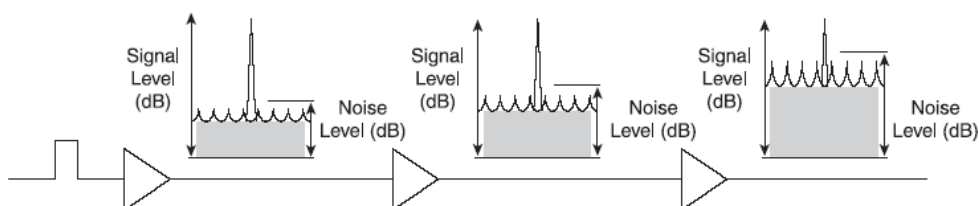


Figure 2-3 noise accumulation in optically amplified link source:[19]

Several methods can be found in the literature presenting the calculation of the noise induced signal quality deterioration [19] [43] [48]. Most of the calculations are based on OSNR calculation and its conversion to the Q-factor. In this dissertation I also followed this method.

The noise power generated by the EDFA is given by the recursive formula:

$$P_{ASEi} = P_{ASEbefore\ i} \cdot G + 2n_{sp}(G-1)h\nu B_0 \quad 2-22$$

Where n_{sp} represents the spontaneous emission factor for the EDFAs, h is Planck's constant, ν is the optical frequency, B_0 is the optical filter bandwidth and G is the gain of the amplifier. $P_{ASEbefore\ i}$ is the noise power before the EDFA at i^{th} channel.

Assuming a direct detecting receiver the variances of the noise at the receiver point while obtaining the eye diagram can be calculated as follows:

$$\sigma_{sp-spi}^2 = R^2(P_{ASEi} / B_0)^2(B_0 - B_e / 2) \cdot 2B_e \quad 2-23$$

$$\sigma_{sig-spi}^2 = 2R^2P_iP_{ASEi} / B_0 \cdot 2B_e \quad 2-24$$

Where σ_{sp-spi}^2 is the spontaneous-spontaneous beat noise in i^{th} channel, $\sigma_{sig-spi}^2$ is the signal-spontaneous beat noise in i^{th} channel; R is the responsivity of the photo detector, B_e is the electric bandwidth of the receiver, and P_i is the optical power at the output.

Neglecting thermal and shot noise of the receiver the σ_{0ASEi} , σ_{1ASEi} can be obtained:

$$\sigma_{0ASEi}^2 = \sigma_{sp-spi}^2 \quad 2-25$$

$$\sigma_{1ASEi}^2 = \sigma_{sig-spi}^2 + \sigma_{sp-spi}^2 \quad 2-26$$

2.1.2.2 Calculation of Crosstalk

The XT in optical systems can be characterized in two different categories: interchannel and intrachannel XT. Interchannel XT occurs in case of non ideal filtering in multiplexers and de-multiplexers. Since the noise component has different wavelength than the signal thus can be easily removed by filtering out. The intrachannel XT occurs in optical switches. Since in this case the disturbing XT noise and the signal has the same wavelength it makes nearly impossible to remove it. In this section we only model and calculate the impact of intrachannel XT coming from optical switches.

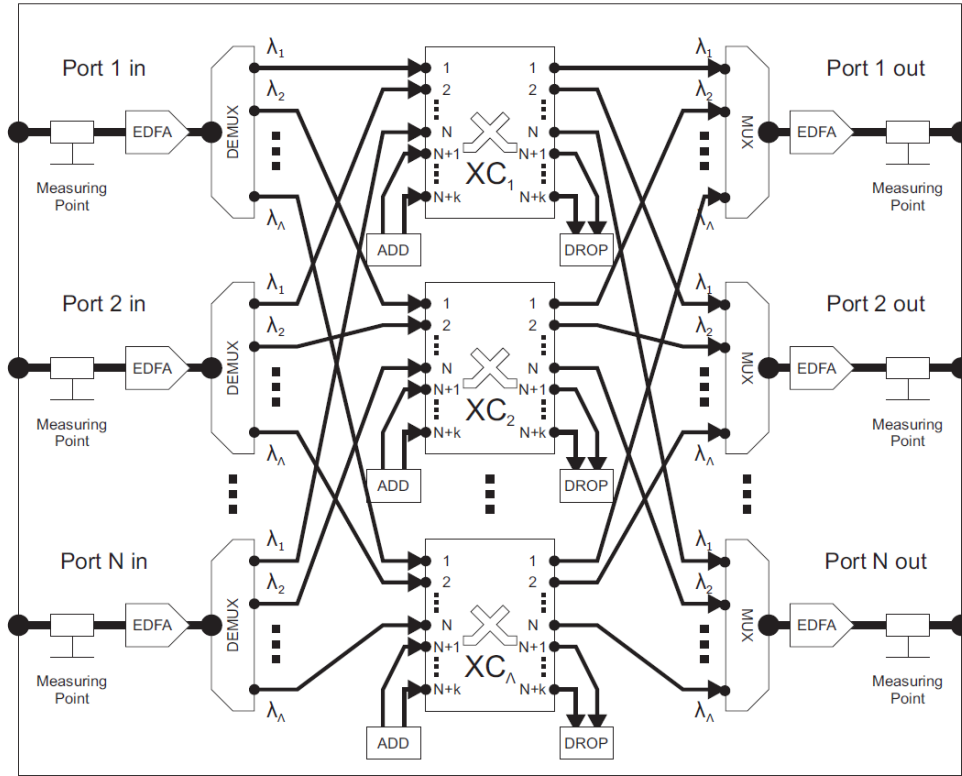


Figure 2-4: Optical cross connect architecture

In Figure 2-4 a basic architecture of an optical node can be seen. It has several fiber input and output ports. The switching is done by $(N+k) \times (N+k)$ switches as indicated in figure. The origin of intrachannel XT is also from these switches.

The XT power generated by the EDFA is given by the recursive formula:

$$P_{XTi} = P_{XTbefore\ i} \cdot L_{sw} + \sum_{j=1}^{N+k} X_{sw} P_{ij} L_{sw} \tag{2-27}$$

where P_{XTi} is the power of XT at i^{th} channel after the switch, the $P_{XTbefore\ i}$ the power of XT at i^{th} channel before the switch X_{sw} the XT parameter of the switch, L_{sw} the insertion loss of the switch and the P_{ij} is the signal power at port j . The index i refers to i^{th} channel however since a switch is dedicated to one channel it has no meaning in this particularly case. It was used to be consequent with the calculation presented in previous section.

Assuming a direct detecting receiver as introduced in section 2.1.2 the variances of the XT at the receiver point:

$$\sigma_{XTi}^2 = \sigma_{sig-xt}^2 = 2\xi_p R^2 P_i b_k P_{xti} \tag{2-28}$$

where $\xi_p = 1/2$ (see [49]) representing the polarization mismatch factor between the signal and crosstalk lightwaves, P_i and P_{xti} are average the signal and of the XT power at i^{th} channel respectively, while b_k is the constant introduced in equation 2-19.

In case of ASE and crosstalk noise the novelty was that receiver model was restricted to a noise free model. This was necessary to fulfill the requests coming from the step by step calculation. Since the model calculates the Q-value after each step, each EDFA or node, and at this point the signal remains in the optical layer a virtual receiver has to be considered to obtained a Q-value. This virtual receiver is noiseless. Obviously at the end of the connection a where the signal is detected, the noise of the receiver can be taken into account.

2.1.2.3 Calculation of fiber nonlinearities

The response of any dielectric to light becomes nonlinear for intense electromagnetic fields, and optical fibers are no exception. On a fundamental level, the origin of nonlinear response is related to anharmonic motion of bound electrons under the influence of an applied field. As a result, the total polarization P induced by electric dipoles is not linear in the electric field E

$$P = \varepsilon_0 \left(\chi^1 E + \chi^2 : EE + \chi^3 : EEE + \dots \right) \quad 2-29$$

where ε_0 is the vacuum permittivity and $\chi^{(j)}$ ($j=1,2, \dots$) is j^{th} order susceptibility. In general, $\chi^{(j)}$ is a tensor of rank $j+1$. The linear susceptibility $\chi^{(1)}$ represents the dominant contribution to P . Its effects are included through the refractive index n and the attenuation coefficient α . The second-order susceptibility $\chi^{(2)}$ is responsible for such nonlinear effects as second-harmonic generation and sum-frequency generation [50]. However, it is nonzero only for media that lack an inversion symmetry at the molecular level. As SiO_2 is a symmetric molecule, $\chi^{(2)}$ vanishes for silica glasses. As a result, optical fibers do not normally exhibit second-order nonlinear effects. The lowest-order nonlinear effects in optical fibers originate from the third-order susceptibility $\chi^{(3)}$ which is responsible for phenomena such as third-harmonic generation, four-wave mixing, and nonlinear refraction. Unless special efforts are made to achieve phase matching, the nonlinear processes that involve generation of new frequencies (e.g. third-harmonic generation and four-wave mixing) are not efficient in optical fibers. Most of the nonlinear effects in optical fibers therefore originate from nonlinear refraction, a phenomenon referring to the intensity dependence of the refractive index. In its simplest form, the refractive index can be written as:

$$\tilde{n}(\omega, |E^2|) = n(\omega) + n_2 |E^2| \tag{2-30}$$

where $n(\omega)$ is the linear part of the refractive index E^2 is the optical intensity inside the fiber, and n_2 is the nonlinear-index coefficient related to $\chi^{(3)}$ by the relation:

$$n_2 = \frac{3}{8n} \text{Re}(\chi_{xxxx}^3) \tag{2-31}$$

where Re stands for the real part and the optical field is assumed to be linearly polarized so that only one component $\chi^{(3)}_{xxxx}$ of the fourth-rank tensor contributes to the refractive index [51].

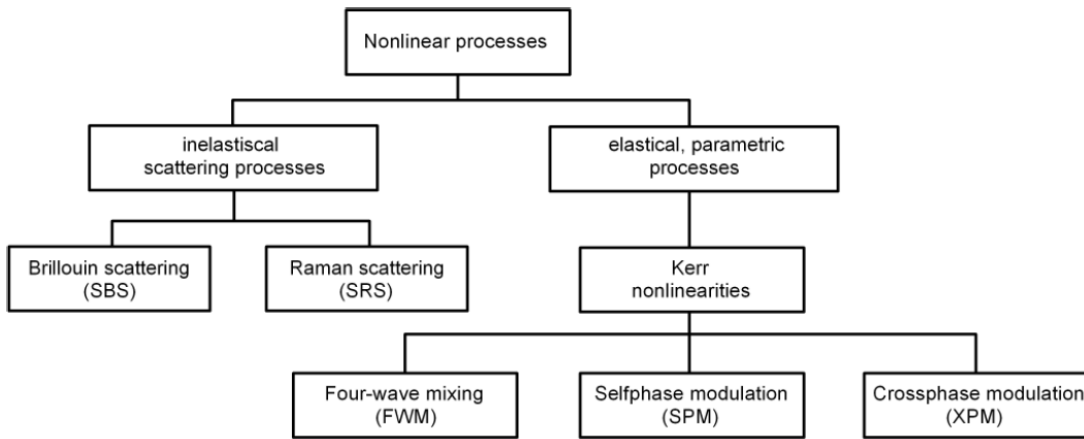


Figure 2-5: Nonlinear processes in optical transmission

Basically, the nonlinear processes can be divided into in-elastic and elastic (parametric) processes (Figure 2-5). The in-elastic processes are dependent on the imaginary part of $\chi^{(3)}$ and become evident above some specific power threshold level. The elastic processes known as Kerr nonlinearities are characterized by the dependence on the real part of $\chi^{(3)}$. The Kerr nonlinearities are self-phase modulation (SPM), cross-phase modulation (XPM), four-wave mixing (FWM) as well as intra-pulse processes such as intra-channel four-wave mixing (IFWM) and intra-channel cross-phase modulation (IXPM), which become important at increased channel bit rates. Stimulated Raman Scattering (SRS) and Stimulated Brillouin Scattering (SBS) are inelastic processes.

The propagation of optical fields in dielectric fibers is described by Maxwell’s equations. Considering x -polarized light propagation in z direction the nonlinear Schrödinger equation (NLSE) can be obtained [51]:

$$\begin{aligned} \frac{\partial}{\partial z} A(z, t) = & -\frac{\alpha}{2} A(z, t) + j \frac{\beta_2}{2} \frac{\partial^2}{\partial T^2} A(z, t) + \frac{\beta_3}{6} \frac{\partial^3}{\partial T^3} A(z, t) \\ & - \frac{\gamma}{\omega_0} \frac{\partial}{\partial t} (|A(z, t)|^2 A(z, t)) - j\gamma |A(z, t)|^2 A(z, t) - j\gamma T_R \frac{\partial}{\partial t} |A(z, t)|^2 A(z, t) \end{aligned} \quad 2-32$$

where α represents the fiber attenuation, T is measured with the frame of reference moving with the pulse at group velocity v_g ($T=t-z/v_g$), T_R refers to the slope of the Raman gain, and γ is the nonlinear coefficient of the fiber, $A(z, t)$ is the field amplitude, ω_0 the carrier frequency and $\beta(\omega)$ is the propagation constant given by:

$$\beta(\omega) \approx \beta_0 + \beta_1(\Delta\omega) + \frac{\beta_2}{2}(\Delta\omega)^2 + \frac{\beta_3}{6}(\Delta\omega)^3 \quad 2-33$$

The terms on the left hand side of Equation 2-32 describe the fiber propagation limitations. The first term is the linear attenuation, the second and third describes the group velocity dispersions (GVD) and the last one represents the nonlinear Kerr effect, self-steepening and stimulated Raman scattering (SRS) group. In the following sections, these effects will be further described. The self-steepening is a higher order nonlinear effect, which originates from the intensity dependence of the group velocity [51]. Since it occurs only for ultra-short optical pulses with widths smaller than 1 ps [51], this effect is not considered in this work.

In the next sections from 2.1.2.3.1 to 2.1.2.3.3 the basic idea of the calculations are presented. The detailed calculation can be found in the references. The aim was to show how this calculation can be taken into account in the previously presented (section 2.1.2) Q-factor calculation method. The novelty is as mentioned before that it is assumed that the influence of nonlinearity on to the evolution of the others is very small, i.e., the nonlinearities result in a larger or smaller perturbation around the mean value of a channel. The phenomena under consideration (FWM, XPM, and SRS) are treated as statistically independent, and their overall contribution to the Q-factor is approximated by a Gaussian variable. Also the calculation of each effect noise variance is not a trivial task.

2.1.2.3.1 Calculation of XPM

When two or more optical fields having different wavelengths propagate simultaneously inside a fiber, they interact with each other through fiber nonlinearity. The fiber nonlinearity can couple two fields through cross-phase modulation (XPM) without inducing any energy transfer between them. Cross-phase modulation is always accompanied by self-phase

modulation (SPM) and occurs because the effective refractive index seen by an optical beam in a nonlinear medium depends not only on the intensity of the beam but also on the intensity of other co-propagating beams [51]. Since the XPM has twice higher impact onto the signal quality than the SPM [51] thus in this work the effects of SPM are neglected.

The impairment due to XPM can be expressed as XPM-induced noise. It is caused by high-power co-propagating wavelengths which introduce a slight phase shift of the pulses edges in the channel of interest. While the phase-to-intensity (PM/IM) conversion, induced through GVD by a phase modulation present at the input of the fiber, can be perfectly undone by a compensating fiber, the one induced by XPM components generated away from the input cannot be perfectly compensated, and the resulting residual intensity distortion impairs the performance of intensity modulated, direct detected systems. Such intensity distortion has been mostly studied by means of computer simulations, because the nonlinear Schrödinger equation is not analytically solvable for general pulses when both the nonlinear and the dispersive terms are present. Simulations involving XPM are almost prohibitively time consuming, because they require the propagation of all the WDM channels. The key idea is the following based on [52]. The XPM at the end of the link is the sum of the XPM contributions generated in each infinitesimal fiber segment. Each infinitesimal XPM contribution gives an infinitesimal intensity distortion by PM/IM conversion at the end of the link. Here we also assume that such infinitesimal contributions add up to give the total output intensity distortion. The noise variance coming from XPM, at i^{th} channel, σ_{XPMi} , can be calculated as follows [52]-[53]. Here the novelty was the equation 2-34 and 2-35 where from the XPM transfer function it is able to calculate the noise variance due to XPM:

$$\sigma_{XPMi}^2 = \sum_{j \neq i} \sigma_{XPMij}^2 \tag{2-34}$$

where σ_{XPMi}^2 the noise variance square due to XPM at i^{th} channel. σ_{XPMij}^2 is given by the following Fourier transform:

$$\sigma_{XPMij}^2 = \frac{1}{2\pi} \int_{-\pi B_0}^{\pi B_0} |H_{XPMij}(\omega)|^2 \cdot S_j(\omega) d\omega \tag{2-35}$$

where ω is the angular frequency, H_{XPMij} is the transfer function of the crosstalk at the i^{th} channel coming from channel j^{th} and S_j is the spectral density of the j^{th} channel B_0 is the optical bandwidth. H_{XPMij} can be calculated with the following expression:

$$H_{\text{XPM}_{ij}}(\omega) = 4\gamma_i P_i(0) e^{-\alpha L} e^{-j\omega L/v_g L} \frac{1}{a^2 + b^2} [a \sin(\beta L) - b \cos(\beta L) + b e^{-\alpha L}] \quad 2-36$$

where γ_i is the nonlinear index of the fiber for the i^{th} channel, $P_i(0)$ is the power of the i^{th} channel at the fiber input. L is the fiber length, v_g is the group velocity in the fiber and a and b is given by the following expression:

$$a = \alpha - j\omega d_{ji} \quad 2-37$$

$$b = \omega^2 D_i \lambda_i^2 / (4\pi c) \quad 2-38$$

where d_{ji} is the walkoff parameter, β is the propagation constant, D_i is the dispersion coefficient of the i^{th} channel. The spectral density of the signal (S_j) assuming NRZ modulation is:

$$S_j = \left(\frac{P_j}{2}\right)^2 \frac{1}{T_b} |G(\omega)|^2 \quad 2-39$$

where T_b is the bit time and $G(\omega)$ in case of rectangular pulse is given by the following expression.

$$G(\omega) = T_b \frac{\sin(\omega T_b / 2)}{\omega T_b / 2} \quad 2-40$$

2.1.2.3.2 Calculation of FWM

Four-wave mixing is a further development of the Kerr nonlinearity in DWDM transmission systems, the occurrence of which requires three co-propagating waves A_j , A_k and A_l on considerable power levels. Then, the third-order susceptibility $\chi^{(3)}$ causes nonlinear polarization of the waveguide material, resulting in a transfer of optical power to the mixing frequencies $\omega_i = \omega_j + \omega_k - \omega_l$, $j, k \neq l$. It is possible to get de-generated four-wave mixing with two channels as well. In this case the generated frequency will be $\omega_i = 2\omega_j - \omega_k$. In DWDM systems with equidistant spectral channel separation, these newly generated frequencies interfere with existing carriers, causing crosstalk.

The crosstalk power P_{jkl} in a piece of fiber of length L can be approximately derived by use of the multi-channel NLSE (equation 2-32), whose GVD, SMP, XPM and SRS terms have been discarded. Just the terms for fiber attenuation and FWM remain.

The noise variance due to FWM, σ_{FWM_i} , can be calculated as follows [54]-[55]:

$$\sigma_{FWMi}^2 = 4PP_{FWMi} \frac{B_e}{B_o} \quad 2-41$$

where P is the average channel power inserted into the fiber, B_e and B_o are the electrical and optical bandwidth respectively and

$$P_{FWMi}(L) = \sum_{\substack{j+k-l=i \\ j,k \neq l}} P_{jkl}(L) \quad 2-42$$

Where j, k, l the channel numbers causing the noise and i is the channel which is disturbed, L is the length of the fiber.

$$P_{jkl}(L) = (d_{jkl} \xi_{pol} \gamma_i)^2 \frac{(1 - e^{-\alpha L})^2 + 4e^{-\alpha L} \sin^2(\Delta\beta_{jkl} L / 2)}{\alpha^2 + \Delta\beta_{jkl}^2} P^3 e^{-\alpha L} \quad 2-43$$

where

$$d_{jkl} = \begin{cases} 1 & j = k \\ 2 & j \neq k \end{cases} \quad 2-44$$

ξ_{pol} is the polarization factor which in our case is 1, γ_i is the nonlinear coefficient and α the attenuation of the fiber,

$$\Delta\beta_{jkl} = \frac{2\pi\lambda_l^2}{c} |j-l||k-l| \Delta f^2 \left[D(\lambda_l) + \frac{\lambda_l^2}{2c} (|j-l| + |k-l|) \Delta f \frac{dD(\lambda_l)}{d\lambda} \right] \quad 2-45$$

where c is the speed of light in vacuum, Δf is the channel spacing, D is the dispersion coefficient and λ_l is the wavelength of channel l_{th} .

2.1.2.3.3 Calculation of SRS

In multi-wavelength optical transmission systems employing silica fiber, any monochromatic pump wave (i.e. wavelength channel) experiences inelastic scattering by molecular vibrations. Any longer-wavelength channels, if present, are amplified coherently, causing the depletion of the pumping shorter-wavelength channels. Due to the fact that optical signals are modulated by random sequences, this power transfer shows statistical behavior. This statistical behavior according to [56]-[57] can be derived to a noise fluctuation σ_{SRSi} and to a mean value μ_{SRSi} changing.

$$\mu_{\text{SRSi}} = e^{\frac{\mu_x + \sigma_x^2}{2}} \text{ and } \sigma_{\text{SRSi}} = \mu_x^2 (e^{\sigma_x^2} - 1) \quad 2-46$$

where:

$$\sigma_x^2 = \sum_{j \neq i} \sigma_{xji}^2 \text{ and } \mu_x = \sum_{j \neq i} \mu_{xji} \quad 2-47$$

also:

$$\sigma_{xji}^2 \approx \frac{1}{8\pi T_b} \int_{-\infty}^{\infty} |Q_{ji}(\omega)|^2 d\omega \text{ and } \mu_{xji} = \frac{Q_{ji}(0)}{2T_b} \quad 2-48$$

where i and j are the interacting channels, T_b the bit time, $Q(\omega)$ the Fourier transform of the signal power coming from SRS, in case of NRZ modulation:

$$Q_{ji}(\omega) = K'(j-i) |P_j(\omega)| \sqrt{\frac{(1 - e^{-\alpha_j L})^2 + 4e^{-\alpha_j L} \sin^2\left(\omega d_{ji} \frac{L}{2}\right)}{\alpha_j^2 + (\omega d_{ji})^2}} \quad 2-49$$

where $P_j(\omega)$ is the power spectra of the j^{th} channel, j and i are the channel numbers, d_{ji} the channel walkoff ($d_{ji} = 1/v_{gi} - 1/v_{gj} \sim D \cdot (\lambda_j - \lambda_i)$) and:

$$K' = \frac{g'_R \Delta f}{2A_{\text{eff}}} \quad 2-50$$

where g'_R is the Raman-gain slope, A_{eff} is the effective core area of the fiber.

2.1.2.4 Calculation of PMD

In conventional single-mode fibers, birefringence is not constant along the fiber but changes randomly, both in magnitude and direction, because of variations in the core shape (elliptical rather than circular) and the anisotropic stress acting on the core. As a result, light launched into the fiber with linear polarization quickly reaches a state of arbitrary polarization. Moreover, different frequency components of a pulse acquire different polarization states, resulting in pulse broadening. This phenomenon is called polarization-mode dispersion (PMD), Figure 2-6 .

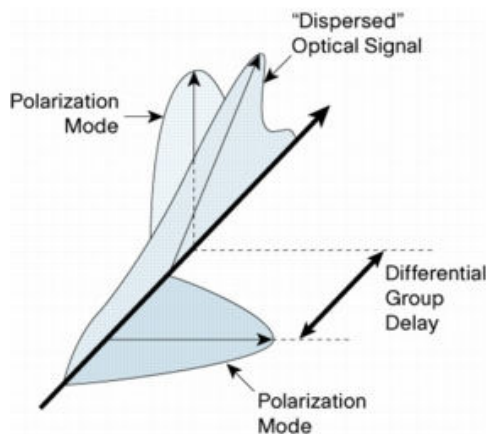


Figure 2-6: Polarization Mode Dispersion

Polarization mode dispersion (PMD) is one of the most important degradation effects in long haul and high data rate transmission systems. It is widely recognized that 40 Gb/s data transmission rates impose very strict requirements on the fiber plant and transmission systems deployed in the field. However, for a data rate of 10 Gb/s the PMD design rules are not so severe, still has to be taken into account. In particular, PMD can be serious limitation on certain fiber links operating at 10 Gb/s [46].

Considering the pulse propagation in the fiber, it can be distinguished between two orthogonal polarization axes called principle states of polarization (PSPs). These axes are not necessarily in the vertical and horizontal planes. In fact, their random orientation depends upon the stresses in the fiber. The light polarized along one of the axes experiences a different refractive index than light polarized along the other axis. This effect is known as birefringence. As the index of refraction is a measure of how fast light moves through the material, the linear-polarized light launched into one principal axis travels through the fiber faster than the light launched into the other axis. It also means that the relative phase of the light in the two axes changes as it propagates along the fiber. This phase difference changes the overall state of polarization (SOP) of the light leaving the fiber [46]. An optical pulse with the polarization aligned with one of the principal axes emerges at the fiber output in the same state of polarization without any PMD impact. For a pulse with randomly oriented polarization, one part of the pulse is transmitted along one of the principal axes, and the other part is transmitted along the other principal axis. The received pulse becomes broadened, because the two parts arrive with a delay time $\Delta\tau$, called differential group delay (DGD) (Figure 2-6). The total pulse broadening due to PMD can be estimated from the time delay $\Delta\tau$ between the two polarization components (Figure 2-6). In a fiber with length L , the DGD is given by [46]:

$$\Delta\tau = \left| \frac{L}{v_{gx}} - \frac{L}{v_{gy}} \right| = L |\beta_{1x} - \beta_{1y}| = L\Delta\beta_1 = L \frac{\omega\Delta n_g}{c} \quad 2-51$$

where x and y are the two orthogonal polarized fiber modes and $\Delta\beta_1$ is group delay difference related to the fiber birefringence. The DGD between the polarization states in a non-polarization preserving fiber is a random variable, with a mean value $\langle\Delta\tau\rangle$. The time-averaged DGD between the two orthogonal SOPs in a fiber can be defined as:

$$\langle\Delta\tau\rangle = D_{PMD}\sqrt{L} \quad 2-52$$

where D_{PMD} stands for the fiber PMD parameter, measured in [ps/km^{1/2}], and L is the fiber length. Typical values of D_{PMD} are in the range of 0,1 to 1 [ps/km^{1/2}], although in old fibers D_{PMD} larger than 1 [ps/km^{1/2}] can occur. Nowadays, fiber manufactures offer fibers with D_{PMD} smaller than 0.05 [ps/km^{1/2}].

Several methods have been proposed in literature for the PMD induced penalty. The most widely accepted is the separate calculation of DGD, from other effects, as presented in [4] or [19]. The problem with these methods is that it excludes the other effects such as noise or nonlinearities. In this thesis the effects of the PMD are taken into account by investigating the influence of PMD on the Q-factor. In such a way it is possible to simultaneously handle the noise related effects and PMD.

Any DGD between the PSPs distorts the optical pulses and gives rise to inter-symbol interference (ISI), which manifests in reduced receiver eye-opening. Therefore, PMD-induced performance degradation in IM-DD transmission systems is assessed by an eye-opening penalty along the lines according to [58]. This eye-opening penalty (EOP) is subsequently translated to a Q-factor penalty. Based on the work published in [59] the EOP can be calculated as follows:

$$EOP_{dB} \approx A(\Delta\tau/T_b)^2 \gamma(1-\gamma) \quad 2-53$$

where EOP_{dB} is the eye-opening (or closure) penalty in dB. A is the pulse form factor which is 21,4 in case of NRZ rectangular pulses [59], $\Delta\tau$ is the DGD in [s] due to PMD and γ is the power distribution factor.

This approximation considers first-order PMD only, i.e. DGDs are way smaller than the bit period ($\Delta\tau \ll T_b$). The PMD-induced instantaneous DGD (and thus the instantaneous EOP) varies with changing environmental conditions. Measurements show that the instantaneous DGD behaves according to a Maxwellian probability density function (PDF).

If defining DGD excursions beyond to a given limit as outage, then the Maxwellian PDF allows to formulate an outage probability (OP) due to the tail of the distribution beyond a certain threshold. This interrelation has been formulated by [59] in order to yield an OSNR penalty. Here, an intermediate result of their calculation is used where the Q-factor penalty can be identified by inspection.

Considering the DGD PDF reported in [61]:

$$pdf(\Delta\tau) = \frac{32}{\pi^2} \frac{\Delta\tau^2}{\langle\Delta\tau\rangle^3} e^{-\frac{4}{\pi}(\Delta\tau/\langle\Delta\tau\rangle)^2} \tag{2-54}$$

For this Maxwellian-distributed instantaneous DGD $\Delta\tau$ and random power splitting, the PDF of the EOP is found to be negative-exponentially distributed [59]:

$$pdf(EOP_{dB}) = \eta \cdot e^{-\eta \cdot EOP_{dB}} \tag{2-55}$$

where

$$\eta = \frac{16}{A \pi \langle\Delta\tau\rangle^2 B^2} \tag{2-56}$$

By transformation of equation 2-55 from logarithmic to linear scale,

$$pdf(Y) = pdf_{EOP_{dB}}(f^{-1}(Y)) \left/ \frac{d}{dEOP_{dB}} \right. f(f^{-1}(Y)) \tag{2-57}$$

where Y eye opening (or closure) due to PMD effects

$$Y = f(EOP_{dB}) = 10^{\frac{EOP_{dB}}{10}} \tag{2-58}$$

$$EOP_{dB} = f^{-1}(Y) = 10 \cdot \log_{10} Y$$

the PDF of the eye closure Y is obtained, which is in turn transformed to the PDF of the Q-factor by making use of the fact that the eye closure reduces the Q-factor:

$$Q \approx Q_{ASE} / Y \tag{2-59}$$

$$pdf(Q) = \begin{cases} \frac{10}{\ln 10} \eta / Q \cdot (Q_{ASE} / Q)^{-\frac{10}{\ln 10} \eta} & 0 \leq Q \leq Q_{ASE} \\ 0 & elsewhere \end{cases}$$

where Q_{ASE} is the baseline Q-factor due to ASE or other noise sources.

The outage probability OP , as mentioned above, determines to which probabilistic extent the maximum tolerable instantaneous DGD $\Delta\tau_{max}$ is exceeded:

$$OP = \int_{\Delta\tau_{max}}^{+\infty} pdf(\Delta\tau)d\Delta\tau \tag{2-60}$$

$$= \int_0^{Q_{min}} pdf(Q)dQ \tag{2-61}$$

$$= (Q_{min} / Q_{ASE})^{\frac{10}{\ln 10} \eta} \tag{2-62}$$

Where Q_{min} is the minimal acceptable Q-factor considering both noise related effects and PMD.

Solving equation 2-62 for $QP_{PMD} = Q_{min} / Q_{ASE}$ yields the desired PMD-induced Q-factor penalty as a function of the outage probability OP :

$$QP_{PMD} = OP^{\frac{\ln 10}{10} \frac{A\pi \langle \Delta\tau \rangle^2 B^2}{16}} \tag{2-63}$$

where QP_{PMD} is the Q-factor penalty due to PMD, B is the bit rate.

The novelty of the method is that based on the previously presented calculation, while knowing the Q-factor when just the noise related effects are taken into account, and an accepted outage probability, the Q-factor for both the PMD and noise can be obtained.

2.1.3 Validation of the calculation

The calculation method presented in previous section 2.1.2 is a highly complex method using several sub-calculations. The validation of it is a difficult task. As first step the calculation presented for ASE and PMD was compared with the results obtained with commercially available software VPI Transmission Maker [62] where very similar results were obtained. In case of nonlinearities this is not possible since in case of higher total power where the nonlinearities have influence (> 18 dBm) the calculation time increases drastically (upto several weeks even months). Here I compared the optimal signal power (see section 2.2) using the previously presented method, and the commercially available products EDFA output power like the Cisco and Huawei ones. Here I again found very good match. The results for nonlinearities were also compared with the results of commercially available simulation

softwer Optisystem [63] in case of CWDM systems where the calculation time is much less than in case of DWDM systems. Figure 2-7 shows the simulation results compared to the calculation results of the model for 60 km fiber length. The aim of this comparison was to find the maximum Q-factors. The OptiSystem simulation results show the maximums such as the calculation results. The powers of the maximums are nearly equal in the two cases. As it is to be seen there is a good correspondence between the estimated progresses of the two graphs. The Q factor calculation by OptiSystem for power values over 26 dBm was impossible, as well as the calculation for higher fiber lengths than 60km. These calculations require an incredible amount of time, one more point in the 60km case requires about 1 week of running. The results were published in [64].

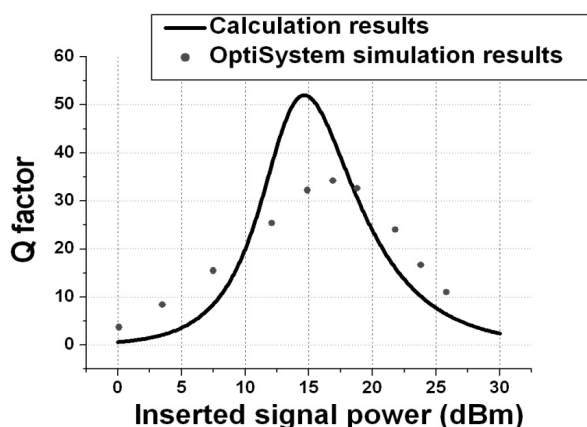


Figure 2-7: Comparison of the calculation results and the OptiSystem simulation results

Also these calculations were used in [65][66][67] where the analytical results were compared with real measurements and also with simulations. The data from the Table 2-1 were obtained from a cooperation study between BME and Magyar Telekom [65]. The M1-M8 means the names of the measuring points. In these points the analytical, the VPI simulation and the experimental data were compared. As it is to be seen, the results match very well except from the M6 point where the dispersion was not compensated. It was a total 700ps/nm dispersion. At this point the analytical calculation and the simulations matched well but not with the experiment measurements. Finally we have investigated this problem and it turned out that the measuring equipment was wrong and the calculations and simulations gave the correct results.

| | M1 | M2 | M3 | M4 | M5 | M6 | M7 | M8 |
|-------------------|-------|-------|-------|-------|-------|-------------------|-------|-------|
| Analytical | 25,64 | 27,82 | 28,73 | 29,07 | 32,54 | 29,97 +700ps = 10 | 27,94 | 27,15 |
| Simulation | 27,78 | 23,43 | 30,8 | 29,7 | 32,76 | 10,52 | 26,02 | 29,5 |
| Experiment | 31,93 | 26,01 | 30,35 | 32,7 | 29,89 | 22,12 | 25,82 | 24,19 |

Table 2-1: Analytical, simulation and experimental data comparison.

As conclusion the presented analytical calculation method for Q-factor estimation gives accurate results for systems up to 10Gb/s channel bit rate OOK modulation and direct detection, i.e. the nowadays mostly deployed systems.

It is also very important to distinguish between the influences of different optical effects considering different network scenarios. For example in access networks the dominant physical constraint is the insertion loss, however in case of metro or long haul networks besides the insertion loss other physical effects have to be taken into account as well. Since in this dissertation the focus is on the metro and long haul networks it is important to investigate which physical effects are important in these networks. In both cases the most important effect is the noise; however the origin is changes in the two cases. In case of metro networks the crosstalk (XT) in the optical nodes has high impact. In lack of dispersion mapping the nonlinear interaction is also important.

In case of long-haul networks despite the accurate dispersion mapping, due to high signal power the nonlinear interaction is also very important. In this case the dispersion distortions have high impacts. Since the polarization mode dispersion (PMD) depends from the length of the optical links, this also has high influence onto the signal quality. Considering the chromatic dispersion, due to the several inline compensation points, the residual dispersion can be high enough not to be considered as a neglecting effect.

As conclusion, the main degrading effect in both cases is the amplifier noise. In case of metro networks the XT and the nonlinearities are important, in case of long-haul networks the nonlinearities the PMD and the residual dispersion is important, besides the ASE noise from the amplifier.

2.2 Claim 1.2: Calculation of optimal signal power for WDM optical networks

Claim 1.2: "I have calculated for different network scenarios the optimal signal power for intensity modulated direct detection 10 Gbit/s point-to-point wavelength division multiplexed optical systems."

In Claim 1.1, a model to calculate analytically the signal quality deterioration due to physical impairments was presented. In claim 1.2, based on simple network scenario and the method mentioned before, the exact value of the optimal signal power is calculated. As a result the exact values are given for the optimal signal power at the transmitter point, or at the output of the inline amplifiers for 10 Gbit/s WDM-OOK-DD systems.

2.2.1 Introduction

In the last twenty years the WDM technology had an incredible evolution. Nearly all physical effects can be compensated in an all-optical way. The only effect that cannot be compensated is the noise. Clearly there are techniques to decrease the noise distortion such as bandwidth filters, however the total eraser is very difficult to be done all-optically. Thanks to technology evolution low-noise amplifier techniques have appeared, such as Raman or parametric amplifiers, or even EDFA and SOA with low noise figures. The crosstalk of the nodes is drastically decreasing as the technology evolves and the noise of the transmitters can be very low as well.

The only phenomena that still limit the optical networks are the nonlinear effects. Although, there are optical fibers with low nonlinear coefficients, it is commercially nearly impossible to replace the already deployed fibers with new ones. The only solution is to maximize the signal power inserted into the optical fiber. To increase the size of optical networks the maximization of the signal power is needed. Moreover, the nonlinear effects highly depend on the network bit rate. While increasing the bit rate from 2.5 Gbit/s to 10 or 40 Gbit/s or even higher the maximally allowed signal power in one optical fiber is decreasing and therefore the size of the all-optical network is decreasing as well.

Nowadays in case of optical networks system designers have very strict rules regarding the optical power inserted into optical fibers in order not to reach the nonlinear region of them. A model of the nonlinear behavior would lead to a more accurate system design. Using the proposed scheme it is possible to determine a signal power range where the signal quality deterioration due to nonlinear effects is tolerated. This way it is possible to maximize the

signal power used in optical fibers, to increase the size of the optical network or to minimize the number of inline amplifiers. It has to be mentioned that there are other existing techniques like the use of other modulation formats, or dispersion mapping which decrease the influence of nonlinearities onto the signal quality [68]-[70]. Best results can be reached combining these techniques and maximizing the signal power.

Using the model presented in section 2.1.2 it is possible to calculate the optimal signal powers of the transmitters and inline amplifiers in typical optical networks. The emphasis for network designers is to give the maximum signal power which can be used for different network scenarios. The results are also compared with the Brillouin threshold.

2.2.2 Model description

In Figure 2-8 the used model is depicted. The goal of the calculation was to increase the total power at point P after the EDFA and calculate the signal quality at point Q. In this way the optimal signal power for a point-point WDM optical network can be obtained.

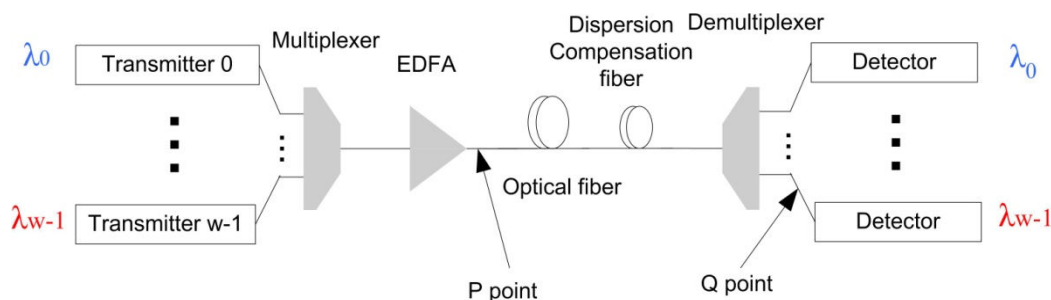


Figure 2-8: Model used for calculating the optimal signal powers in WDM optical networks

The results can be extended to multiple amplified systems since the optimal signal power will not change in case of using more EDFAs, only the signal quality will decrease. To demonstrate the effects of nonlinearity onto the signal quality, ideal transmitters and receivers were assumed. The idea behind it was that in case of low signal power where the impact of nonlinearity onto the signal quality is negligible a noisy transmitter-receiver would lead to false results. The crosstalk from the mux-demux was also neglected. Table 2-2 contains the main parameters of the model.

| Symbol | Quantity | Value |
|-------------|--------------------------------------|--------------------------------|
| B_o | Optical bandwidth of the receiver | 40 GHz |
| B_e | Electrical bandwidth of the receiver | 7 GHz |
| f_b | Bit rate | 10 Gbit/s |
| S | Dispersion slope | 0.085 ps/(nm ² km) |
| D | Dispersion coefficient | 17 ps/(nm km) |
| λ_o | Highest channel wavelength | 1550 nm |
| c | Speed of light | 300,000 km/s |
| α | Attenuation coefficient | 0.21 dB/km |
| γ | Nonlinear index | $1.18 \cdot 10^{-3}$ 1/(Wm) |
| NF | EDFA noise figure | 4.5 dB |
| R | Responsivity of the photo detector | 1 |
| g_R | Raman gain slope | $7.482 \cdot 10^{-27}$ m/(WHz) |
| A_{eff} | Effective core area | 80 μm^2 |

Table 2-2 Main parameters of the optical system

2.2.3 Results

As mentioned in previous section, I increased the signal power inserted in the optical fiber and determined the signal quality at the receiver side. I also compared the signal quality for each nonlinear effect with the signal quality obtained when only the ASE noise is taken into

consideration. As it was expected while increasing the gain of the amplifier the ASE noise is increasing which leads to a decreased OSNR. This results in a decreased signal quality when only the ASE is taken into account. See in Figure 2-10 - Figure 2-15, the solid line marked with *ASE*. In these figures the total input power inserted in the fiber is plotted versus the Q-factor. It was mentioned before that I use ideal transmitters and receivers which means that the receiver sensitivity is infinite. The curve corresponding to ****+ASE* means the respective nonlinear effect and the effects of ASE onto the signal quality, where ***** is the corresponding nonlinear effect. *XPM* means the cross-phase modulation, *FWM* means the four-wave mixing and *SRS* means the stimulated Raman scattering. The curves signed with *TOTAL* were obtained when all the nonlinear effects were taken into account.

In the next section, I present the results obtained for channel spacing of 50 and of 100 GHz and for different fiber lengths and different channel numbers. The highest wavelength means the channel with wavelength 1550 nm. The lowest and medium wavelengths are changing for every calculation, depending on the channel spacing and channel number used. In Figure 2-9 I plotted the spectra of the channels and indicated the channel numbers for 16 channels. Of course, in case of 80 channels the enumeration goes to 79 instead of 15. All these results were published in [47].

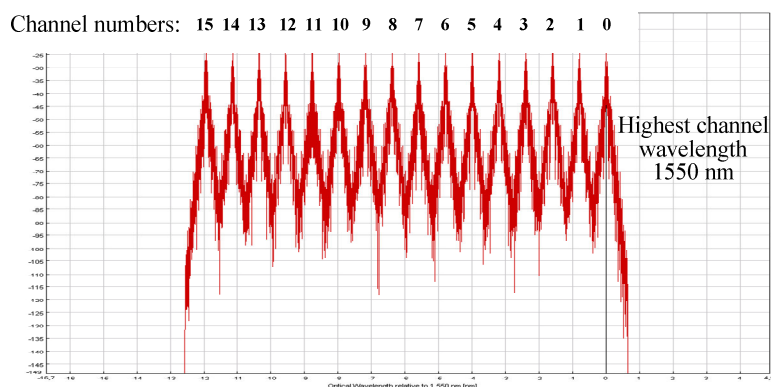


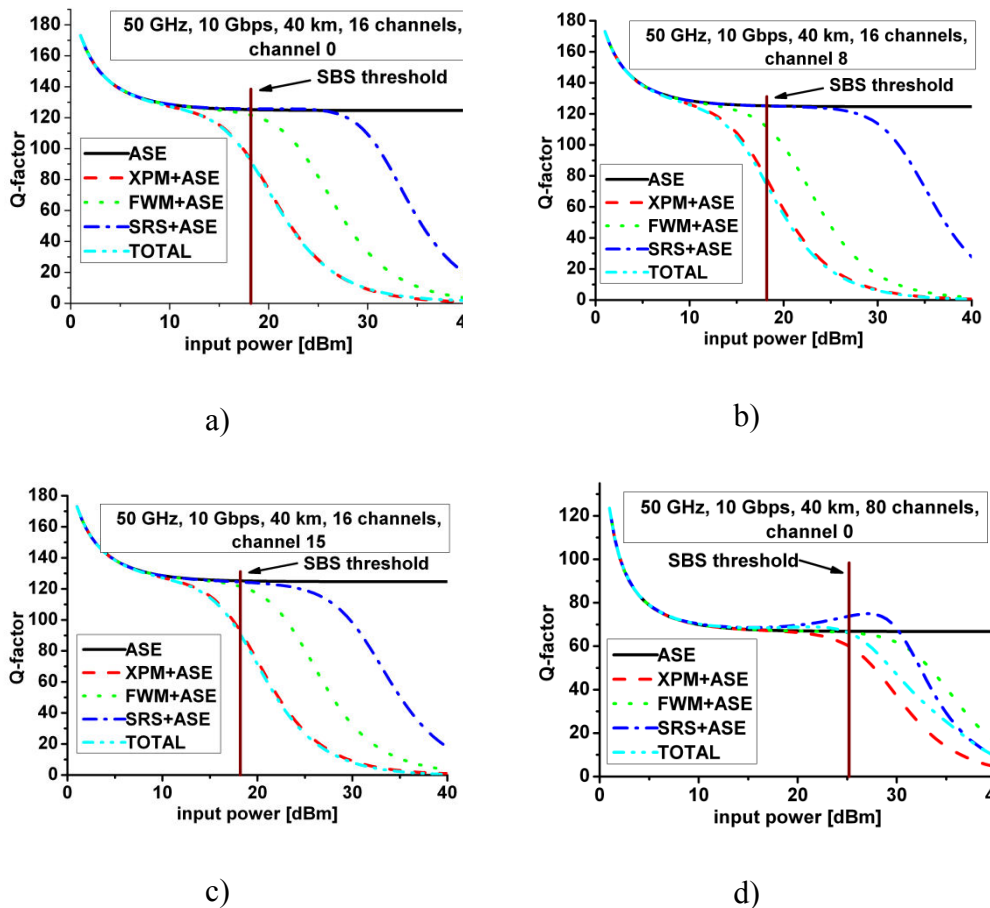
Figure 2-9: Number of channels

2.2.3.1 50 GHz channel spacing

From Figure 2-10 to Figure 2-12, the results are presented for 50-GHz channel spacing. In Figure 2-10 the results for 40-km fiber length are plotted. In Figure 2-10-a the results obtained for the highest channel using 16 channels are plotted. As it is to be seen the SRS has lower impact than the FWM and the main constraint is the XPM for this network scenario. As it is to be seen the *TOTAL* curve is nearly the same as the *XPM* curve. For the medium channel, Figure 2-10-b, I got nearly the same results except for the FWM. This is due to the fact that

more parasite signals appear on the center wavelengths, than on the peripheral ones. A little change can be observed on the XPM curve, too. This is because XPM has stronger impact in case of more neighboring channels i.e., in middle wavelengths. Figure 2-10-c is nearly the same as the Figure 2-10-a. This is the consequence of the fact that Raman scattering is negligible when using 16 channels. In Figure 2-10 d-e-f, results for 80 channels are plotted. As can be seen there is a significant difference between results obtained for 16 channels. In Figure 2-10, channel for 0, the XPM is still the most dominating effect. Raman scattering has very interesting behavior. The signal power of low frequency channels is increasing thus the signal quality is also increasing. Due to Raman crosstalk, noise is generated which deteriorates the signal quality. These two effects lead to the behavior seen in Figure 2-10-d.

In Figure 2-11 and Figure 2-12 the same results can be seen as those of Figure 2-10 for fiber lengths of 80 and 120 km. In each figure I also plotted the Brillouin threshold. The results are similar to the 40-km case. There is only small signal quality deterioration as I increase the fiber length. This is the result of the longer interaction length between the channels. However, as the nonlinear effects are dominant at high signal power close to the fiber input, the increased fiber length causes a negligible nonlinear distortion.



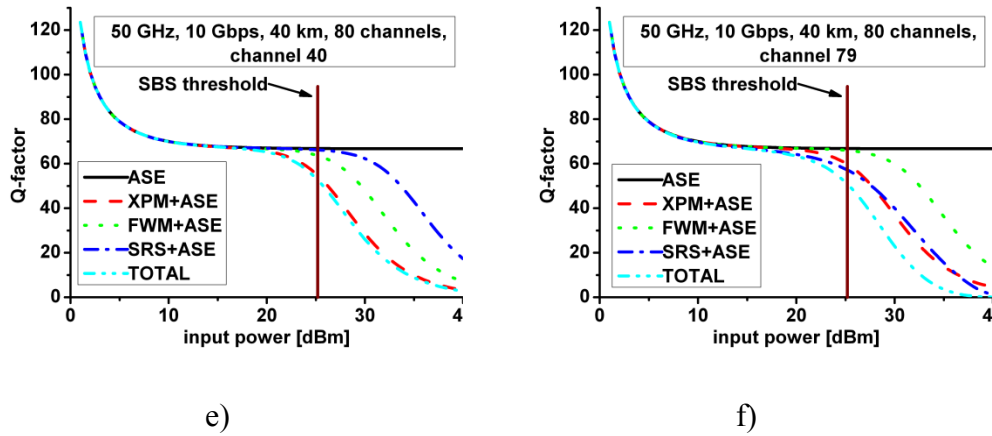
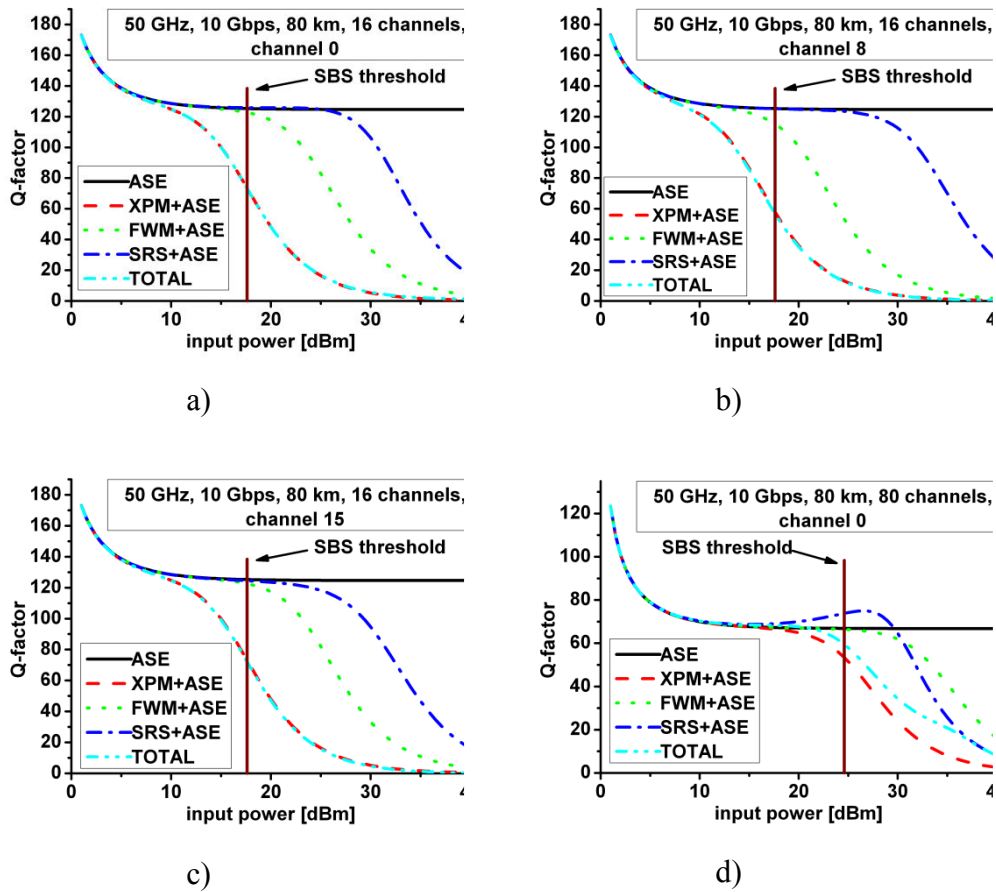
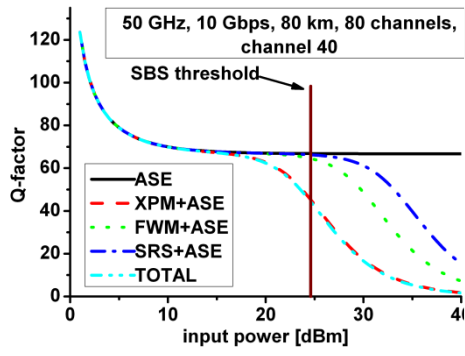
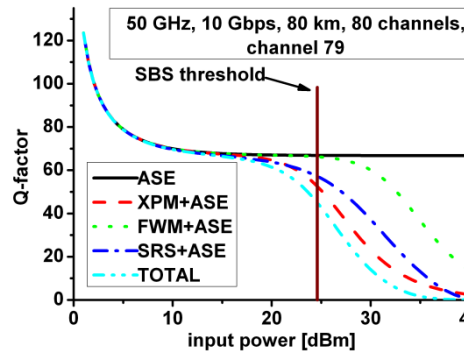


Figure 2-10: Q-factor as function of the input power for a 40-km transmission line using 50-GHz channel spacing taking into account ASE noise and nonlinear effects using 16 channels a) the longest, b) a medium, c) the shortest wavelength channel; using 80 channels d) the longest e) a medium f) the smallest wavelength channel



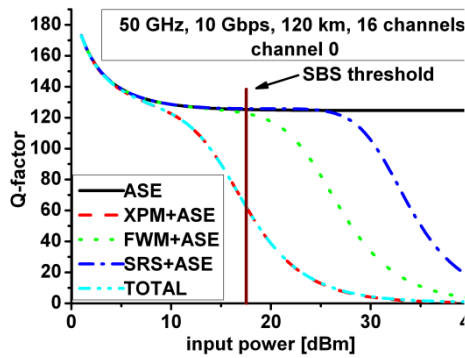


e)

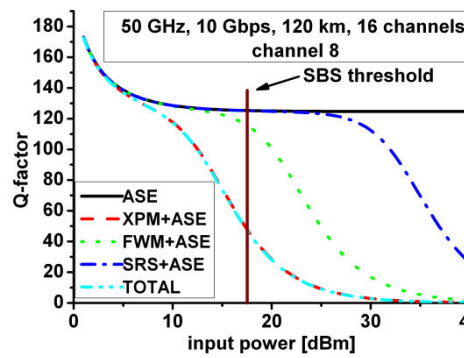


f)

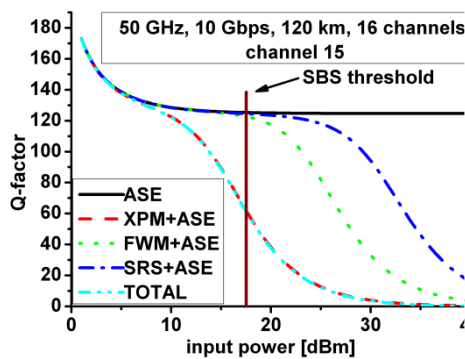
Figure 2-11: Q-factor as function of the input power for a 80-km transmission line using 50-GHz channel spacing taking into account ASE noise and nonlinear effects using 16 channels a) the longest, b) a medium, c) the shortest wavelength; using 80 channels d) the longest, e) a medium, f) the shortest wavelength channel



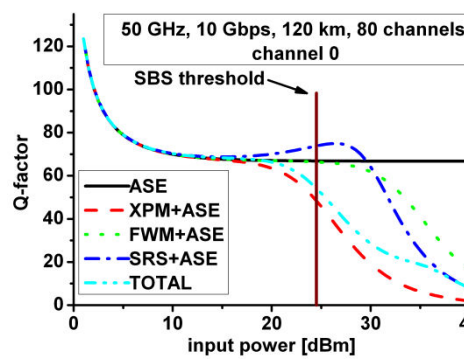
a)



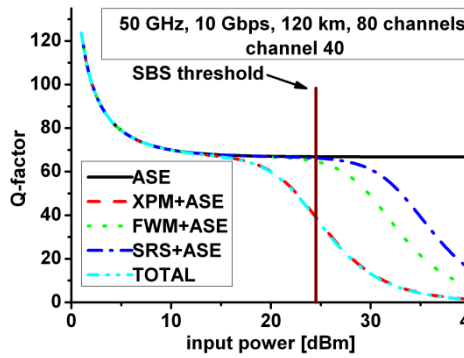
b)



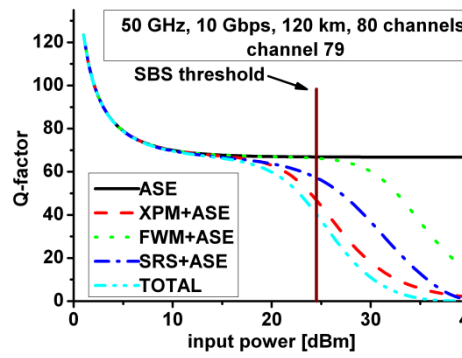
c)



d)



e)



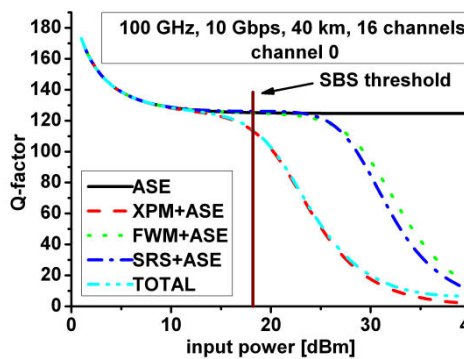
f)

Figure 2-12: Q-factor as function of the input power for a 120-km transmission line using 50-GHz channel spacing taking into account ASE noise and nonlinear effects using 16 channels a) the longest b) a medium c) the shortest wavelength channel; using 80 channels d) the longest e) a medium f) the shortest wavelength channel

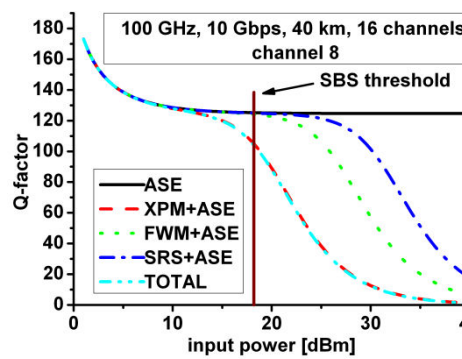
2.2.3.2 100 GHz channel spacing

From Figure 2-13 to Figure 2-15 the results are presented for 100-GHz channel spacing. In Figure 2-13 the results for 40 km fiber length are presented. In case of 16 channels, Figure 2-13 a-b-c, the results are nearly the same as presented for 50-GHz channel spacing. Using 80 channels the increased frequency difference between the high and low wavelength channels increase the Raman effect, so Raman scattering becomes the dominating effect. For the middle channels the XPM is still the dominating effect.

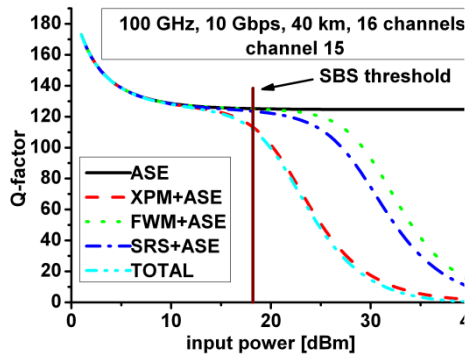
In Figure 2-14 and Figure 2-15 the same results can be seen as in Figure 2-13 for fiber lengths of 80 and of 120 km. A small signal quality deterioration can be observed, for the same reason as for the 50-GHz case.



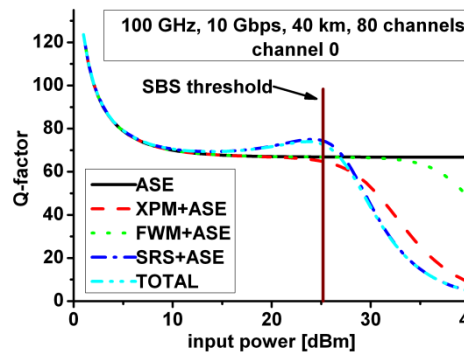
a)



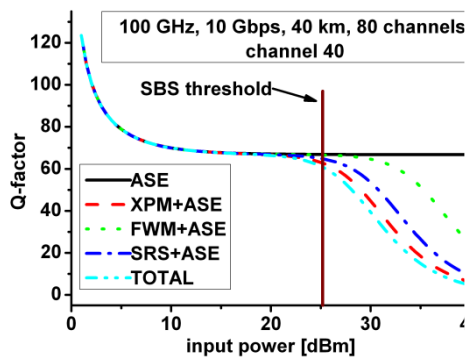
b)



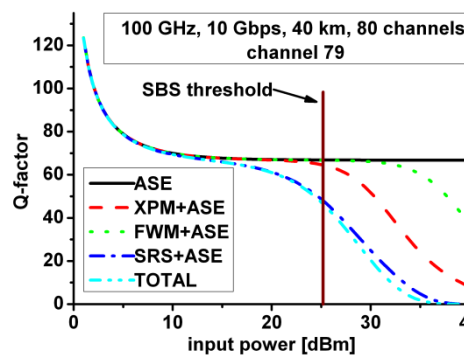
c)



d)

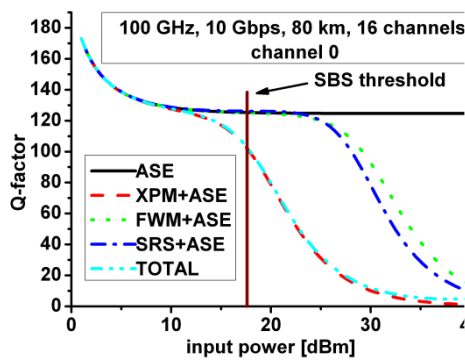


e)

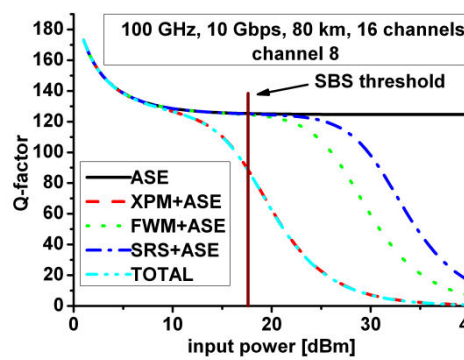


f)

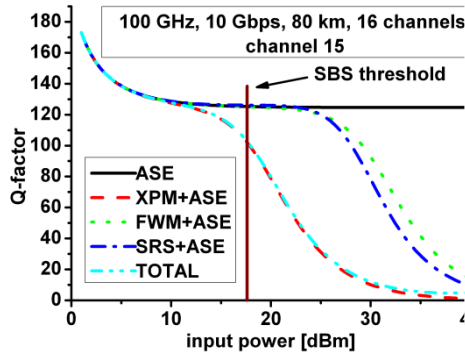
Figure 2-13: Q-factor as function of the input power for a 40-km transmission line using 100-GHz channel spacing taking into account ASE noise and nonlinear effects using 16 channels a) the longest b) a medium c) the shortest wavelength; using 80 channels d) the longest e) a medium f) the shortest wavelength



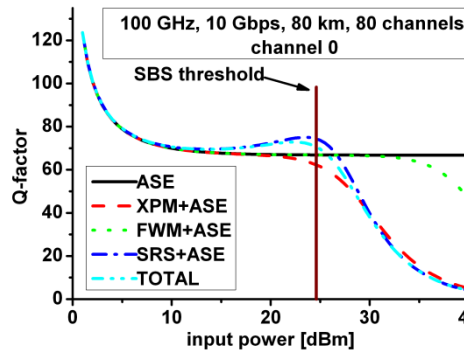
a)



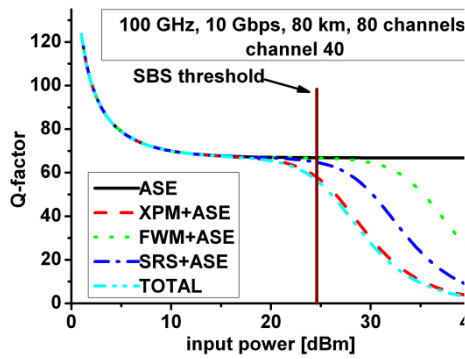
b)



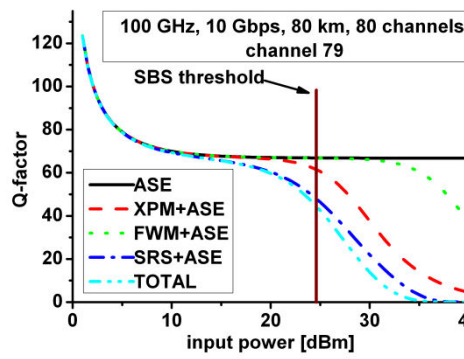
c)



d)

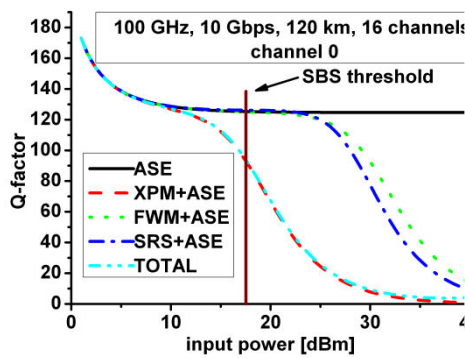


e)

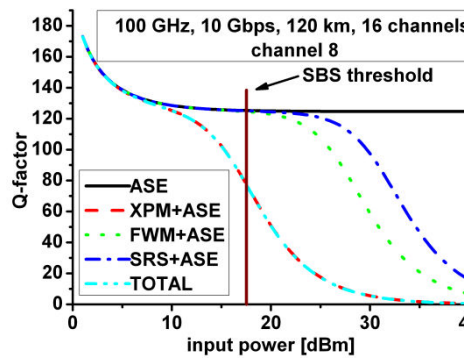


f)

Figure 2-14: Q-factor as function of the input power for a 80-km transmission line using 100-GHz channel spacing taking into account ASE noise and nonlinear effects using 16 channels a) the longest b) a medium c) the shortest wavelength channel; using 80 channels d) the longest e) a medium f) the shortest wavelength channel



a)



b)

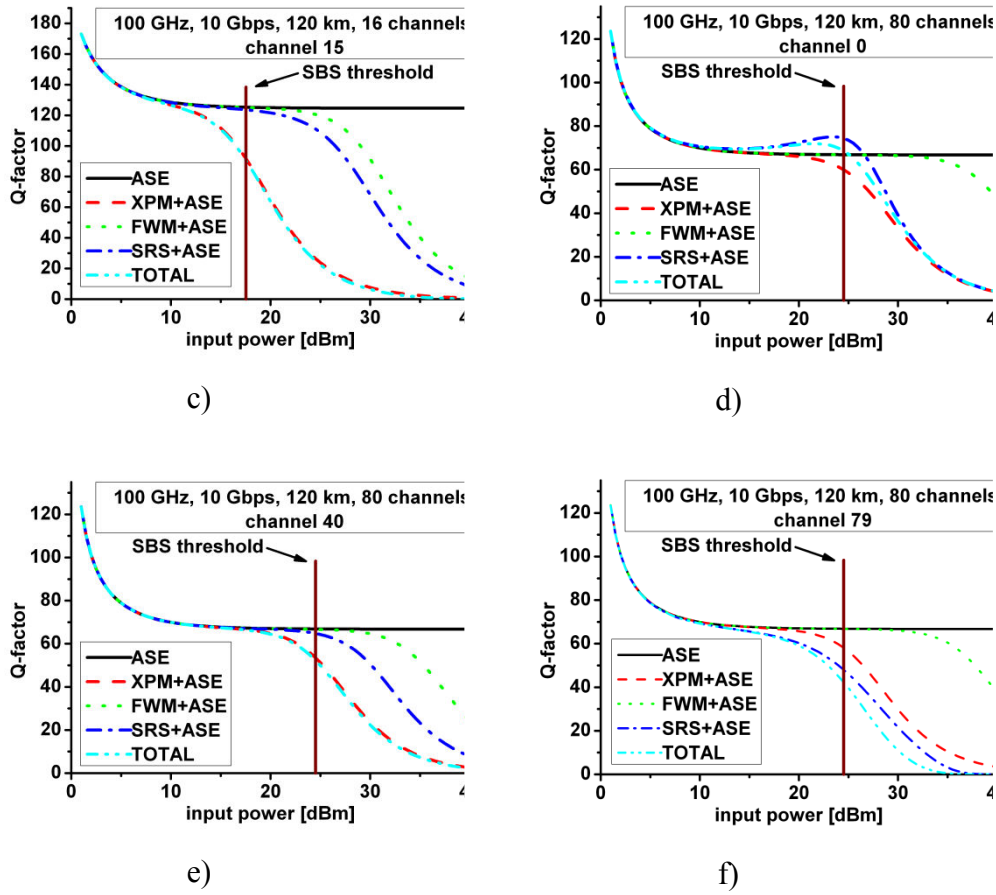


Figure 2-15: Q-factor as function of the input power for a 120-km transmission line using 100-GHz channel spacing taking into account ASE noise and nonlinear effects using 16 channels a) the longest b) a medium c) the shortest wavelength channel; using 80 channels d) the longest e) a medium f) the shortest wavelength channel

2.2.3.3 Optimal signal power versus number of channels

To define the optimal signal power, I introduced the Q-factor penalty of the nonlinear effects. The Q-penalty of the nonlinearities can be obtained as follows:

$$QP = \frac{Q_{ASE}}{Q_{TOTAL}} \tag{2-64}$$

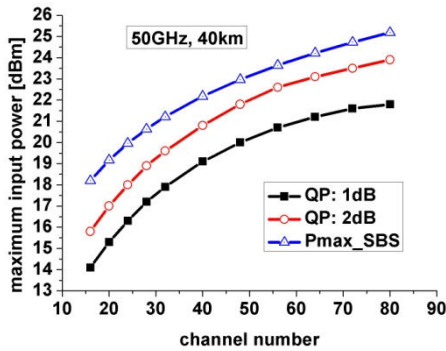
Where Q_{ASE} is the Q-factor when only the ASE is taken into account as described in previous section and Q_{TOTAL} is the Q-factor when the effects of nonlinearities are taken into account besides the effect of ASE.

The QP can be expressed in dB where conversion is:

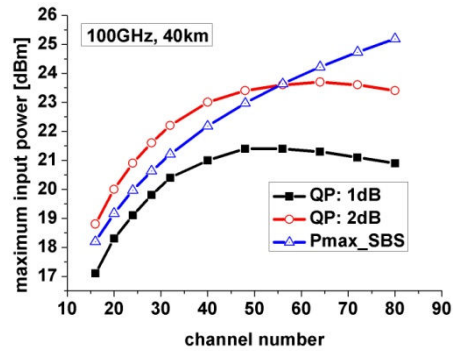
$$QP_{dB} = 20 \cdot \log QP \tag{2-65}$$

I defined for the QP_{dB} two margins, 1 and 2 dB. These are the typical margin values where the influences of the certain physical effects are tolerated. The results can be seen in Figure 2-16. As a comparison I also plotted the curve corresponding to Brillouin threshold. The results were obtained as follows:

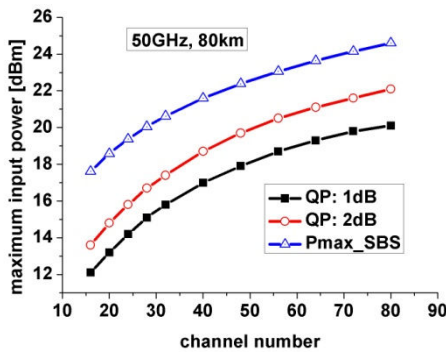
- I calculated the Q-factor of the ASE and the nonlinearities as presented in previous section for different number of channels.
- I took the worst channel and calculated the signal power corresponding to 1 or 2 QP_{dB}



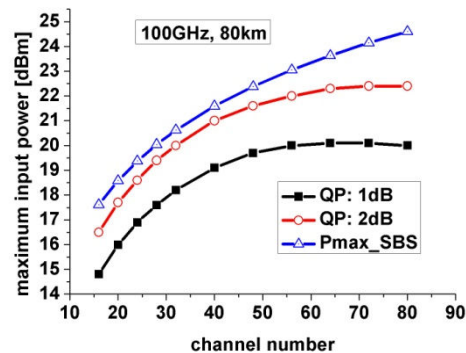
a)



b)



c)



d)

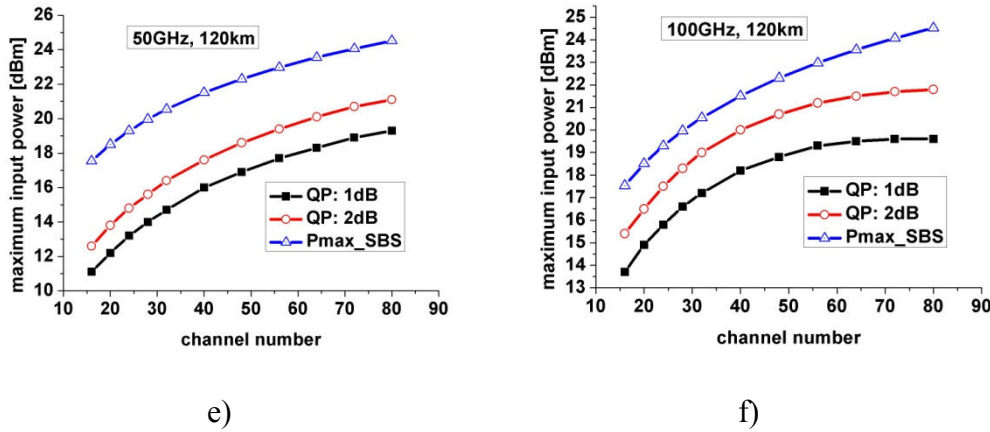


Figure 2-16. Maximum total signal power to avoid the nonlinearities for different number of channels for 40-km fiber length a) 50-GHz channel spacing b) 100-GHz channel spacing; for 80-km fiber length c) 50-GHz channel spacing d) 100-GHz channel spacing; for 120-km fiber length e) 50-GHz channel spacing f) 100-GHz channel spacing

As it is to be seen in nearly all cases the Brillouin threshold has higher values than the maximum allowable signal power corresponding to 1 and 2-dB QP_{dB} .

The other interesting property is that while increasing the channel number the maximum signal power is increasing, too. It has to be mentioned that the maximum signal power means the total signal power inserted into the optical fiber. The results show that the optimum signal power is approximately 12 dBm for 16 channels and about 21 dBm for 80 channels.

2.2.3.4 Maximum communication length

In this section the way to determine the maximum communication length is presented having in mind that a typical detector has -26 dBm receiver sensitivity and the signal quality for error free operation has Q-factor of 9.5. The results show the maximum distance for point-to-point systems where no inline amplifiers are used.

In this case the insertion loss of the dispersion compensation unit (DCU) has to be taken into account. I also assumed that the dispersion coefficient of the DCU fiber is -90 ps/(nm km) and the attenuation coefficient is 0.6 dB/km. The length of the DCU fiber was exactly the same as the length of the optical fiber multiplied by 17/90, to overcome the effects of dispersion at the receiver side. To remember the fiber dispersion coefficient was 17 ps/(nm km) Table 2-2. I also plotted the SBS threshold. It has to be mentioned that the SBS threshold is defined for a single channel. For WDM systems where the number channels is different the SBS threshold will change, as it is to be seen in Figure 2-17. Of course the SBS threshold plotted by a straight line has no physical correspondence. It should be a point at each channel number at a certain input power which gives a position of a horizontal line. Just for better

illustration purpose a straight line was plotted. As it is to be seen in this case when no inline amplifier is used and only the nonlinearities are the limiting factors on an optical link the main constraint is the Brillouin scattering, and the maximum communication length is about 110 km with an input power 20-28 dBm depending on the number of channels.

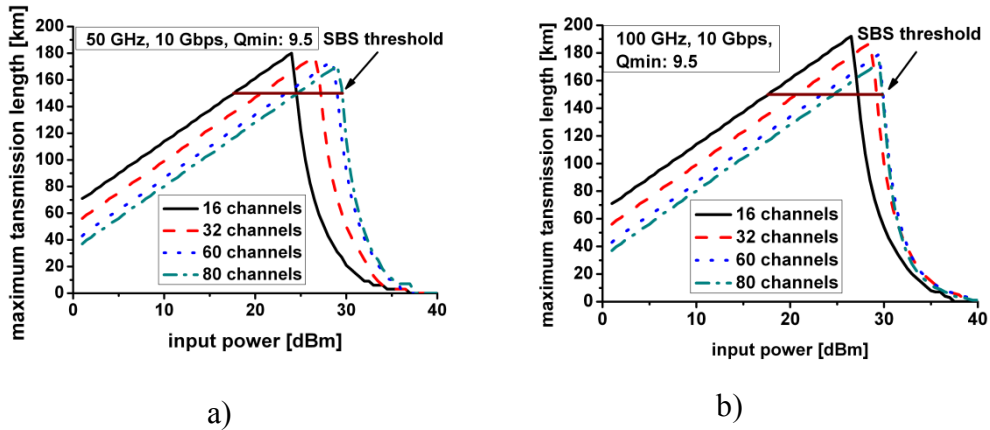


Figure 2-17:. Maximum communication length without inline amplifier

2.2.4 Conclusion

In this section the dependency of the nonlinear effects on the signal power was presented. By analytical calculations the optimal signal powers for different network scenarios were determined. I also demonstrated for different network scenarios what the most limiting nonlinear effects are. I also calculated the maximum connection length based on nonlinear behavior of the optical fibers for point-to-point systems. These results are useful tools for network designers for improving their optical network or even redesigning their power budget.

Chapter 3

Physical impairment based routing

3.1 Claim 2.1: Dynamic IA-RWA algorithm

"I have proposed a novel dynamic IA-RWA algorithm which can take into account the physical constraints of the optical layer considering a multilayer network environment. "

In both, metropolitan optical networks (MON) and long haul optical networks (LHON) the signal quality is often influenced by the physical impairments, therefore a proper impairment based routing decision is needed. In the absence of all-optical 3R regenerators, the quality of transmission has a strong impact on the feasibility of all-optical transmission. It is assumed that signal regeneration can be done only in electrical layer. Once the signal is in electrical layer there are some features supported e.g., the traffic grooming. I have shown, that by taking into account both, the physical impairments characterized by the Q-factor, as I propose in section 2.1.2, and the features of electrical layer, will have a strong impact onto the routing that is based on impairment constraints. The claim 2.1 presents a method for that.

3.1.1 Introduction

IA-RWA may be used in transparent networks as a tool for performance engineering with the goal of choosing feasible paths, while obtaining the optimal routes regarding the RWA problem. As it was mentioned in section 1.3.1, many excellent papers have been written about constraint based routing which obeys physical effects [35]-[39]. The main difference of the proposed model and the already published ones is that, in this case the features of electrical layer can also be taken into account. The other difference is that in this case, the physical effects are modeled in a very complex and accurate way.

There is no doubt, that the near future info-communications will be based on optical networks. In general for networks of practical size, the number of available wavelengths is lower by a few orders of magnitude than the number of connections to be established. The only solution here is to join some of the connections to fit into the available wavelength-links. This is referred to as traffic grooming. The main idea of the optimization is that it is assumed that in the optical layer, there is no signal regeneration, and the noise and signal distortion accumulate along a lightpath. Actually, re-amplification, re-shaping, and re-timing, which are collectively known as 3R regeneration, are necessary to overcome these impairments. Although, 3R optical regeneration has been demonstrated in laboratories, only electrical 3R regeneration is economically viable in current networks.

It was already mentioned that in the electric layer it is possible to do traffic grooming. If we investigate the physical limitations in the optical domain, and take them into consideration,

we will have to include new optical-electrical-optical conversion just to ensure the quality prescriptions. These new optical-electrical-optical conversions will have influence onto the RWA process.

3.1.2 Graph model

Several graph models have been proposed for representing WR networks with traffic grooming capability [72]. The applicability of these models, obviously varies; the one most closely conforming to the demands of this work has been proposed by Cinkler et al. [73][74]. In this work a slightly modified version of it is presented. The adaptation has been done by Szigeti et al. for the purposes of IDRSIM [75] and was presented a little later with some changes in [76]. The purpose of this model is to facilitate the solution of the RWA problem by assigning a graph to a WR network in which path computation algorithms (Dijkstra, Bellman-Ford, Suurballe, etc.) may be used to route calls.

Figure 3-1 illustrates a hybrid node type, used in this work which consists of an OXC and an attached electronic switching and processing layer. Any incoming signal may be forwarded towards an arbitrary output port on the same wavelength. Furthermore, a limited number of signals may be switched towards the electronic layer via dedicated ports of the internal cross-connects. For OXCs, one port is required on internal switch for every port of the OXC. The same applies for the node type being discussed, however, additional ports on internal switches may be connected to the input ports of the electronic layer in order to allow electronic processing. The number of such extra ports determines the number of signals on each wavelength that can be forwarded towards the electronic part of the node: if there are as many extra ports as optical - optical ports, every incoming signal can be processed electronically (in this case, each internal switch has twice as many ports as the node itself).

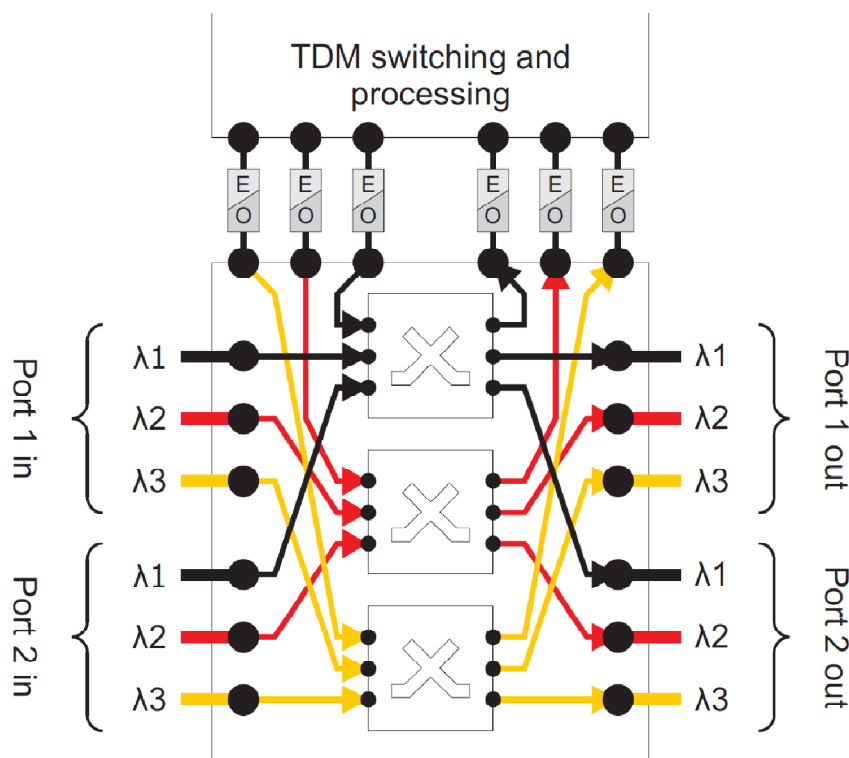


Figure 3-1: Representation of network nodes

It has to be mentioned that IDRSIM [75] supports other type of nodes such as pure OXCs or electrical cross connects. In this thesis just the presented node architecture is used since the aim was to investigate the IA-RWA in case of multilayer environment.

3.1.3 Routing model

The Intra-Domain Routing IDRSIM Simulator [75] provides a discrete event simulation environment for routing simulations in sub-rate multiplexed wavelength routed (WR) networks using graph models. In accordance with the graph model, the network architecture consists of two transport layers: an electronic and an optical one. The control planes of the two layers are allowed to inter-operate by the generalized multi protocol label switching (GMPLS) peer interconnection model. The optical layer performs WR network switching over Wavelength-Division Multiplexing, while the electronic layer adds dynamic traffic grooming time division multiplexing (TDM) capability to the network functionality. In order to enhance the performance of this feature, it is allowed lightpaths to be torn when an add or drop operation is requested at an intermediate node of a lightpath. The program takes a network topology and a traffic sample as inputs. Starting with an empty network (containing no active calls), it takes the traffic demands of the sample one by one and routes them using Dijkstra's shortest path algorithm in the logical graph built from the physical topology, realizing the routing function. During the conduction of the traffic sample, several measures

are recorded, including the blocking ratio of the sample, the hop and lambda counts of individual calls and the network load as a function of time. A route can be blocked due to the RWA problem, or because of the physical impairments. A route is blocked due to RWA problem if there is not enough resource to route the demand between the source and destination node. This happens when all the wavelengths are used or in case of grooming there is not enough free capacity to groom the demands. A route is considered blocked due to physical impairments if value of Q of the route is lower than 7.5, which is a typical requirement for connection quality in case of metro-core networks, without forward error correction schemes.

The setup of the algorithm can be split in two main parts. The first one is the routing part and the second one is the calculation of physical impairments (CPI), (Figure 3-2). The communications between these two parts are as follows: The routing algorithm chose an optimal route, between the source and destination node and it sends the description of the route to CPI. The description of the route contains the lengths of the optical fibers between the nodes. The CPI calculates the signal quality based on the calculation presented in chapter 2 and if it is adequate it sends a message back to the routing part, that the connection can be established. If the signal quality is not adequate the CPI determines the maximum reachable node (MRN) along the path and sends this information back to the routing model. The routing model establishes the connection between the source and the MRN, than chooses another route between the MRN and the destination node. If the MRN is the source node e.g. there is no possible connection due to the physical layer, the route is blocked.

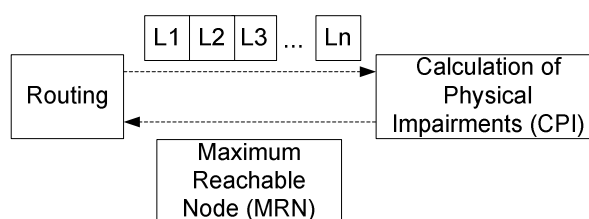


Figure 3-2: Set-up of the algorithm

The used network scenario is the basic topology proposed by COST 266 project [77], Figure 3-3. The bit-rate is 10Gbit/s per wavelength. All traffic samples were created using a Poisson-like birth process having geometrically distributed inter-arrival times with a mean of 10 time units; the source and destination nodes were distributed uniformly among the possibilities with the exclusion of calls whose endpoints are the same. The bandwidth requested by each call followed a binomial distribution of a mean of 100, 1000 or 10000 Mbit/s, while the holding times had, again, a geometric distribution with an average obtained to have 0 blocking in case of 80% network load.

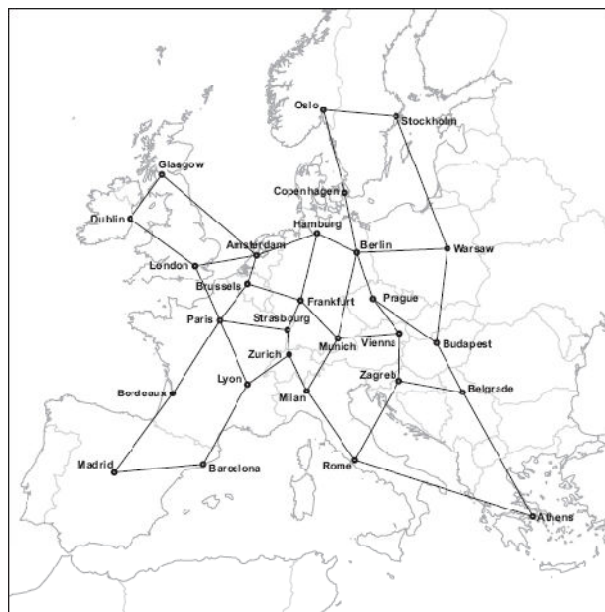


Figure 3-3: Used network scenario

3.1.4 Results

The results can be divided into two subcategories. The first set of results shows the mutual impact of physical impairments and grooming in multilayer networks as presented in [76].

In the second group the cross impact is also investigated, however here the grooming capability of the nodes are decreased by decreasing the number of O/E ports in the node switches.

3.1.4.1 Physical impairments and grooming

To perform the effects of grooming onto the IA-RWA four simulation types were made.

- The first one when there is no grooming in the RWA and the physical effects are negligible
- The second one when there is grooming and the physical effects are negligible
- The third one when there is no grooming in the RWA and the physical effects are taken into consideration
- The fourth one when there is grooming and the physical effects are taken into consideration

As it was mentioned before, the routing is done by a shortest path algorithm when each link has its own cost. By using different cost values for the links of the network one can optimize an RWA oriented, or a physical impairment oriented routing. For this purpose I use four metrics.

- The first one where the cost of each link is the same. Will be referred as hop routing.
- The second one when the cost of each link is equal to the length of the link. Will be referred as length routing.
- The third one when the cost of the link is equal to the $1/Q$ where the Q is the Q-factor of the link
- The fourth one when the cost of the link is equal to the $1/Q^2$ where the Q is the Q-factor of the link

In the case of the third and of the fourth metrics the Q-factor of each link is calculated as a point-to-point connection between the two end nodes of the link. The Q-factor based routings are not obviously the best routings for the point of view of the physical layer. This is due to the nonlinear behavior of the Q-factor. If we have two lightpaths, each lightpath has its representative Q , for example Q_1 and Q_2 . Consider a route which contains these two lightpaths in chain. The overall Q cannot be calculated from these two Q-factors, other information is also needed as presented in section 2.1.2. The only assumption which we can make, is that, if Q_1 and Q_2 have high values than the overall Q will be high as well. The exact flow chart of the algorithm can be seen in Figure 3-4.

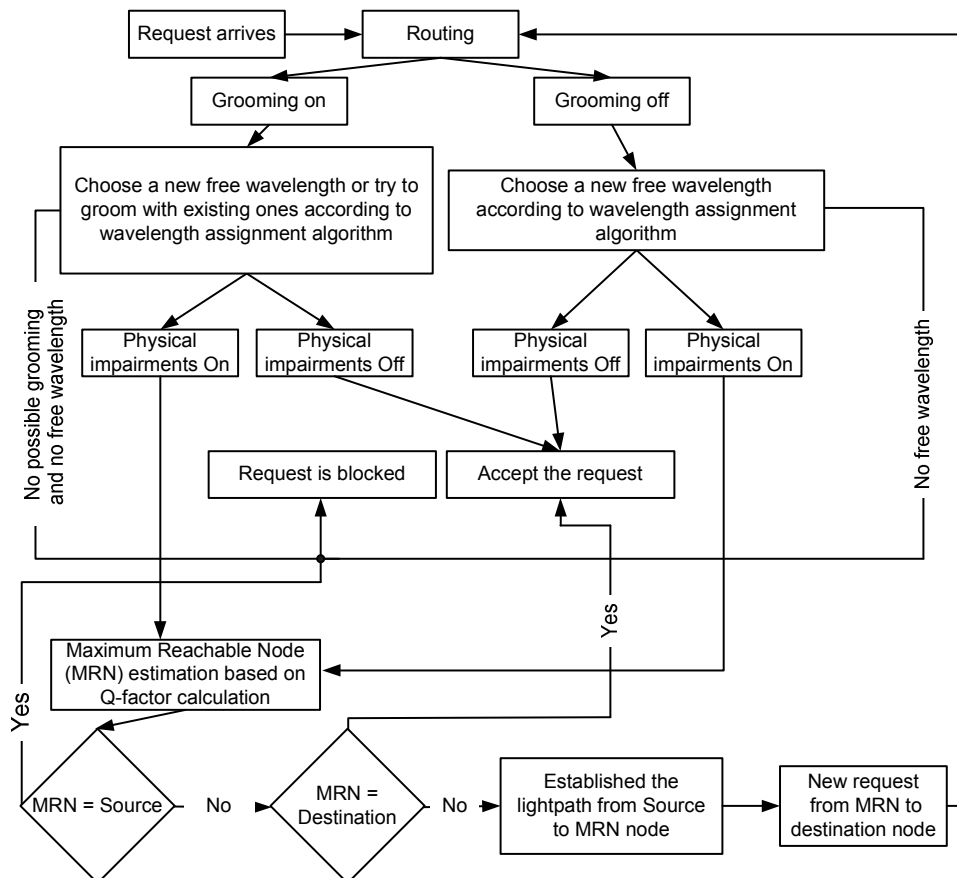


Figure 3-4: Flow chart of the algorithm

The physical impairment calculation was done based on calculations presented in Claim 1.1, section 2.1.2. The main physical parameters of the network can be seen in Table 3-1.

| | | |
|-----------|-------------|------------------------------------|
| Nf | 4,8 dB | Noise figure of the EDFA |
| X_{sw} | 40dB | Crosstalk of the switch |
| D_{pmd} | 0,1ps/nm*km | PMD coefficient of the fiber |
| Alpha | 0.2 dB/km | Fiber Attenuation |
| L_{tap} | 1dB | Attenuation of the measuring point |
| L_{mx} | 4dB | Attenuation of the multiplexer |
| L_{dmx} | 4dB | Attenuation of the demultiplexer |
| L_{sw} | 8dB | Attenuation of the switch |
| OP | 10^{-3} | Outage probability |
| P_{out} | 8dBm | Total Output of an EDFA |

Table 3-1 : The main physical parameters of the network

The four metrics used for representing the cost values of the links were compared, in Figure 3-5-Figure 3-6. In Figure 3-5 the calculation of the physical impairments was switched off and the grooming capability was switched on, and in Figure 3-6 both modules were switched on. In the X axis the scale of the network can be seen. The meaning of it is that we changed the used network link lengths, by multiplying the original lengths with the scale parameter. This resulted in increase of impairments. On the Y axis the blocking ratio is plotted. In Figure 3-5 it is to be seen that the best metric from the point of view of the blocking ratio is the hop-metric followed by $1/Q$ and $1/Q^2$ metrics while length metric yields the worst results. It is expected that in case when the physical impairments are switched off the scale of the network has no influence onto the blocking ratio. This is true when the grooming is switched off. In case of grooming there are several routing decisions which have the same probability so it is done randomly. These random decisions lead to the non-deterministic behavior.

In Figure 3-6 when the physical effects are taken into consideration the differences between the four metrics decrease. To understand this behavior the blocking ratio dependency

on to the physical effects was investigated, see Figure 3-7. In the X axis the network scale and in the Y axis the blocking ratio due to physical effects is plotted. This blocking ratio contains only the blockings due to physical effects without rerouting. This means that the routing module chooses an optimal lightpath and the CPI module calculates its Q-factor. If the Q is lower than 7,5 then the request is blocked. This is a more simplified scenario than the one presented before. In Figure 3-7 it is to be seen that the characteristics of the curves are what we expected. In case of low network scales, where the lengths of the links are very small, where the physical effects have no influence, the blocking ratio is very low. While increasing the link lengths, the influence of the physical effects increases, the blocking ratio is increasing. The four metrics were compared from the point of view of blocking ratio due to physical impairments i.e. grooming and rerouting capabilities were not used at all. Length routing has the best performance while hop routing has the worst. Between these two are the Q-based routings. Of course it is possible to find a metric which is the function of Q , $f(Q)$, that gives better results than the length based metric, however this is not the scope of the thesis.

Returning to Figure 3-6 the blocking ratio subsidence between the four metrics is due to the constraints on the physical effects. In the aspect of physical effects the best metric is the length followed by the $1/Q^2$, and the $1/Q$ while the worst is the hop metric. From the point of view of RWA the order of these four metrics is reverse. Taking into account both the physical effects and the RWA problem, as it was done, will lead to this behavior.

The other interesting property is that while increasing the scale of the network the blocking ratio can decrease. This is due to the fact that increasing the lengths of the network increases the influence of the physical effects. The effect of this influence is that we have to do more O/E/O regenerations. If there are more points where the signal goes to the electrical layer, and we are capable to groom in these nodes, the network will be more optimally used. This can lead to decreased blocking ratio.

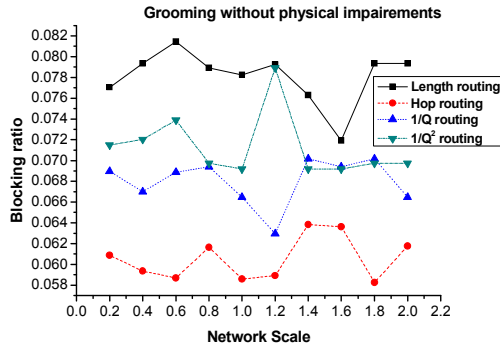


Figure 3-5: Blocking ratio dependency from the scale of the network in case of grooming without physical effects

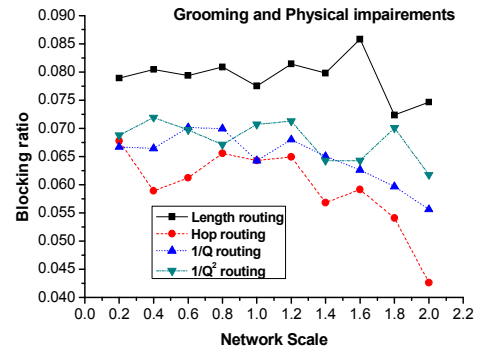


Figure 3-6 Blocking ratio dependency from the scale of the network in case of grooming and physical effects

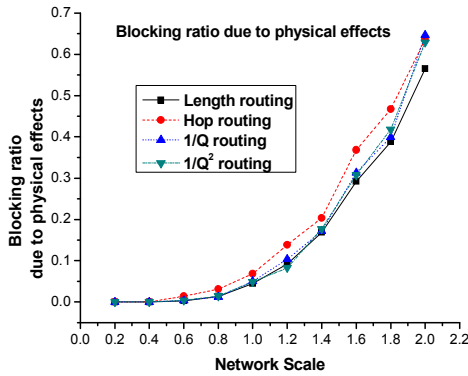


Figure 3-7: The dependence of the blocking ratio on physical effects from the as the network scales

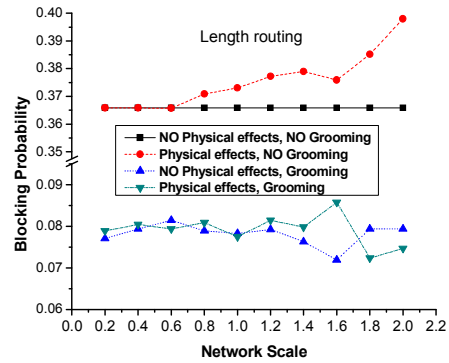


Figure 3-8 The dependency of the blocking ratio from the scale of the network for the four routing scenarios using length routing metric

In Figure 3-8 the blocking ratio dependency, on the scale of the network is plotted for the four routing scenarios, using the length routing metric. The characteristics of the curves were the same for each metric. As it was expected, there is a huge difference in the blocking ratio when the grooming capability is switched on or off in this specific network scenario. The other interesting property is that in case when the grooming is switched off and the physical impairments constraints are taken into consideration while increasing the scale of the network the blocking ratio is increasing. This is because increasing the lengths of the network the physical effects become dominating so we have to do more often O/E/O regeneration which increases the overall load of the network. In case when the nodes are capable to groom this trend of blocking growth cannot be observed. As it was mentioned before, see Figure 3-6, the blocking ratio is even decreasing while increasing the scale of the network.

3.1.4.2 O/E/O constrained grooming in IA-RWA

In this section based on previous result the performance of optical networks are investigating for different demand and node parameters. As the first step I have defined three parameters to investigate.

The first one is the scale of the network. As it was shown before this parameter has high influence onto the signal quality, i.e., the blocking ratio due to physical effects. In the following simulations to get comparable results a scale between 25% to 65% was used.

The other important parameter is the average bandwidth of the demands. This parameter has high influence onto the grooming capability of the network. Each link contains 16 wavelengths. An average network load of 60% was considered. Assuming that every wavelength operates at 10 Gbit/s, I generated 3 traffic samples, a 10 Mbit/s, a 1 Gbit/s, and a 5 Gbit/s as mean value for the bandwidth of the demands. These three values represent very low bandwidth request, an average bandwidth request, and a very high bandwidth request for the demands. Each traffic sample contains around 200000 demands. For comparison reasons, to fulfill the 60% network load, for the three different traffic samples the holding time was changed.

The last important parameter was the number of optical-electronic-optical (O/E/O) converters in the switch. It was assumed that all the nodes in the network are OXCs. The schematic of it was already presented in Figure 2-4. This node may handle A wavelengths and N ports. The “ADD” and “DROP” boxes represent connections from and to the electronic layer, respectively; the device may drop k lightpaths to and add k lightpaths from the electronic layer on each wavelength. During the tuning simulations it has been observed, that the number of built in O/E/O converters has to be between 20 and 80. 80 equals to the logically infinite value, which means every call can be lead to the electronic layer at any node of the network. This is defined by the highest degree of the nodes in the given network, multiplied by the number of wavelengths. In the simulation five steps were chosen: 20, 24, 28, 36...80. It was noted that from 36 till 80 there is no significant change in the results. This parameter besides the grooming capability of the nodes has another very important meaning. Since the cost of an optical node is highly influenced by the number of O/E/O converters, thus this parameter also represents the cost of the network.

Having the computational capacity of the nowadays PCs, and the simulation space, marked by the three orthogonal parameters: bandwidth, converter number and expansion; results in 162 different cases, it was decided to obtain access to an available supercomputer. Assuming that a simulation takes from 1 day up to 3 days, it would take almost a year to run all of them

on an average computer. Fortunately the National Information Infrastructure Development Institute of Hungary provides computation time for scientific research and educational purposes. The network consist of two SunFire 15000 HPCs, each of these has 72 processors and 164GB system memory which takes the load, and a SunFire 480R with 4 processors and 8GB memory which works as a user terminal. All the following results were obtained from this environment.

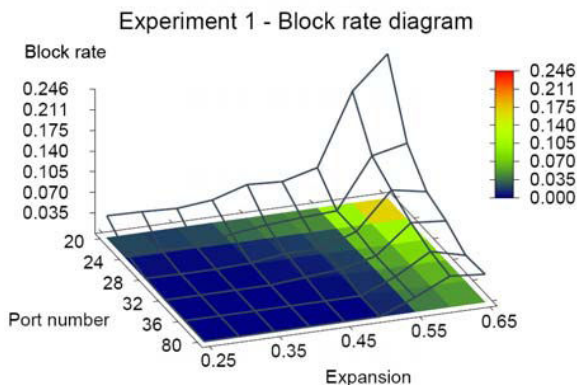


Figure 3-9: Blocking ratio in experiment 1

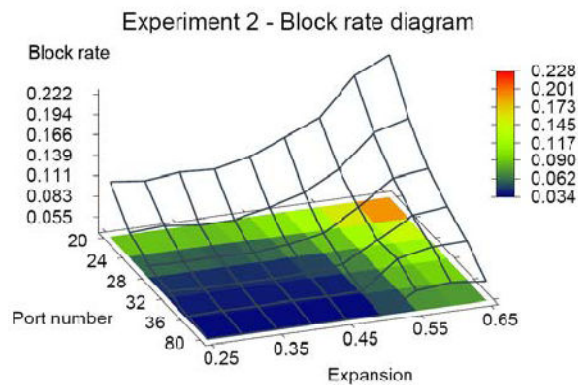


Figure 3-10: Blocking ratio in experiment 2

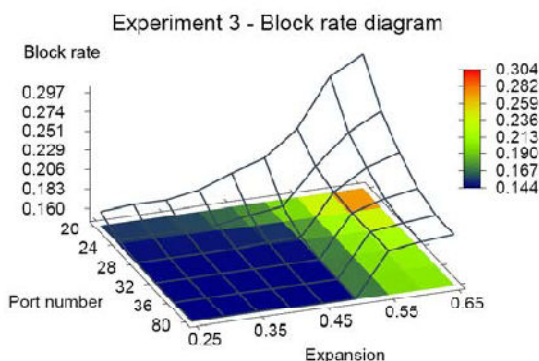


Figure 3-11 Blocking ratio in experiment 3

Figure 3-9 - Figure 3-11 show the blocking ratio of the simulations. The figures show the expected tendencies. If the length of the links increases, the blocking grows, because the physical effects will not allow connections. If only a few converters are used, the blocking grows, because the network nodes cannot perform enough wavelength conversions, and traffic groomings to allow the new calls enter into the network. The results for the experiment 1 (Figure 3-24) were obtained when the average bandwidth of the demands was 10 Mbit/s, experiment 2 (Figure 3-25) when 1 Gbit/s and experiment 3 (Figure 3-26) when 5Gbit/s. A very important conclusion can be made regarding the required O/E/O regenerations based on the blocking ratio. As it is to be seen based on the tolerable blocking ratio of the network it is possible to determine the number of O/E/O regenerators in the node.

To investigate the cross-layer influence of the optical and electronic layers the concept of optical and electronic hops was introduced.

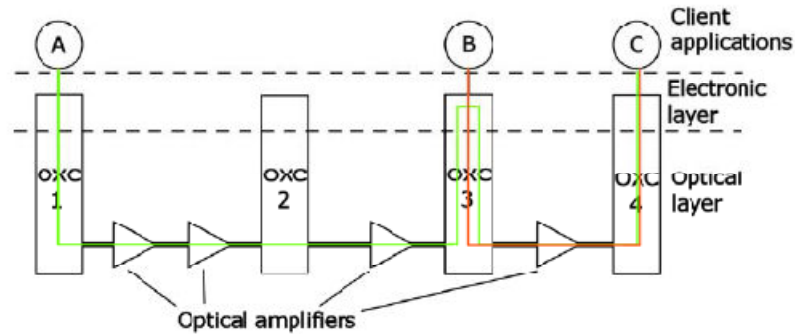


Figure 3-12: Optical and electronic hops in a two layer network scenario

For the better understanding the meaning of optical and electronic hops, let us take an example. Figure 3-12 illustrates the scenario where client *A* communicates with client *C* (green line) and client *B* with client *C*. The *A*-to-*C* path contains two electronic hops, because the signal reaches the electronic layer at *OXC3*. The number of optical hops equals three for *A*-to-*C* because it traverses through *OXC2*, although it leaves it unchanged. The optical amplifiers do not count into these values. The *B*-to-*C* path contains one optical and one electronic hop, following the previous logic. If the total bandwidth of both connections is not greater than the capacity of one lambda channel, then they can use the same lightpath between *OXC3* and *OXC4*.

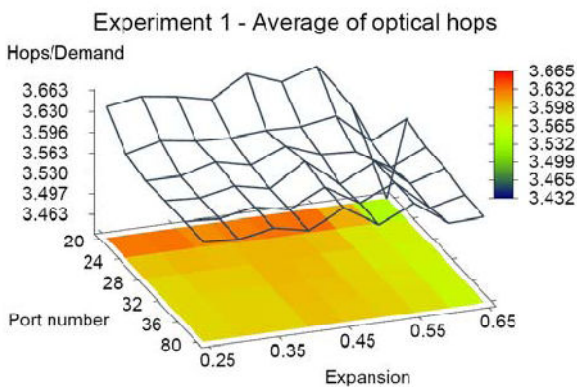


Figure 3-13: Average optical hops in experiment 1

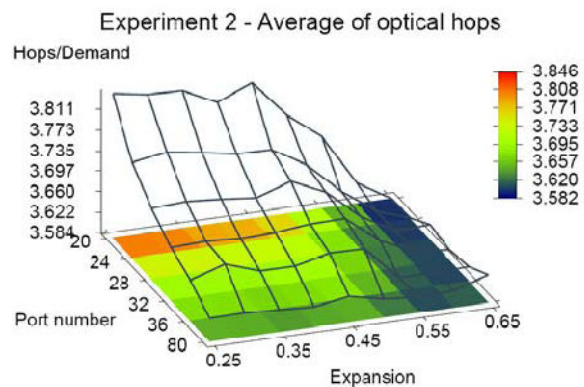


Figure 3-14: Average optical hops in experiment 2

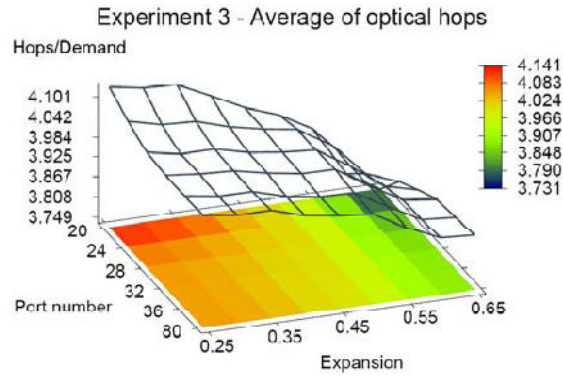


Figure 3-15: Average optical hops in experiment 3

The average optical hops show the optical layer performance. The higher is this number the longer all-optical connections are established. In all three experiment cases, while increasing the number of regenerators the more O/E/O regenerations can be done, which leads to a decreasing tendency in the number of optical hops. It also has to be mentioned that all the results are affected by the blocking ratio, since the longest is a connection the more likely is it blocked. In case of optical and electrical hops only the established connections are counted. This is the reason why an average hop number decrement can be seen at long expansion and low port numbers.

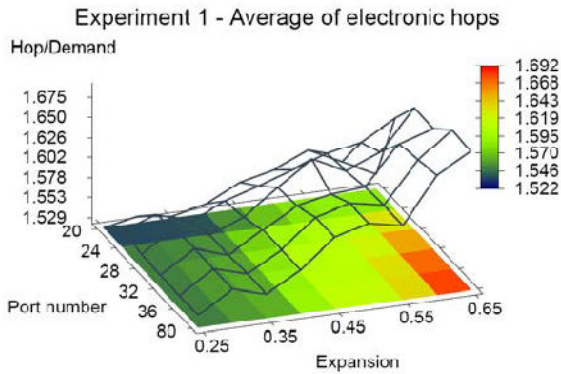


Figure 3-16: Average electronic hops in experiment 1

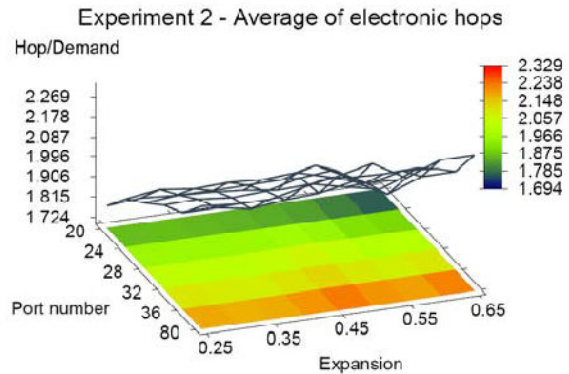


Figure 3-17: Average electronic hops in experiment 2

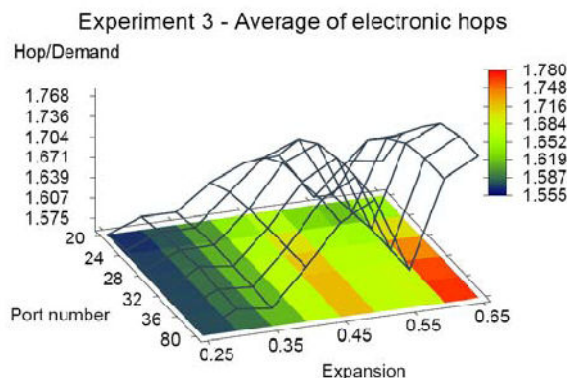


Figure 3-18: Average electronic hops in experiment 3

The number of average electrical hops determines the influence of electrical layer. It has to be mentioned that several reasons can be, to convert the signal in electrical layer:

- signal regeneration, due to physical impairments the signal quality is not adequate
- wavelength conversion, due to wavelength continuity constraint in one link the lightpath wavelength has been already used
- traffic grooming, the bandwidth of a lightpath is usually higher than the bandwidth of the demands, thus several demands can be groomed together

In Figure 3-16 - Figure 3-18 the average electronic hops are plotted. The results show that while increasing the length of the links the physical effects will have increasingly more influence, thus O/E/O regeneration has to be done more often. Also it has to be mentioned that as in case of optical hops the blocking ratio here also effects the results the same way as it was presented before.

3.1.5 Conclusion

In Claim 2.1 a novel method for IA-RWA is presented. According to the authors knowledge this is the first routing algorithm published which has the following features:

- handles multilayer networks, i.e. can take into account the electric layer performances such as grooming or wavelength conversion
- the model of the optical layer calculates the ASE, XT, PMD and also the fiber nonlinearities as presented in Claim 1.1

Based on the proposed routing model several results were obtained, as presented, regarding the design and operability of optical networks.

3.2 Claim 2.2: Adaptive configuration method

"I have proposed an adaptive configuration method, where the signal powers are tuned based on OSNR requirements in metro WDM networks. I have shown that it gives in every case the same or better configurability than the traditional methods."

In claim 2.2 I propose a novel network configuration method where the control plane has influence on the signal powers of the channels. The basic idea is to tune the signal power of each channel separately, according to the OSNR requirements at the receiver side. I also present, that the nowadays used metro WDM optical networks support such things and the proposed idea can be implemented in routing schemes.

3.2.1 Introduction

The WDM networks have successfully solved the capacity issues, but the continuously changing traffic still causes serious problem for the operators. Emerging demands often cannot be satisfied without modifying the network design, which is quite costly and difficult, so operators try to avoid this situation whenever possible. There is a strong need for a system that can deliver the same capacity as WDM, with the design and provisioning flexibility of SONET/SDH. The solution must ensure flexibility for dynamically changing future demands.

The reconfigurable optical network offers the possibility to increase or change services between sites with no advanced engineering or planning, and without disrupting existing services. In the past, reconfigurable optical networking technology was too expensive or delicate to be widely deployed. With recently matured silicon-based integrated planar lightwave circuit components, reconfigurable optical add/drop multiplexers (ROADMs) are now being installed by many operators. The technology called ROADM represents a real breakthrough for WDM networks by providing the flexibility and functionality required in present complex networking environments. Older, or fixed, OADMs cannot configure capacity at a node without manual reconfiguration and typically support reconfiguration of only a limited number of wavelengths. In contrast, ROADMs allow service providers to reconfigure add and drop capacity at a node remotely, reducing operating expenses by eliminating the time and complexity involved in manual reconfiguration.

ROADM by itself is not enough. Increased data management capabilities on individual wavelengths are also needed to exploit the benefits of ROADM in metro and backbone WDM networks. For instance, ROADM rings are very sensitive to topology changes and need strict monitoring and control of wavelength power to keep the system in balance. The real

innovation lies in the system engineering related to the ROADM function, addressing per-wavelength power measurement and management, and per-wavelength fault isolation. Almost every optical system vendor has commercial ROADM with wavelength monitoring functions (see e.g. [78]-[81]).

The next step towards a fully reconfigurable WDM optical network is the deployment of tunable small form-factor pluggable (SFP) interfaces, where the wavelength allocation is modified according to the network changes. The tunable dispersion compensation elements mean another innovation. Nowadays these are ready-made products and can be purchased [82],[83]. The evolution of optical networks seems to tend towards a fully reconfigurable network where the control and the management plane (CP and MP) have new functions, such as determining the signal quality, tuning the wavelength frequency, setting dispersion compensation units, and – by using variable optical attenuators – setting the channel powers. Of course traditional functions (such as routing) remain the main function of the CP and MP.

In this section I propose a new configuration method where the control plane handles the routing and the signal power allocation jointly. The method was presented in [84], and [85]. The basic idea is to tune the channel powers to fulfill the demands of the IA-RWA, i.e., to fulfill the OSNR requirements. Let us assume a very simple scenario, Figure 3-19. In this case we have two wavelengths λ_1 and λ_2 . In Case “A” due to physical constraints node A can only reach node C in all-optical way. If there is a demand between node A - D this can only be established with signal regeneration either in node B or in node C . In Case “B” it is possible to increase the signal power of λ_2 to fulfill the OSNR request at node D . In this way it is possible to establish an all-optical connection between nodes A - D .

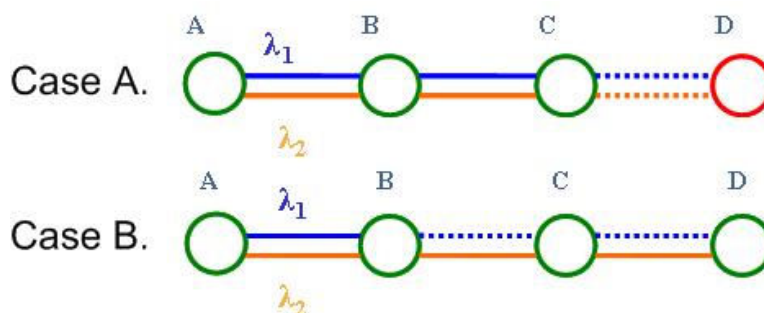


Figure 3-19 The difference of OSNR based routing and traditional routing schemes

3.2.2 Physical feasibility

Currently the power of certain channels within a fiber is set to equal levels. This is one of the remaining practices of point-to-point optical networks. Naturally using this kind of channel power allocation is a technical simplification. The other reason for using the same

channel powers is the nonlinear effects, which in this case have the smallest impact on the signal quality, see section 2.1.2.3. The idea is to use different channel powers according to the length of the path of the connection request to fulfill the optical signal to noise ratio (OSNR) to achieve bit-error free detection. E.g. for a long distance connection we can increase the signal power of the dedicated wavelength, while for a short distance connection lower wavelength power is satisfactory.

Partly the same idea has been already implemented in the Alcatel-Lucent product [89]. The difference between the proposed scheme and the product of Alcatel-Lucent is that in [89] just the minimal signal power for point-to-point links is set up, and the routing and signal power is not jointly optimize. The similarity is that both deal with different channel powers in optical fibers.

In the following sections from 3.2.2.1-3.2.2.3 the feasibility of such configuration scheme is investigated. Each section is dedicated to the main components of an optical network.

3.2.2.1 Feasibility of different channel powers in the same optical fiber

The linear effects occurring in optical fibers such as insertion loss or dispersion do not depend on the signal power however, since the nonlinear effects highly depend on the used dispersion mapping the dispersion has to be considered as a bottleneck of the proposed scheme. In case of metro WDM networks where due to short distances dispersion mapping is not used the method can be implemented. In case of long haul networks, where well balanced power budget and accurate dispersion maps are used, the proposed method cannot be used.

The other interesting question is about the nonlinear effects, since these effects highly depend on the used signal powers. In metro WDM networks the signal power of the optical channels is determined by Cross-Phase (XPM) modulation and Raman scattering and not from the Brillouin threshold [47]. This means that the total power inserted in fiber has an upper bound and not the channel powers. In this case it is possible to increase the powers of some channels up to the Brillouin threshold and at the same time the other channel powers have to be decreased to fulfill the XPM and Raman scattering constraints. The only question is, how much signal power difference can be allowed between the maximum and minimum signal power, which will be referred to as n-factor, Figure 3-20.

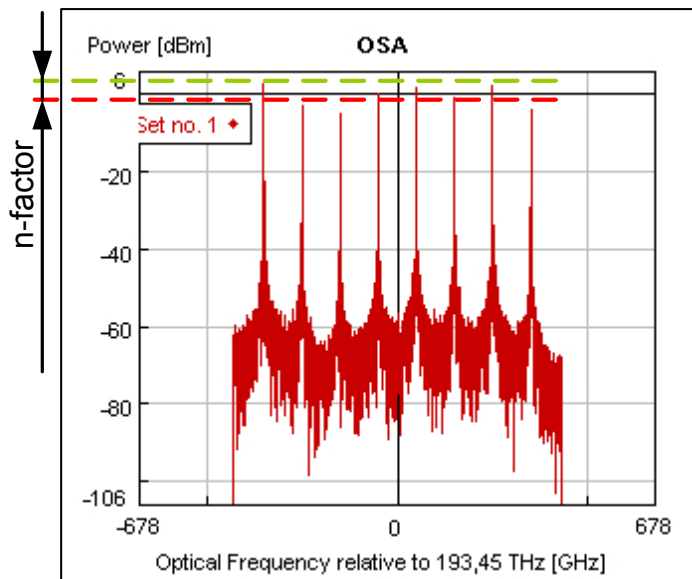


Figure 3-20: The maximum and minimum channel power in a same optical fiber

In Table 3-2 the corresponding channel powers for different n-factor values are shown in mW and dBm. These values were obtained in a real case study work [85]. As it is to be seen these values are much lower than the Brillouin threshold thus the nonlinear behavior of the optical fiber will not cause problems for such configuration scheme.

| | n-factor | | | | | Brillouin threshold |
|-------------|----------|------|------|------|------|---------------------|
| | 1 | 1,2 | 1,4 | 1,6 | 1,8 | |
| Pimax (mW) | 1,25 | 1,5 | 1,75 | 2 | 2,25 | ~ 5 |
| Pimax (dBm) | 0,96 | 1,76 | 2,43 | 3,01 | 3,52 | ~ 7 |

Table 3-2: n-factor values in mW and in dBm respectively

3.2.2.2 Feasibility of different channel power considering all-optical nodes

As it was mentioned in section 3.2.1 the demand for reconfigurable all-optical networks has been triggered the development of several new elements such as ROADMs, or tunable transmitters, etc. These components become readymade products, moreover some of them have been already deployed. Also due to dynamicity of the optical layer several new functions have been introduced. In case of point to point optical links, all the channels travelling in one optical fiber had nearly the same parameters. (Here the wavelength dependency of the elements is not considered). In case of dynamic optical networks each channel, (each

wavelength traveling in the same fiber), will have different noise distortion, dispersion and other degrading effects, since their "history", (their route), is different from each other [90]. To overcome this problem per-wavelength monitoring and equalization techniques have been introduced.

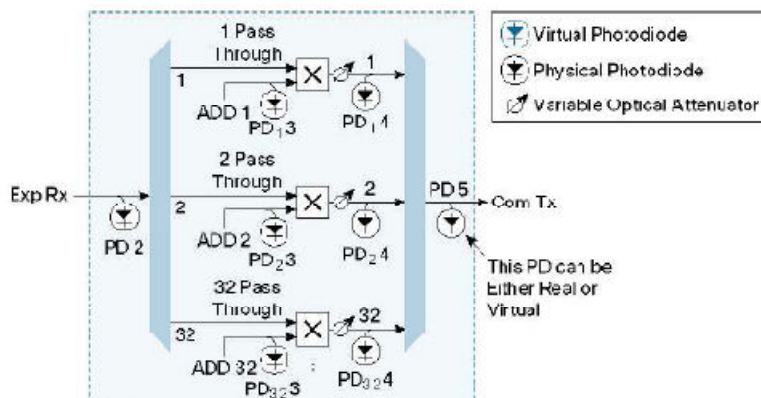


Figure 3-21 Cisco 15454 ROADM switching module

Source: http://www.cisco.com/en/US/products/hw/optical/ps2006/products_data_sheet0900aeced803fc52f.htm

In Figure 3-21 the CISCO 15454 ROADM switching module can be seen. This is a readymade product [78]. As it is to be seen in these switching modules already there are variable optical attenuators (VOA) for the purpose to equalize the channel power. These VOAs can be used to tune the signal powers according to the routing schemes presented before. The only new function is to extend the control or management plane to have influence onto the VOAs.

As conclusion the presented configuration method can be deployed in networks based on reconfigurable optical nodes.

3.2.2.3 Feasibility of different channel power considering optical amplifiers

An interesting question is how the Erbium Doped Fiber Amplifiers (EDFAs) react to the use of different channel power allocations. For this purpose I made simulations using the VPI TMM/CM Version 7.5 simulation tool [62]. It is assumed a system with 8 channels which are multiplexed and then amplified using EDFA rate propagation modules. The aim was to investigate the difference between the uniform and the adaptive channel power allocations. Following the amplifier an attenuator was placed with attenuation equal to the gain of the EDFA. The results can be seen in Figure 3-22. On the horizontal axis the number of hops is plotted, i.e., the number of EDFAs and attenuators connected in a series. On the vertical axis the "powers of ones" is plotted, where the "power of ones" is the power of the signal level when transmitting the mark one in case of two level OOK modulation format. The first three curves represent the adaptive channel power allocation where the "powers of ones" are set to

0.4 mW, 3.4 mW for channel two, seven and for all the other channels the power is 1.6 mW, respectively. These values were obtained using adaptive signal power routing presented in [91]. These values are the maximum, minimum and average channel powers, respectively. The values for channel two, four and seven were plotted. As it was expected, if the number of hops increases, after a certain number of inline amplifiers “the power of ones” decreases, i.e., the signal quality becomes very poor. The interesting thing is, that if the number of consecutive amplifiers is lower than this value, “the power of ones” remains nearly the same. Because of this behavior the EDFA supports adaptive signal allocation.

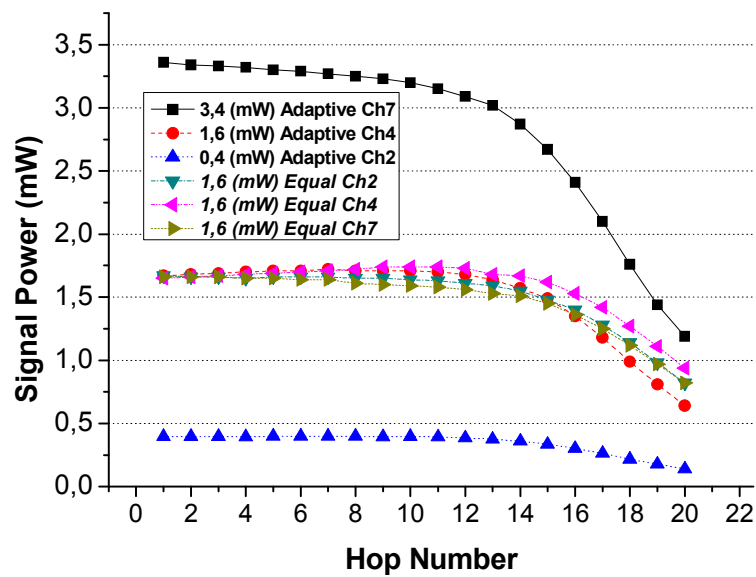


Figure 3-22: Signal power dependency from the number of EDFAs in chain

To compare the performance of the two power allocation schemes I made exactly the same simulations as it was described formerly, but without allowing different channel powers. In this case for all channels (channel 2, 4 and 7) the “powers of ones” were set to the same value (1.6 mW). See the last three curves in Figure 3-22. It can be seen that the three curves are very close to each other. The only difference is due to the wavelength dependency of the EDFA. It is interesting that the results obtained for adaptive and uniform allocation schemes are nearly the same. Difference can be seen only for high numbers of hops, where the signal quality is very poor. These results lead us to the conclusion that the so far deployed EDFAs behave similarly in case of both uniform and non-uniform channel power allocations in a single optical fiber.

3.2.3 Conclusion

In this section a novel configuration scheme was introduced for configuring the optical network. The method has been patented in [84]. The basic idea of the method is to tune the signal power according to the OSNR requests of the receiver. It was also presented that the nowadays used optical networks fully support the proposed method just the management and control plane has to be extended.

3.3 Claim 2.3: Heuristic RWA for the adaptive configuration scheme

"I have proposed a heuristic routing method for the adaptive signal power based configuration method. The algorithm depending from the input parameters can give back the globally optimal solution, or the simplest shortest path routing solution, thus makes a trade-off between scalability and complexity of the method."

As presented in section 3.2 the idea behind the adaptive configuration method is to tune the powers of each channel travelling in the same fiber according to the OSNR request at the receiver side. Also there are several constraints like the Brillouin threshold or the other nonlinearities.

In this section a novel routing algorithm and its advantages are presented. This algorithm is able to handle the adaptive signal power configuration scheme and is also suitable to compare the proposed and traditional configuration schemes.

3.3.1 Introduction

In recent years there has been a few publications which apply the same idea of different channel power allocation. This problem was considered in [86]-[88]. In [86] a general OSNR network model was developed and the OSNR optimization problem was formulated as a non-cooperative game between channels. A distributed iterative algorithm was also proposed which was further improved in [87] and [88]. In these publications the focus is on finding an equilibrium based on game-theory models to the overall network OSNR. Also as it was mentioned before the newest Alcatel-Lucent WDM product [92] benefits from the advantage of different channel powers. As it is to be seen to use different signal powers within optical fiber can be done, moreover the authors know error free operation optical networks where the signal powers differ from each other, although this wasn't done intentionally. In this specific case the tuning of signal power was not done in ROADM-s.

To the best of the authors knowledge the joint optimization of the routing and the signal power was presented first by the author in [91] and extended in [85], patented in [84]. All the previously mentioned methods treat the RWA and the signal power allocation as two independent problems.

The routing algorithm is an integer linear programming (ILP) based method which gives the globally optimal solution. Since the problem is an NP-hard problem, the scalability of the algorithm is very poor, usually for practical size networks the number of wavelengths is

limited to eight. To improved the scalability a pre-filtering technique has been proposed, to decrease the number of variables, i.e. to decrease the complexity of ILP.

3.3.2 Graph model

The graph model is slightly similar to the one presented in section 3.1.2. The wavelength graph (WL graph), which can be regarded as a detailed virtual representation of the network, is derived from the physical network considering the topology and the switching capabilities of the devices, nodes. The technique allows arbitrary mesh topologies, different types of nodes and joint optimization of multiple layers. A simpler version of the model has been first proposed in [93].

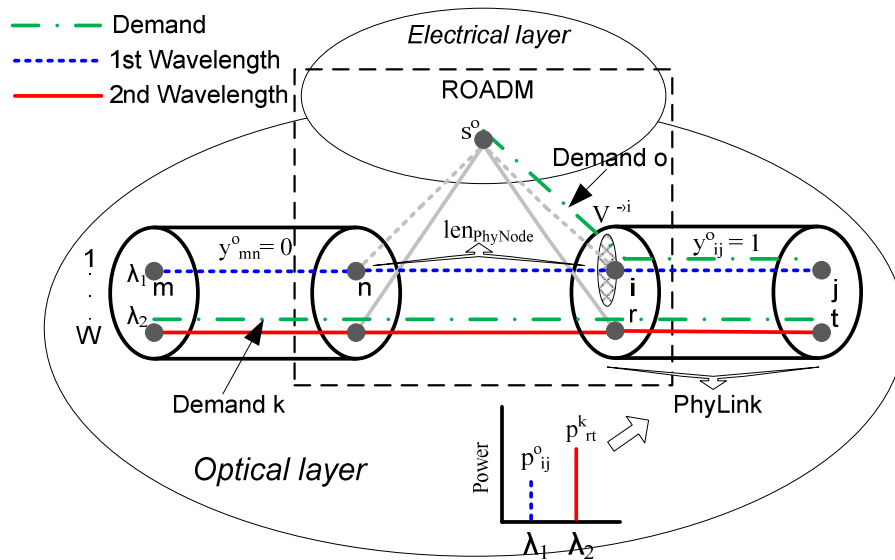


Figure 3-23: Model of switching device with optical and electronic switching capabilities,

The model of an ROADM switching device assumed in the proposed method is shown in Figure 3-23. The device can perform optical switching and electrical ending of the demands. The device illustrated in Figure 3-23 has an input and an output interface with a physical link (or fiber) connected to each. Each physical interface supports in this specific case two wavelengths ($W=2$), marked by blue dashed and red solid lines. The signal powers of the wavelengths in the right hand side physical link are different – as shown by the small subfigure. The example also comprises two demands (indicated by dash-dotted line): demand “ k ” passes though the switch in the optics, while demand “ o ” originates in this device in the electronic layer (s^o). A certain length of fiber ($len_{PhyNode}$) is assigned to each internal edge, e.g., edge (n, i) , which corresponds to the amount of signal distortion that the switching functionality introduces in the demand path. The edges representing O/E or E/O conversion are marked by grey color.

In routing it is assumed that the noise and the signal distortion accumulate along the lightpath. Actually, re-amplification, re-shaping, and re-timing – which are collectively known as 3R regeneration – are necessary to overcome these impairments. Although 3R optical regeneration has been demonstrated in laboratories, only electronic 3R regeneration is economically viable in current networks.

The constraints of maximum input power in each fiber, and maximum allowed distance as a function of the input power of the lightpath have to be met.

It is assumed that a whole lightpath is assigned to each demand from source to destination node. The signal enters into the optical layer at the source node and leaves it at the destination node. Wavelength conversion, grooming or regeneration is not allowed elsewhere along the path. This model represents an all-optical network model.

3.3.3 Routing model

As it was mentioned before, the routing method is an ILP based one. This theses does not include the ILP description of the method published in [91], since this is a part of the coauthors theses, however for better understanding it is given in chapter 5, appendix.

3.3.3.1 Relation between channel power and maximum allowed distance

Since the ILP, is a linear programming method the main difficulty in the routing algorithm was to give a linear relationship between the channel power and maximum distance. To investigate this relationship, let us consider a noise limited system where other physical effects can be taken into account as power-penalty:

Considering a chain of amplifiers, the OSNR of the end point can be calculated as follows: [19]:

$$\text{OSNR}_{\text{dB}} = 58 + P_{\text{in}} - \Gamma(\text{dB}) - \text{NF}_{\text{dB}} - 10 \cdot \log N - M \quad 3-1$$

where noise figure (NF) is the same for every amplifier and the span loss ($\Gamma(\text{dB})$) is the same for every span. P_{in} is the input power in dBm, M is the margin for other physical effects, and N is the number of spans. It is assumed that in every l km there is an inline amplifier. This means that if the link length is L , N is $\text{Int}(L/l)$ where Int means the integer part of the division.

Having into mind that

$$Q_{dB} = OSNR_{dB} + 10 \cdot \log\left(\frac{B_0}{B_e}\right) \quad 3-2$$

where B_0 is the optical bandwidth and B_e is the electronic bandwidth of the receiver.

The logarithmic Q_{dB} and the linear Q have the following relation:

$$Q_{dB} = 20 \cdot \log(Q) \quad 3-3$$

Substituting equation 3-2 and 3-3 into 3-1 we obtain the linear relation between the maximum allowable distance and the signal power.

$$L = L_c \cdot P_{mW} \quad 3-4$$

where P_{mW} is the input power in mW, L is the maximum allowable distance, and L_c is the linear factor between them.

$$L_c = 1/10^{\left(\frac{20 \cdot \log Q - 10 \cdot \log\left(\frac{B_0}{B_e}\right) - 58 + \Gamma_{dB} + NF + M}{10}\right)} \quad 3-5$$

For typical values used in telecommunications the L_c is between 500 and 2000 [km/mW].

The effects of an optical node on the signal quality are similar to the impact of an about 90 km long optical fiber, since it has nearly the same attenuation. Using the approximation mentioned previously in the routing algorithm, when the physical effects are taken into consideration, we substituted each node with a 90 km optical fiber. Naturally, more accurate models can be implemented for characterizing the networks, such the one presented in section 2.1.2, but in this case the goal was the RWA method not the detailed modeling of the physical layer.

Based on previously presented calculation it is possible to make a linear relationship between the signal power and maximum allowable distance. In the ILP formulation this was included in constraint 5-17. As it was mentioned before this was one of the main elements of the ILP, since this constraint makes the relationship between the "power-based" variables (p_{ij}^0), and "link-based" variables (y_{ij}^0).

3.3.3.2 Heuristic method for adaptive RWA

The RWA problem described is an NP-hard problem, thus the scalability is very poor. In case of globally optimal solution the maximum wavelength number was eight, where it was possible to get results, for COST266 BT network topology [77]. The bottleneck is both the calculation time and the simulation engine performance. Considering a typical metro WDM network where the number of wavelengths is between 16-60, it is clear that the only solution is to use some kind of heuristic method. Here a heuristic method is proposed which takes the advantage of the complexity of globally optimal solution and also it is able to give results for higher channel numbers as well.

The idea of the heuristic is to decrease the number of variables. This is done by preprocessing the variables before solving the ILP method presented in appendix. The algorithm has the following steps:

- for every demand calculate the shortest path
- determine a previously defined maximum deviation
- calculate for every demand and every edge that if the demand goes through the edge how much will be the total length of the route
- if the route length is higher than the shortest path plus the *maximum deviation* then this variable is excluded from the ILP description, thus decreasing the number of variables.

The heuristic presented has several advantages. If the *maximum deviation* is infinite, or high enough, the heuristic method gives back the globally optimal solution. In the other hand, if the *maximum deviation* is zero that we got a shortest path routing for adaptive configuration method, which scales well with the number of wavelengths. Of course by changing the input parameter *maximum deviation* it is possible to make a trade off between the calculation complexity and the scalability.

Considering the complexity of the problem, both the heuristics and the globally optimal solutions are NP hard problems. In case of the heuristics due to the pre-filtering technique the number of variables are decreasing, thus a more simplified ILP problem has to be solved. The pre-filtering algorithm has a polynomial complexity. Considering the ILP description, Table 3-3 shows an example for different network scenarios. The first row shows the number of wavelengths the second is the number of demands, the third stands for the method and the last three rows show the complexity of the problem, the number of rows, columns and nonzero elements while solving the ILP. The first method is mentioned as “FIX method” here it is not

allowed to tune the signal powers of the channels. The second method is the adaptive routing where a globally optimal solution is given for the adaptive routing scheme. The third one is the heuristic. Here the results are given for the case where the maximum deviation is zero i.e. shortest path routing is done. Obviously if the maximum deviation parameter is infinite we get the same complexity as in case of adaptive routing.

| Wavelength | Demands | Method | Row | Columns | Nonzero |
|------------|---------|-----------|--------|---------|---------|
| 8 | 15 | Fix | 83605 | 82992 | 343096 |
| | | Adaptive | 83605 | 83007 | 343141 |
| | | Heuristic | 5413 | 4143 | 16973 |
| 8 | 40 | Fix | 300821 | 305656 | 1257909 |
| | | Adaptive | 300821 | 305711 | 1257909 |
| | | Heuristic | 23446 | 18768 | 78440 |
| 4 | 15 | Fix | 41881 | 41496 | 171548 |
| | | Adaptive | 41881 | 41511 | 171593 |
| | | Heuristic | 2769 | 2079 | 8509 |

Table 3-3: Complexity of different methods.

3.3.4 Results

It is a very hard task to illustrate the efficiency of the algorithm since it gives obviously better results than the traditional RWA algorithms. This is due to the additional degree of freedom namely, the tune ability of the signal power. In this section some of the benefits of the algorithm are illustrated having in mind that for different input parameters the results would be slightly different.

In the simulations the well-known Cost 266 reference network [77] is used. Since this network is a long haul network I have decreased the lengths of the links by 25% to get a metro size optical network. The nodes are fully optical nodes and the signal cannot be 3R regenerated or converted into the electronics once it is in the optical layer. To demonstrate the advantage of the proposed method I have introduced the concept of “maximum routed demands”. This means that I have randomly generated a certain number of demands, a traffic matrix. If these demands could be routed, I increased the number of demands, e.g. the size of the traffic matrix, and route it again. This process continues until it is not possible to route more demands anymore. This way it is possible to find the maximum number of demands which can be routed. The bandwidths of the demands were equal with the capacity of one channel. The source and destination pairs were chosen randomly.

The absence of solution can have two reasons: the RWA does not succeed, or the distance between the source and destination node is too long, i.e. the signal quality will be inadequate. The bandwidths of the demands were equal to the capacity of one channel.

I have compared the proposed algorithm with the traditional RWA algorithm (Figure 3-24- Figure 3-25). Here in this case the *maximum deviation* parameter was infinite, i.e. the ILP is solved which gives the globally optimal solution. On the y-axis the maximum number of routed demands is depicted, while on the x-axis the used routing schemes. *RWA* means that the traditional routing scheme is used where each channel has the same signal power. It has to be mentioned that the n-factor parameter gives the maximum possible deviation between the channel powers, see equation 5-7 in chapter 5, appendix. The $n = 1$ routing scheme is similar to the *RWA* routing scheme. The only difference is that in case of $n = 1$ the channel powers can be lower than the average of the powers. In *RWA* case this variation is not allowed. In $n > 1$ cases I used the proposed routing algorithm with n equal to the depicted numbers. The result marked as “MAX” is the number of maximum routed demands in case when physical effects are neglected. The *scale parameters* mean that I changed the lengths of the used network link by multiplying the original lengths with the scale parameter. In Figure 3-24 the scale is 1, i.e., the original link lengths are used. In Figure 3-25 the scale parameter is 1.25. (The geographical distances are decreased to 25%)

In Figure 3-24 and Figure 3-25 it can be seen that the traditional RWA algorithm can route 19 and 1 demands, respectively. While by increasing the n-factor more and more demands can be routed until we reach a limit, where the RWA problem is infeasible in itself (without considering physical effects). These results show that using the proposed RWA scheme it is possible to reach the same number of routed demands as in case of neglecting the physical impairments.

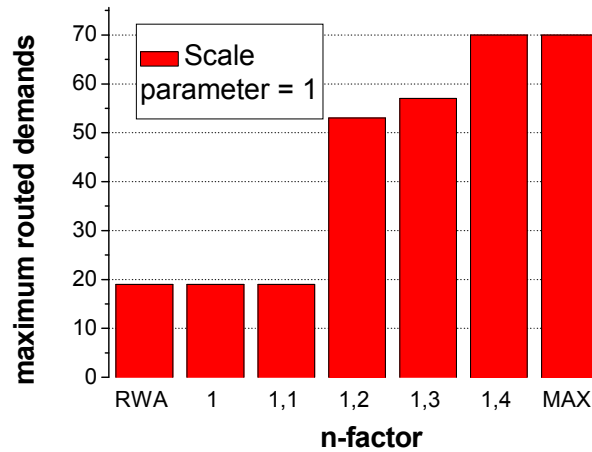


Figure 3-24: Maximum number of routed demands versus n-factor parameter in case of COST 266 topology

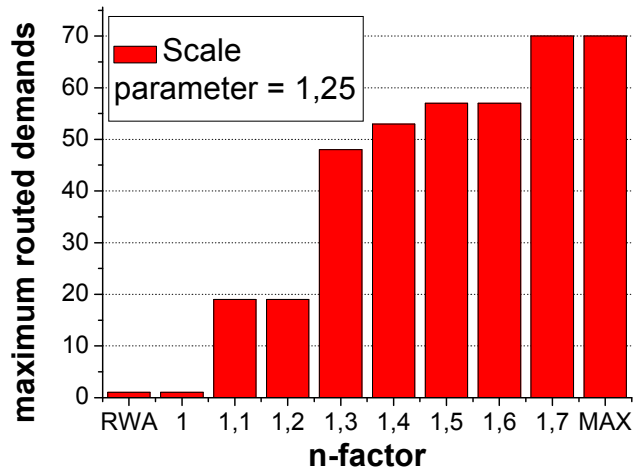


Figure 3-25: Maximum number of routed demands versus n-factor parameter in case of COST 266 topology, scale 1.25

The results lead to a conclusion that just a small amount of n-factor increase, highly increases the number of maximally routed demands.

To investigate the dependency of the proposed method on the number of wavelengths I made simulations using the COST266 network topology and different wavelength numbers (see Figure 3-26). Here also the *maximum deviation* parameter was infinite. The figure shows that while increasing the number of channels the maximum number of routed demands is increasing. This behavior is what it is expected when solving the RWA problem. The interesting property is that, if we double the number of wavelengths and the n-factor is high enough, the maximum number of routed demands is more than double in each case. This behavior is due to the way how the proposed algorithm works. If we have more wavelengths,

there are more possible variations how the signal power can be allocated. Consequently, if the number of wavelengths is increased, the performance of the proposed algorithm will improve.

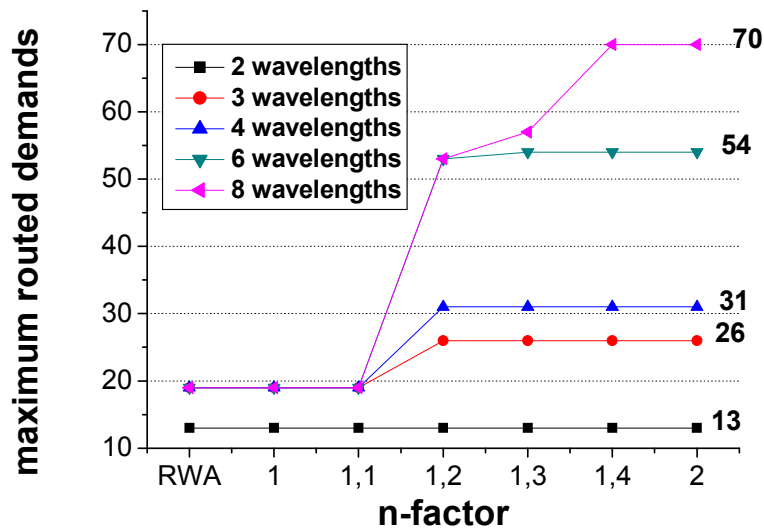


Figure 3-26: Maximum number of routed demands versus n-factor parameter in case of COST 266 topology, for different wavelength numbers

In the previous figures the performance of the algorithm was presented in case of globally optimal solution. As it was mentioned the proposed scheme is able to scale while changing the maximum allowable distance. In Figure 3-27 the performance of the method is presented in case of eight wavelength network. Two extreme cases are compared when the maximum allowable distance is zero, i.e. all demands are routed in shortest path, and when the maximum allowable distance is infinite, i.e. the globally optimal solution. As it is to be seen in case of low n-factor values the two methods give the same result but while increasing the tune-ability of the signal powers, as it was expected, the globally optimal solution performs better than the shortest path routing. The emphasis is on, that even for the simplest shortest path routing, if it is allowed to tune the signal power much more demands can be routed in all-optical domain than in case when this is not allowed. In Figure 3-28 the results for sixteen wavelength network topology is shown in case of shortest path routing. As it is to be seen the number of routed demands is highly increasing while increasing the n-factor.

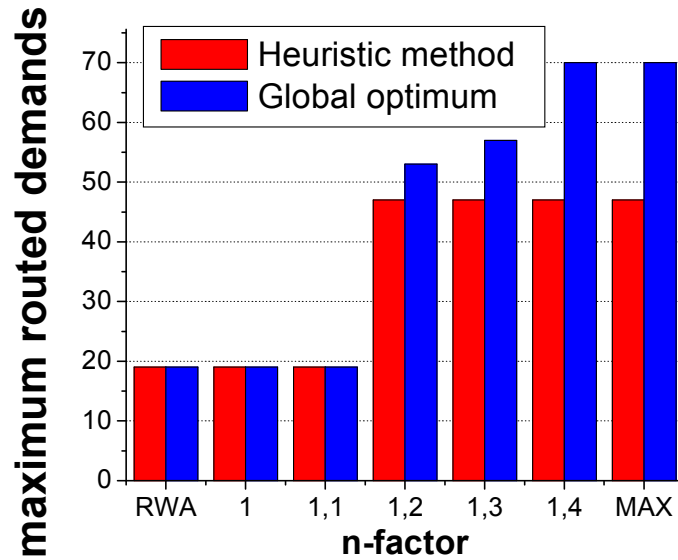


Figure 3-27: The performance of heuristic method in case of globally optimal solution and shortest path routing

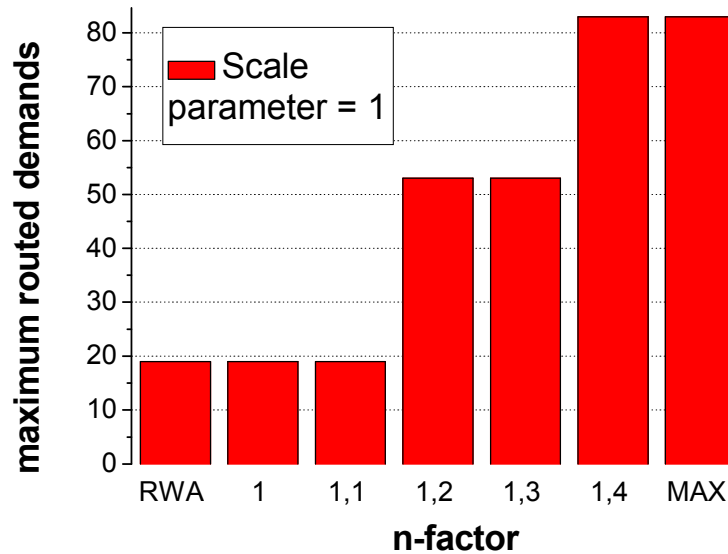


Figure 3-28: Shortest path results in case of 16 wavelengths

3.3.5 Conclusion

In this section a new RWA algorithm is presented where the power of WDM channels can be adjusted. The proposed algorithms perform joint optimization of routing (RWA) and determining the signal powers of WDM channels. The proposed methods can be used in existing WDM optical networks where the nodes support signal power tuning. A heuristic

method is given which, by using a scale parameter, can make a tradeoff between the complex global optimal solution and the simplest shortest path routing.

Chapter 4

Conclusion:

The need to explore and identify more suitable M&C methods to incorporate in wavelength division multiplexing (WDM) networks in general can be solved by taking into account the impact of physical impairments in the network performance, ranging from physical to management layer issues. The dissertation came to the conclusion that without taking the physical impairments into account optimum network performance would be difficult to achieve.

The aim of the dissertation was to present novel and efficient method for configuring the optical networks. Not only algorithms but well adopted models are presented for re/optimizing it. The obtained results have shown that both modeling and algorithmic approaches contains novelties and their development has potentials.

The dissertation at first investigates the modeling issues of different physical impairments. It presents an advanced analytical model which is suitable for characterizing the performance of nowadays used WDM networks. This is done by calculating the optimal signal power for different network scenarios. Also due to its structure, and fast computation time, the presented model is suitable for implementing in impairment aware routing and wavelength assignment algorithms (IA-RWA).

In the second part of the dissertation novel IA-RWA algorithms and methods are presented. In the first part a dynamic RWA method is shown, which is able to interoperate between the optical and electrical layer, besides taking the benefits of the highly complex and accurate physical impairments modeling method. Afterward a novel configuration method is presented where the control and management plane has influence onto the WDM channel powers. Also to overcome the scalability problems a heuristic algorithm is presented for adaptive configuration method.

Bibliography

- [1] K. L. Chen, H. M. Cheung, K. C. Chan, "From optical performance monitoring to optical network management: research progress and challenges (Invited)", ICOCN 2004
- [2] M. Saleh, J. M. Simmons, "Evolution toward the next-generation core optical network", IEEE/OSA. J. Lightwave Technology. 24(9), 3303–3321, 2006. doi:10.1109/JLT.2006.880608
- [3] H. Zang, J.P. Jue, B. Mukherjee, "A review of routing and wavelength assignment approaches for wavelength-routed optical WDM networks.", SPIE/Baltzer Opt. Netw. Mag. 1(1), 47–60, 2000
- [4] A. Hodzic "Investigations of high bit rate optical transmission systems employing a channel data rate of 40 Gb/s" PhD thesis, Von der Fakultät IV - Elektrotechnik und Informatik - der Technischen Universität Berlin zur Erlangung des akademischen Grades, Berlin, Germany, 2004
- [5] G. Cancellieri, "Single-Mode Optical Fibers", Pergamon Press, Elmsford, NY, 1991.
- [6] J. A. Buck, "Fundamentals of Optical Fibers", Wiley, New York, 1995.
- [7] International Telecommunication Union, Telecommunication Standardization Sector, Series G, Transmission system and media, digital systems and networks, Transmission media characteristics – Optical fibre cables ITU-T G650-G659
- [8] "Cisco 15454 ROADM module"
http://www.cisco.com/en/US/prod/collateral/optical/ps5724/ps2006/ps5320/product_data_sheet0900aecd803fc52f.html
- [9] D. Breuer, K. Petermann. "Comparison of NRZ and RZ modulation format for 40-Gb/s TDM standard-fiber systems", IEEE Photonics Technology Letters, 9(3):398–400, March 1997.
- [10] G. Mohs, C. Furst, H. Geiger, G. Fischer. "Advantages of nonlinear RZ and NRZ on 10 Gb/s single-span links.", Optical Fiber Communication Conference (OFC), 4(FC2):35–37, March 2000.
- [11] H. Sunnerud, M. Karlsson, and P. A. Andrekson. "A comparison between NRZ and RZ data formats with respect to PMD-induced system degradations", IEEE Photonics Technology Letters, 13(5):448–450, May 2001

- [12] R. Gross. "Differential encoder for QPSK systems", IEE Electronics Letters, 27(14):1256–1257, July 1991.
- [13] A. H. Gnauck, et al., "2.5 Tb/s (64x42.7 Gb/s) transmission over 40x100 km NZDSF using RZ-DPSK format and all-Raman-amplified spans" Optical Fiber Communication Conference (OFC), Postdeadline Paper(FC2), March 2002.
- [14] V. S. Grigoryan, P. S. Cho, I. Shpanter. "Nonlinear penalty reduction of RZ-DBPSK versus RZOOK modulation format in fiber communications" European Conference on Optical Communication (ECOC), 3(P3.29), September 2002
- [15] B. Wedding, B. Franz, and B. Junginger. "10-Gb/s optical transmission up to 253 km via standard singlemode fiber using the method of dispersion-supported transmission", Journal of Lightwave Technology, 12(10):1720–1727, October 1994.
- [16] S. Benedetto and P. Poggiolini. "Theory of polarization shift keying modulation. IEEE Transaction on Communication", 40(4):708–721, April 1992.
- [17] A. Carena, et al. "Polarization modulation in ultra-long haul transmission systems: A promising alternative to intensity modulation", European Conference on Optical Communication (ECOC), 1:429–430, September 1998.
- [18] S. Benedetto, R. Gaudino, P. Poggiolini. "Direct detection of optical digital transmission based on polarization shift keying", IEEE Journal of Selected Areas in Communications, 3(3):531–542, April 1995.
- [19] T. Antony, A. Gumaste, "WDM Network Design", Cisco Press Feb 7, 2003
- [20] E. Mannie *Ed.*, "Generalized Multi-Protocol Label Switching (GMPLS) Architecture", RFC 3945, Oct. 2004.
- [21] Recommendation G.8080/Y.1304, "Architecture for the Automatically Switched Optical Network (ASON)", ITU-T, Tech. Rep., Nov. 2001.
- [22] Z. Zhang, *et al.*, "Lightpath routing for intelligent optical networks", IEEE Network, vol. 15, no. 4, July-Aug. 2001
- [23] Keyao Zhu, Hongyue Zhu, Biswanath Mukherjee: "Traffic Grooming in Optical WDM Mesh Networks", Springer, 2005
- [24] Arun K. Somani: "Survivability and Traffic Grooming in WDM Optical Networks", Cambridge University Press, 2005
- [25] Eytan Modiano, Philip J. Lin: "Traffic Grooming in WDM Networks", IEEE Communications Magazine, vol. 39, no. 7, July 2001, pp. 124–129

- [26] Angela L. Chiu, Eytan Modiano: "Traffic Grooming Algorithms for Reducing Electronic Multiplexing Costs in WDM Ring Networks", *Journal of Lightwave Technology*, vol. 18, no. 1, Jan 2000, pp. 2–12
- [27] Timothy Y. Chow, Philip J. Lin: "The Ring Grooming Problem", *Networks*, vol. 44, no. 3, October 2004, pp. 194–202
- [28] Ori Gerstel, Rajiv Ramaswami, Galen Sasaki: "Cost Effective Traffic Grooming in WDM Rings", *IEEE/ACM Transactions on Networking*, vol. 8, no. 5, October 2000, pp. 618–630
- [29] D. Banerjee, B. Mukherjee: "Wavelength routed optical networks: linear formulation resource budgeting tradeoff and a reconfiguration study". *IEEE/ACM Trans. Netw.* 8(5), 684–696 (2000)
- [30] S Yan, M. Ali, J. Deogun: "Route optimization of multicast sessions in sparse light-splitting optical networks". *IEEE GLOBECOM* 4, 2134–2138 (2001)
- [31] B. Mukherjee, S. Ramamurthy, D. Banerjee, A. Mukherjee,: "Some principles for designing a wide-area WDM optical network." *IEEE/ACM Trans. Netw.* 4(5), 684–696 (1996)
- [32] M Ali, B. Ramamurthy, J.S. Deogun: "Routing algorithms for all-optical networks with power consideration: the unicast case." In: *Proceedings of the 8th IEEE ICCCN*, pp. 335–340 (1999)
- [33] N. Banerjee, V. Mehta, S Pandey: "A genetic algorithm approach for solving the routing and wavelength assignment problem in WDM networks." In: *3rd IEEE/IEE International Conference on Networking*, pp. 70–78 (2004)
- [34] L. Zong, B. Ramamurthy: "Optimization of amplifier placement in switch-based optical network." *Proc. IEEE ICC* 1, 224–228 (2001)
- [35] I. Tomkos, D. Vogiatzis, C. Mas, I Zacharopoulos, A Tzanakaki, E Varvarigos: "Performance engineering of metropolitan area optical networks through impairment constraint routing." *IEEE Opt. Commun. Mag.* 42, 40–47 (2004)
- [36] G. Markidis, S Sygletos, A Tzanakaki, I Tomkos,: "Impairment aware based routing and wavelength assignment in transparent long haul networks." *Optical network design and monitoring*. In: *Lecture Notes in Computer Science (series), Optical Network Design and Modeling* (pp. 48–57). Springer Berlin / Heidelberg (2007)
- [37] J.H. Brandt-Pearce, M. Pointurier, Y Subramaniam,: "QoT aware routing in impairment-constrained optical networks." In: *Proceedings of GLOBECOM*, pp. 26–30, Washington DC (2007)

- [38] M. Ezzahdi, S Zahr, M Koubaa, N. Puech, N., M. Gagnaire,: "LERP: a quality of transmission dependent heuristic for routing and wavelength assignment in hybrid WDM networks" In: Proceedings of ICCCN, pp. 125–136 (2006)
- [39] T. Deng, S. Subramaniam,: "Adaptive QoS routing in dynamic wavelength-routed optical networks." Proc. BROADNETS **1**, 184–193 (2005)
- [40] D.C. Kilper, R. Bach, D.J. Blumenthal, D Einstein, T. Landolsi, L. Ostar, M. Preiss, A.E. Willner: "Optical performance monitoring. " IEEE/OSA. J. Lightwave Technol. 22(1),294–304 (2004). doi:10.1109/JLT.2003.822154
- [41] ITU-T Draft New Recom. G.697. Optical Monitoring for DWDM Systems (2004)
- [42] N. S. Bergano, F.W. Kerfoot, C.R. Davidson "Margin measurements in optical amplifier systems," IEEE Photon. Technol. Lett. Vol. 5, pp. 304-306, Mar. 1993
- [43] G. P. Agrawal, "Fiber-Optic Communication Systems". New York: Wiley, 1997
- [44] VPI University Program, "Photonic Curriculum Version 5.0" 2009, Lecture Series: Ber and Q-factor.
- [45] E. Desurvire, D. Bayart, B. Desthieux, and S. Bigo. "Erbium-doped Fiber Amplifiers - Device and System Developments. " Number ISBN 0-471-41903-6. A John Wiley and Sons, Inc., Publication, 2002.
- [46] Sz. Zsigmond "Polarizációs Módus Diszperzió és kompenzációs lehetőségei WDM hálózatokban ", Híradástechnika, vol. LXI., pp. 11-16, 2006
- [47] D. Mazroa, Sz. Zsigmond, T. Cinkler, "Determining the Maximum Signal Power in 10 Gbit/s WDM Optical Networks", Photonic Network Communications Vol. 18 Issues 1, 2009, pp 77.
- [48] B. Ramamurthy, D. Datta, H. Feng, J. P. Heritage, B. Mukherjee, "Impact of Transmission Impairments on the Teletraffic Performance of Wavelength-Routed Optical Networks," IEEE/OSA J. Lightwave Tech., vol. 17, no. 10, Oct. 1999, pp. 1713–23.
- [49] H. Takahashi, K. Oda, and H. Toba, "Impact of crosstalk in an arrayed-waveguide multiplexer on N*N optical interconnection," J. Lightwave Technol., vol. 14, pp. 1097–1105, June 1996.
- [50] Y. R. Shen, "Principles of Nonlinear Optics" Wiley, New York, 1984.
- [51] G. P. Agrawal, "Nonlinear Fiber Optics". Academic Press, 3 edition, 2001

- [52] A. Cartaxo, "Impact of modulation frequency on cross-phase modulation effect in intensity modulation—direct detection WDM systems," *IEEE Photonics Technology Letters*, vol. 10, pp. 1268-1270, Sept. 1998.
- [53] T.K. Chiang, N. Kagi, M.E. Marhic, L.G. Kazovsky. "Cross-phase modulation in fiber links with multiple optical amplifiers and dispersion compensators". *IEEE J. Lightwave Technol.*, 14:249-259. 1996
- [54] W. Zeiler, F. Di Pasquale, P. Bayvel, J.E. Midwinter. "Modeling of Four-Wave Mixing and Gain Peaking in Amplified WDM Optical Communication Systems and Networks". *IEEE J. Lightwave Technol.*, 14(9):1933-1942. 1996
- [55] K. Inoue, K.Nakanishi, K.Oda, H.Toba. "Crosstalk and Power penalty due to fiber four-wave mixing in multichannel transmission" *IEEE J. Lightwave Technol.*, 12(8):1423-1439. 1994
- [56] D. Cotter, A.M. Hill. "Stimulated Raman crosstalk in optical transmission: Effects of group velocity dispersion." *IEEE Electron. Lett.*, 20:185-187. 1984
- [57] K.-P. Ho. "Statistical Properties of Stimulated Raman Crosstalk in WDM Systems." *IEEE J. Lightwave Technol.*, 18(7):915-921. 2000
- [58] C.-J. Chen. "System impairment due to polarization mode dispersion." *Proc. Optical Fiber Conference and Exhibit (OFC)*, 77–79, paper WE2-1. 1999
- [59] J. Kissing, T. Gravemann, E. Voges. "Analytical probability density function for the Q factor due to pm� and noise." *IEEE Photon. Technol. Lett.*, vol. 15(4):611-613. 2003
- [60] I.P. Kaminow, T. Koch "Optical fiber telecommunications" vol. IIIA, Academic Press. 1997
- [61] C.T. Allen, P.K. Kondamuri, D.L. Richards, D.C. Hague. "Measured Temporal and Spectral PMD Characteristics and Their Implications for Network-Level Mitigation Approaches." *IEEE J. Lightwave Technol.*, 21(1):79-86. 2003
- [62] VPI Transmission Maker <http://www.vpiphotonics.com/>
- [63] OptiSystem <http://www.optiwave.com/>
- [64] Á. Szabó, Sz. Zsigmond, T. Cinkler, "Impact of Physical Effects onto the Optimal Signal Power in CWDM Optical Networks", *Mediterranean Journal of Electronics and Communications (MEDJEC)* under acceptance
- [65] Sz. Zsigmond et. al.: "A DWDM gerinchálózatokban használható nagysebességű jelek alkalmazhatóságának elméleti és gyakorlati méréseken alapuló", Készült a PKI Távközlésfejlesztési Intézet megbízásából BME-TMIT által teljesítve, 2006.

- [66] Sz. Zsigmond et. al.: “Optikai crossconnect-ek (OXC) alkalmazása a transzportálózatokban”, Készült a PKI Távközlésfejlesztési Intézet megbízásából BME-TMIT által teljesítve, 2005.
- [67] Sz. Zsigmond et. al.: “SFP és XFP modulok alkalmazásai feltételeinek vizsgálata számítógépes szimulációval”, Készült a PKI Távközlésfejlesztési Intézet megbízásából BME-TMIT által teljesítve, 2007
- [68] R. A. Saunders, B. L. Patel, H. J. Harvey and A. Robinson, “Impact of crossphase modulation for WDM systems over positive and negative dispersion NZDSF and methods for its suppression”, *Electron. Lett.*, 32, (24), (1996), pp. 2206-2207.
- [69] H. J. Thiele, R. I. Killey and P. Bayvel, “Influence of transmission distance on XPM-induced intensity distortion in dispersion-managed, amplified fibre links”, *Electron. Lett.*, 35, (5), 1999, pp. 408-409
- [70] I. Neokosmidis *et al.*, “New techniques for the suppression of the fourwave mixing-induced distortion in nonzero dispersion fiber WDM systems”, *IEEE/OSA J. Lightw. Technol.*, vol. 23, no. 3, pp. 1137–1144, Mar. 2005
- [71] J. Strand and A. Chiu, “Impairments and Other Constraints on Optical Layer Routing“, IETF RFC4054, May 2005.
- [72] Keyao Zhu, Hongyue Zhu, Biswanath Mukherjee: “Traffic Grooming in Optical WDM Mesh Networks“, Springer, 2005
- [73] Csaba Gápár, Tibor Cinkler, Gábor Makács, János Tapolcai: “Wavelength Routing With Grooming and Protection“, 7th IFIP Working Conference on Optical Network Design and Modelling, Budapest, Hungary, 3–5 February, 2003
- [74] Tibor Cinkler: “ILP Formulation of Grooming Over Wavelength Routing With Protection“, The 5th Working Conference on Optical Network Design and Modelling, Vienna, Austria, 5–7 February, 2001
- [75] János Szigeti, Péter Hegyi et al.: “IDRSIM (Intra-Domain Routing Simulator)“, Department of Telecommunications and Media Informatics, Budapest University of Technology and Economics, 2004–2009
- [76] Szilárd Zsigmond, Gábor Németh, Tibor Cinkler: “Mutual Impact of Physical Impairments and Grooming in Multilayer Networks“, The 11th International Conference on Optical Network Design and Modelling, Athens, Greece, 29–31 May, 2007
- [77] European Cooperation in the Field of Scientific and Technical Research (Cost) 266 eurpoan project: <http://www.ufe.cz/dpt240/cost266/>

- [78] XC-VXL-10G/2.5G Cross Connect Cards for the Cisco ONS 15454 SDH MSPP, Cisco ONS 15454 60G/5G High-Order/Low-Order XC-VXC Cross-Connect Card <http://www.cisco.com/>
- [79] LambdaXtremeTM , Lambda Unite MMS datasheet <http://www.alcatel-lucent.com/wps/portal>
- [80] MARCONI MHL 3000 CORE datasheet <http://www.ericsson.com>
- [81] OptiX BWS 1600G DWDM datasheet <http://www.huawei.com/>
- [82] LambdaDriver WDM Tunable Cards datasheet <http://www.huawei.com/>
- [83] LambdaDriver Tunable 10GE WDM cards, TM-DXFP20T and TM-DXFP35T DM Tunable Cards <http://www.mrv.com>
- [84] Sz. Zsigmond, M. Perényi, T. Cinkler "Signal Power Based Routing In WDM All-Optical Networks" European Patent Office, PCT/EP2008/056579, submitted by Ericsson
- [85] Sz. Zsigmond, M. Perényi, T. Cinkler, "OSNR Based Routing in WDM Optical Networks", *Híradástechnika*, vol. LXIII., 2008/7 pp. 47-54
- [86] L. Pavel, "Power control for OSNR optimization in optical networks: a noncooperative game approach", in Proc. 43rd IEEE Conf. Decision and Control, 3033-3038, Dec. 2004.
- [87] Y. Pan and L. Pavel, "OSNR optimization in optical networks: extension for capacity constraints", Proc. American Control. Conf., Portland, June 2005.
- [88] L. Pavel, "OSNR Optimization via end-to-end Power Control: A Central Cost Approach", in Proc. IEEE INFOCOM 2005, Miami, March 2005
- [89] Alcatel-Lucent 1626 Light Manager <http://www.alcatel-lucent.com/wps/portal>
- [90] Sz. Zsigmond et al., "An integrated view on monitoring and compensation for dynamic optical networks: from management to physical layer", *Photonic Network Communications Accepted 2008 waiting for publication*
- [91] Sz. Zsigmond, M. Perényi, T. Cinkler "ILP formulation of Signal Power Based Routing for Single and Multilayer Optical Networks", BROADNETS 2008 September 8-11 2008 London
- [92] LambdaXtremeTM , Lambda Unite MMS datasheet: <http://www.alcatel-lucent.com/wps/portal>
- [93] T. Cinkler et al., "Configuration and Re-Configuration of WDM networks", NOC'98, European Conference on Networks and Optical Communications, Manchester, UK, 1998

Index

| | | | |
|------|--|-------|--------------------------------|
| ASE | amplified spontaneous emission | NLSE | nonlinear Schrödinger equation |
| ASK | amplitude shift keying | NRZ | non-return-to-zero |
| ASON | automatic switched optical network | OADM | add-drop-multiplexer |
| BER | bit error rate | OEO | optical-electrical-optical |
| CD | chromatic dispersion | OIM | optical impairment monitoring |
| CP | control plane | OOK | On-Off-keying |
| CPI | calculation of physical impairments | OP | outage probability |
| CWDM | course wavelength division multiplexed | OPM | optical performance monitoring |
| DCU | dispersion compensation unit | OSNR | optical signal to noise ratio |
| DD | direct detection | OXC | optical cross connect |
| DFB | distributed feedback lasers | PDL | polarization dependent loss |
| DGD | differential group delay | PM/IM | phase-to-intensity |
| DPSK | differential phase-shift | PMD | polarization mode |

| | keying | | dispersion |
|--------|--|-------|-------------------------------------|
| DQPSK | differential quadrature phase-shift keying | PolSK | polarization shift keying |
| EDFA | erbium doped fiber amplifier | PSK | phase-shift keying |
| EOP | eye-opening penalty | PSP | principle states of polarization |
| FSK | frequency-shift keying | QoS | quality of service |
| FTTB | fiber-to-the-business | ROADM | reconfigurable add-drop-multiplexer |
| FTTH | fiber-to-the-home | RZ | return-to-zero |
| FWM | four-wave mixing | RWA | routing and wavelength assignment |
| GMPLS | generalized multi-protocol label switching | SBS | stimulated Brillouin scattering |
| GVD | group velocity dispersions | SFP | small form-factor pluggable |
| HSNLab | High-Speed Networks Laboratory | SLA | service level agreement |
| IA-RWA | impairment aware routing and wavelength-assignment | SNR | signal to noise ratio |
| IFWM | intra-channel four-wave mixing | SOA | semiconductor optical amplifier |
| ILP | integer linear programming | SOP | state of polarization |

| | | | |
|--------|---|-----|---------------------------------|
| IM | intensity modulation | SRS | stimulated Raman scattering |
| ISI | inter symbol interference | TDM | time division multiplexing |
| IXPM | intra-channel cross-phase modulation | VOA | variable optical attenuators |
| LHON | long haul optical network | WDM | wavelength division multiplexed |
| M&C | management and control | WR | wavelength routing |
| MAN | metro area network | XPM | cross-phase modulation |
| MON | metropolitan optical network | XT | crosstalk |
| MP | management plane | | |
| MRN | maximum reachable node | | |
| MROADM | multi-degree reconfigurable add-drop-multiplexer | | |
| NICT | National Institute of Information and Communications Technology | | |

Appendix:

In the section the ILP formulation of dynamic network configuration is given.

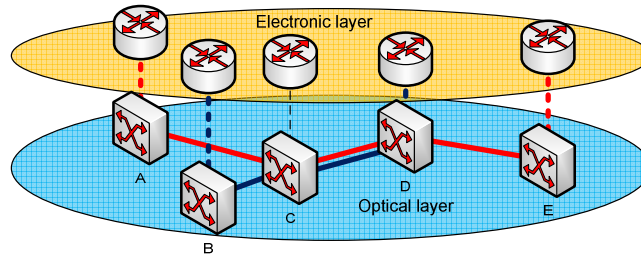


Figure 5-1: End-to-end lightpaths are assigned to each demand. In this example there are two demands (A-E and B-D). Two lightpaths (A-E, B-D) are allocated, no O/E/O is allowed on link C-D.

5.1 Constants

The WL graph contains nodes (V) and edges (A). Edge (i, j) represents one edge in the WL graph. $V^{\rightarrow i}$ and $V^{i \rightarrow}$ represent incoming and outgoing edges of node i , respectively. Symbol A^{sw} denotes the set of edges in the WL graph representing switching function inside a physical device; other edges represent wavelengths of a physical link (A^{pl}). The set of demands in the network is denoted by O .

$$P_{pl}^{\max} = 4\text{-}20 \text{ dBm typically } 10\text{dBm} \quad 5\text{-}1$$

Constant P_{pl}^{\max} means the upper limit of total power in physical link pl in dBm. $P_{pl, \text{lin}}^{\max}$ the same in mW.

$$\text{len}_{ij} \quad 5\text{-}2$$

Constant len_{ij} is the length of the physical link which the wavelength belongs to.

$$\text{len}_{\text{PhyNode}} = 90 \text{ km typically} \quad 5\text{-}3$$

Constant $\text{len}_{\text{PhyNode}}$ corresponds to the length of the fiber a switching device induces to the path of the demand.

$$L_c = 1200 \quad 5-4$$

Constant L_c is the factor of the linear relation between the input power of a demand (in mW) and the maximum distance the signal is allowed to reach.

$$\alpha \quad 5-5$$

Constant α expresses tradeoff between optimization objectives: minimal routing cost or minimal power.

$$s^o, t^o \quad 5-6$$

Symbols s^o and t^o represent source and target of demand o .

$$\beta = \frac{n}{W} \cdot P_{pl \ lin}^{\max} \quad 5-7$$

Constant β is the maximum allowed signal power for one channel in mW. Where n is a real number between 1 and W , and W is the number of wavelengths in a fiber.

5.2 Variables

$$p^o \in \left[0, \frac{\beta}{P_{pl \ lin}^{\max}} \right], \forall o \in O \quad 5-8$$

Variable p^o denotes the input power of demand o divided by $P_{pl \ lin}^{\max}$.

$$p_{ij}^o \in \left[0, \frac{\beta}{P_{pl \ lin}^{\max}} \right], \forall (i, j) \in A, \forall o \in O \quad 5-9$$

Variable p_{ij}^o means the power of demand o on edge (i, j) divided by constant $P_{pl \ lin}^{\max}$.

$$y_{ij}^o \in \{0, 1\}, \forall (i, j) \in A, \forall o \in O \quad 5-10$$

Variable y_{ij}^o tells whether demand o uses edge (i, j) or not. (E.g., variable $y_{mn}^o = 0$ in Figure 3-23 since demand o does not pass through edge (m, n) , which represents the first wavelength. On the other hand, variable $y_{ij}^o = 1$, because demand o does use edge (i, j) .)

5.3 Objective function

Minimize:

$$\alpha \cdot \sum_{\forall o \in O} \sum_{\forall (i, j) \in A / A_{sw}} y_{ij}^o + (1 - \alpha) \cdot \sum_{\forall o \in O} p^o \quad 5-11$$

The objective function expresses that the sum of the used edges should be minimized together with the sum of input powers of demands. If we want to minimize the total cost of the routing, constant cost factors should be assigned to each edge.

Constant α decides whether optimization emphasis is on minimal routing cost (α is close to 1) or on minimal input power (α is close to zero).

5.4 Constraints

$$\sum_{\forall o \in O} \sum_{\forall (i, j) \in pl} p_{ij}^o \leq 1, \quad \forall pl \in \text{PhyLinks} \quad 5-12$$

$$p_{ij}^o \leq y_{ij}^o, \quad \forall (i, j) \in A, \quad \forall o \in O \quad 5-13$$

$$\sum_{\forall j \in V \rightarrow i} p_{ji}^o - \sum_{\forall k \in V \rightarrow i} p_{ik}^o = \begin{cases} -p^o & \text{if } i = s^o \\ 0 & \text{if } i \notin \{s^o, t^o\}, \\ & \forall i \in V, o \in O \\ +p^o & \text{if } i = t^o \end{cases} \quad 5-14$$

$$\sum_{\forall j \in V \rightarrow i} y_{ji}^o - \sum_{\forall k \in V \rightarrow i} y_{ik}^o = \begin{cases} -1 & \text{if } i = s^o \\ 0 & \text{if } i \notin \{s^o, t^o\}, \\ & \forall i \in V, o \in O \\ +1 & \text{if } i = t^o \end{cases} \quad 5-15$$

$$\sum_{\forall o \in O} y_{ij}^o \leq 1, \quad \forall (i, j) \in A \quad 5-16$$

$$\begin{aligned}
& \sum_{\forall (i,j) \in A^{sw}} y_{ij}^o \cdot \text{len}_{\text{PhyNode}} + \sum_{\forall (i,j) \in A^{pl}} y_{ij}^o \cdot \text{len}_{ij} \leq & 5-17 \\
& \leq L(\mathbf{p}^o) = L_c \cdot p^o \cdot P_{pl}^{\max}_{lin}, \quad \forall o \in O
\end{aligned}$$

5.5 Explanation

Constraint 5-12 expresses that the sum power of demands traversing a physical link (fiber) cannot exceed the maximum allowed power of that link. Constraint 5-13 tells that if the power of demand o in edge (i,j) is larger than zero, then edge (i,j) is used by demand o . Constraints 5-14 and 5-15 express the flow-conservation constraint of the power and of the y decision variables, respectively, for every demand. Constraint 5-16 guarantees that a given edge can be used by only one demand. Constraint 5-17 ensures that the total length of demand o should be less than the distance allowed by the input power of demand o .